

# Tailoring the Mechanical Properties of Tissue Engineering Scaffolds made from Decellularized Cartilage

Thèse N° 9059

Présentée le 22 janvier 2019

à la Faculté des sciences et techniques de l'ingénieur  
Laboratoire de biomécanique en orthopédie  
Programme doctoral en biotechnologie et génie biologique

pour l'obtention du grade de Docteur ès Sciences

par

**JENS ANTONS**

Acceptée sur proposition du jury

Prof. N. Stergiopoulos, président du jury  
Prof. D. Pioletti, Prof. L. A. Laurent-Applegate, directeurs de thèse  
Prof. M. Zenobi-Wong, rapporteuse  
Prof. Z. Cui, rapporteur  
Prof. O. Naveiras, rapporteuse

2019



To Anja,  
The love of my life who inspires me every day  
to be the best person I possibly can. . .



## **Acknowledgements**

I would like to express my deep gratitude to my thesis advisor Prof. Dominique P. Pioletti and my thesis co-supervisor Prof. Lee Ann Laurent-Applegate. Together, they have provided me with a supportive environment, which paved the way towards my growth with immeasurable optimism, guidance, useful critiques and mutual respect during the last four years. In this environment, I did not only grow as a scientist, but also as a person and I will forever be grateful to both of you for helping me to be the person I currently am. Moreover, I would like to thank Prof. Nikolaos Stergiopoulos, Prof. Olaia Naveiras, Prof. Marcy Zenobi-Wong and Prof. Zhanfeng Cui for dedicating their precious time and expertise to review my work. I would also like to thank all former and current members of the Laboratory of Biomechanical Orthopedics (LBO) and the Unit of Regenerative Therapy (UTR) for the friendly and highly supportive atmosphere in the lab, all the fun-filled lab ski days, coffee breaks and scientific discussions. I would, especially, like to thank Sandra Jaccoud for helping and advising me with countless experiments in the lab including: cell culture, histology, and for always being around. Sandra was far more than a technical assistant; she has also helped me greatly to improve my French during my Ph.D. and introduced me to important Swiss traditions. Further, I want to thank Dr. Nathalie Hirt-Burri for her enthusiasm, scientific input and some Spanish practice. I am deeply grateful to Naser Nasrollazadeh and Peyman Karami for sharing their profound knowledge of biomechanics and for their thorough scientific discussions. I would like to offer my special thanks to Dr. Andreas Schmocker for his enthusiasm, appreciation and for taking me to climbing sessions with his 30 year old rattling Vespa. Special thanks also to Dr. Alexandre Terrier and Dr. Pierre-Etienne Bourban for their valuable feedback during my PEX examinations, lab meetings and CartiMat reunions. Furthermore, I would like to express my gratitude to Virginie Kokocinski for helping me with all administrative work, train tickets, lab ski days and bringing me bulky bovine knees from the butcher for my experiments. I would also like to thank Yasmine Boulanaache for her cheerfulness and availability to discuss the most important things in life over a delicious coffee- a passion Yasmine shares with me. Special thanks also to Claire Delabarde for introducing me to the French words that really matter and Oriane Poupart for wonderful running sessions at the shore of lake Geneva. Moreover, I would like to express my gratitude to Pierre-Arnaud

Aeberhard, who sadly passed away in June 2018 at age 27. I will always remember his captivating character and his impeccable dancing skills at the gala dinner at Termis Davos in 2017. I would like to offer my special thanks to Dr. Matteo Marascio, who helped me to work with supercritical carbon dioxide and who was always there as a friend with whom I had a great time in his home town Domodossola (Italy), during game nights and Italian evenings. I also learned a great deal about data visualization and useful software from Dr. Valérie Malfroy Camine, who willingly shared her knowledge with me to help me develop as a scientist and to discover my passion for beautiful figures- even though I have never been an artist. I want to express my deepest and sincere appreciation to Dr. Ulrike Kettenberger, who was always there as a critical advisor with strong analytical skills and as a dearest friend. Ulrike and her family with Maxi, Vinci and Flori made my life in Switzerland the most beautiful experience I could wish for. Furthermore, I would like to offer my special thanks to all my students for their excellent work and contribution to my Ph.D. thesis: Lea De Maddalena, Leila Cammoun, Quentin Vermeire, Kathlyn Minisini, El Mehdi Soukrati, Céline Bartolini and Giulia Weissenberger . Moreover, I would like to thank the former lab members: Antoine Derrawat, Caroline Fernandez, Dr. Tanja Hausherr, Dr. Philippe Abdel-Sayed and Dr. Adeliya Latypova. During these four years I also had the honor to be member and president of the EPFL-UNIL Toastmaster Club, which tremendously helped me to improve my presentation skills in a friendly and supportive environment. I had the honor to meet and learn from outstandingly-talented and motivated people. Especially I would like to express the deepest appreciation to Dr. Ossama Khalaf, who helped me as a friend and climbing partner, Vitalijs Zubkovs who made nice skiing trips with me and showed me his beautiful home-country Latvia, Luca Bertagnolio who taught me a lot about public speaking as my mentor and Carina Schey who has inspired me to grow further and to constantly push my limits. I owe my deepest gratitude to my family, especially my parents Anna-Maria and Engelbert Antons for believing in my future plans and for enduring my endless thrilling adventures. Finally, and most importantly the present thesis would have been impossible without the profound love and support from the most incredible person I have ever met in my life: my girlfriend Anja Holzheu. With her immeasurable cheerfulness and profound love she was always able to make me smile and feel comfortable even in the most difficult situations.

Lausanne, 08.11.2018

## Abstract

Due to its limited regeneration capacity, articular cartilage defects are considered a frequent clinical problem. Initial cartilage defects, if left untreated, will progress in severity over time and can eventually lead to degenerative joint diseases such as osteoarthritis. Hence, orthopedic surgeons would like to aim to treat cartilage defects early on to prevent further damage. Healthy articular cartilage consists of hyaline cartilage which assures its proper function. However, the major drawback of current treatments such as Autologous Chondrocyte Implantation or Microfracture is that they cannot guide the formation of a pure hyaline cartilage. Following current treatments a fibrocartilage or a mixture of fibro- and hyaline cartilage fills the defect in the place of hyaline cartilage. Fibrocartilage has the disadvantage that it degrades over time due to its inferior mechanical properties compared to hyaline cartilage. To solve this issue, future treatments should focus on creating pure hyaline cartilage. Recently, it was hypothesized that one possibility to engineer pure hyaline cartilage is the production of scaffolds which mimic the mechanical properties and zonal structure of native cartilage.

The overall goal with my Ph.D. project is the development of a scaffold based on decellularised articular cartilage, which has zone-specific mechanical properties to induce zonal lineage commitment in chondro-progenitors. The Ph.D. project was divided into three major sections. In the first section, the zonal mechanical properties of human articular cartilage were measured by instrumented indentation which was information crucial to targeting the appropriate properties in scaffolds. This resulted in finding a depth-dependent mechanical property gradient. In the second section, a decellularisation method involving supercritical carbon dioxide in combination with a CO<sub>2</sub>-philic detergent was developed that could overcome the limitations of existing complex and time-consuming protocols to decellularise articular cartilage. Using this method, bovine articular cartilage was successfully decellularised while important cell adhesion molecules were maintained. The high matrix density of articular cartilage makes cell infiltration challenging. For that reason, the articular cartilage was processed into a porous scaffold, in the third section of this thesis. The porous scaffold was produced by pepsin-digestion of the decellularised cartilage, lyophilization and covalent

crosslinking. It was demonstrated that the mechanical properties of these scaffolds could be tailored by changing the digest concentration prior to lyophilization. However, the developed scaffold fabrication procedure only enabled the achievement of the mechanical properties of the superficial zone, whereas the mechanical properties were too low to target the middle, deep and calcified zone. Further analysis was therefore only focused on superficial cartilage. The superficial zone-specific protein lubricin was evident on the surface of the scaffolds after 14 and 28 days of cell culture when seeded with human chondro-progenitors. This confirms that mimicking the zone-specific mechanical properties in these prepared scaffolds can produce zonal lineage commitment.

Through the results that have been accumulated in my project, it was possible to demonstrate that scaffolds with superficial zone-specific mechanical properties which are based on decellularised articular cartilage can induce zonal lineage commitment. These results show a promising concept to induce zonal lineage commitment in chondro-progenitors, a valuable feature to engineer pure hyaline cartilage with natural structure in future cartilage treatments.

**Keywords:** Articular cartilage, chondro-progenitors, decellularisation, instrumented indentation, mechanical property gradient, supercritical carbon dioxide



## **Zusammenfassung**

Knorpelschäden sind ein häufig auftretendes klinisches Problem, aufgrund der eingeschränkten Regenerationsfähigkeit von Gelenkknorpel. Unbehandelt vergrößern sich Knorpelschäden progressiv und führen zu ernstzunehmenden Gelenkserkrankungen wie Arthrose. Daher ist eine frühzeitige Behandlung des Gelenkknorpels unerlässlich, um die Situation zu stabilisieren und ein weiteres Fortschreiten aufzuhalten. Nur gesunder, hyaliner Knorpel, stellt die korrekte Funktion unserer Gelenke sicher. Aktuelle Therapieansätze wie die autologe Knorpelzelltransplantation oder Mikrofraktierungen resultieren jedoch oft in mechanisch minderwertigem Faserknorpel oder einer Mischung aus Faser- und hyalinem Knorpel. Die reduzierten Materialeigenschaften führen dann zu einem beschleunigten Verschleiß der reparierten Knorpelstelle. Diese Probleme können nur mit neuen Therapieformen, die die Entstehung von hyalinem Knorpel unterstützen, gelöst werden. Ein Ansatz dafür könnte die Nutzung von Trägermaterial mit Knorpelschicht-spezifischen mechanischen Eigenschaften zur Knorpelgewebezüchtung sein.

Das übergeordnete Ziel dieser Doktorarbeit war die Entwicklung eines Trägermaterials für die Knorpelgewebezüchtung mit der Fähigkeit, Knorpelschicht-spezifisches Verhalten in Chondroprogenitorzellen hervorzurufen. Zur Verwendung kommen soll dazu dezellularisierter Rinderknorpel mit dem der jeweiligen Knorpelschicht angepassten mechanischen Eigenschaften. Die Doktorarbeit ist in drei Teile untergliedert. Im ersten Teil wurden die Knorpelschicht-spezifischen mechanischen Eigenschaften von humanem Gelenkknorpel mittels Eindruckhärteprüfungen ermittelt. Diese Information bildet die Grundlage für die folgende Festlegung der mechanischen Eigenschaften des zu entwickelnden Trägermaterials. Wie zu erwarten zeigten die Messungen einen Anstieg der mechanischen Eigenschaften bei Bewegung der Indenternadel von der Knorpeloberfläche zum Knochen. Im zweiten Teil dieser Arbeit wurde eine Dezellularisierungsmethode basierend auf superkritischem Kohlendioxid und einem Kohlendioxid-philien Lösungsmittel entwickelt. Mit dieser neuen Technik sollen die Nachteile von existierenden Protokollen, die meist komplex und zeitaufwändig sind, überwunden werden. Es wurde gezeigt, dass mit dieser Methode erfolgreich Rinderknorpel unter Erhaltung wichtiger Zelladhäsionsmoleküle dezellularisiert werden kann. Die entstehenden Matrizen können aufgrund ihrer hohen Dichte jedoch kaum von Zellen besiedelt werden, daher wurde die Verarbeitung des Knorpelmaterials zu porösen Strukturen notwendig, ein Prozess der im dritten Teil der Doktorarbeit beschrieben wird. Zur Erreichung dieses Ziels wurde der Rinderknorpel mit Pepsin verdaut, gefriergetrocknet und kovalent quervernetzt. Die mechanischen Eigenschaften der so produzierten Trägerstrukturen konnten durch Anpassung der zu verdauenden Knorpelkonzentration, eingestellt werden. Die

mechanischen Eigenschaften der entstehenden Strukturen waren tendenziell eher niedrig und konnten nur der oberflächlichen Knorpelschicht angepasst werden. Der höhere elastische Modulus der tieferen Knorpelschichten konnte nicht erreicht werden. Alle weiteren Untersuchungen wurden daher auf die oberflächliche Knorpelschicht beschränkt. Die entwickelten Trägerstrukturen wurden in einem weiteren Schritt mit Chondroprogenitorzellen besiedelt und später immunohistochemisch untersucht. Dabei wurde das Protein Lubricin, welches spezifisch für die oberflächliche Knorpelschicht ist, erfolgreich an der Oberfläche der Gerüste nach 14 und 28 Tagen Zellkultur nachgewiesen. Dies bestätigt die Hypothese der vorliegenden Doktorarbeit, dass Knorpelschicht-spezifische mechanische Eigenschaften in natürlichen Trägerstrukturen ausreichen um einen zonalen Zelltyp hervorzurufen.

Zusammenfassend kann gesagt werden, dass die in dieser Arbeit präsentierten Techniken ein attraktives Konzept zur Stimulation eines zonalen Zelltyps in Chondroprogenitorzellen darstellen. Dies ist ein wichtiger Schritt, um bei zukünftigen Knorpelbehandlungen, rein hyalinen Knorpel mit natürlicher Struktur und Funktion erzeugen zu können.

**Schlüsselwörter:** Chondroprogenitorzellen, Dezellularisierung, Eindruckhärteprüfung, Extrazelluläre Matrix, Gelenkknorpel, Gradient von mechanischen Eigenschaften, Indentation, superkritisches Kohlendioxid

# Table of contents

<b>List of figures</b>	<b>xv</b>
<b>List of tables</b>	<b>xvii</b>
<b>Glossary</b>	<b>xix</b>
<b>1 Motivation</b>	<b>1</b>
<b>2 State of the Art</b>	<b>3</b>
2.1 Articular Cartilage . . . . .	3
2.1.1 Composition and Zonal Structure of Articular Cartilage . . . . .	3
2.1.2 Biomechanical Properties of Articular Cartilage . . . . .	7
2.1.3 Articular Cartilage Defects and Osteoarthritis . . . . .	8
2.2 Treatments for Cartilage Lesions and Osteoarthritis . . . . .	10
2.2.1 Pain Alleviation and Prevention . . . . .	12
2.2.2 How To Choose the Surgical Intervention? . . . . .	12
2.2.3 Microfracture . . . . .	14
2.2.4 Autologous Chondrocyte Implantation . . . . .	14
2.2.5 Total Knee Arthroplasty . . . . .	16
2.3 Cartilage Tissue Engineering . . . . .	17
2.3.1 Decellularised Articular Cartilage . . . . .	17
2.3.2 Commercial Products . . . . .	21
2.3.3 Cell Sources . . . . .	21
<b>3 Research Question</b>	<b>27</b>
3.1 Background . . . . .	27
3.2 Objectives . . . . .	27
3.2.1 Aim 1 . . . . .	28
3.2.2 Aim 2 . . . . .	28

3.2.3	Aim 3+4 . . . . .	29
<b>4</b>	<b>Zonal Mechanical Properties of Human Articular Cartilage</b>	<b>31</b>
4.1	Graphical Abstract . . . . .	31
4.2	Abstract . . . . .	31
4.3	Introduction . . . . .	32
4.4	Materials and Methods . . . . .	34
4.4.1	Human cartilage origin and preparation . . . . .	34
4.4.2	Indentation measurements . . . . .	35
4.4.3	Relative depth . . . . .	37
4.4.4	Histology . . . . .	38
4.4.5	Quantification of histology sections . . . . .	38
4.5	Results . . . . .	38
4.5.1	Indentation measurements . . . . .	38
4.5.2	Histological evaluation . . . . .	39
4.6	Discussion . . . . .	39
4.7	Acknowledgements . . . . .	43
<b>5</b>	<b>Decellularised Tissues obtained by a CO<sub>2</sub>-philic Detergent and Supercritical CO<sub>2</sub></b>	<b>47</b>
5.1	Graphical Abstract . . . . .	47
5.2	Abstract . . . . .	47
5.3	Introduction . . . . .	48
5.4	Materials and Methods . . . . .	50
5.4.1	Pre-treatment . . . . .	50
5.4.2	Treatment . . . . .	52
5.4.3	Biological Characterization . . . . .	52
5.4.4	Mechanical and Structural Characterization . . . . .	54
5.4.5	Statistics . . . . .	56
5.5	Results . . . . .	56
5.5.1	Biological Characterization . . . . .	56
5.5.2	Mechanical and Structural Characterization . . . . .	60
5.6	Discussion . . . . .	61
5.7	Acknowledgements . . . . .	67

---

<b>6 Engineering the Superficial Zone in Cartilage Scaffolds based on Decellularised Bovine Articular Cartilage</b>	<b>69</b>
6.1 Graphical Abstract . . . . .	69
6.2 Abstract . . . . .	69
6.3 Introduction . . . . .	70
6.4 Materials and Methods . . . . .	72
6.4.1 Scaffold Fabrication . . . . .	72
6.4.2 Decellularisation with scCO <sub>2</sub> /EtOH . . . . .	74
6.4.3 EDC/NHS Crosslinking . . . . .	74
6.4.4 DNA Extraction . . . . .	75
6.4.5 Statistical Methods . . . . .	77
6.5 Results . . . . .	77
6.6 Discussion . . . . .	87
6.7 Acknowledgements . . . . .	90
<b>7 Discussion and Outlook</b>	<b>93</b>
7.1 Clinical Situation . . . . .	93
7.2 Summary of the Findings, Discussion and Outlook . . . . .	94
<b>References</b>	<b>99</b>
<b>Curriculum Vitae</b>	<b>121</b>



# List of figures

2.1	Articular cartilage in humans. . . . .	4
2.2	Composition of extracellular matrix in articular cartilage. . . . .	5
2.3	Zones present in articular cartilage with chondrocyte and collagen fiber orientation/distribution. . . . .	6
2.4	Articular cartilage defect types. . . . .	9
2.5	Treatments for patients with cartilage lesions and osteoarthritis (knee as example). . . . .	11
2.6	Criteria for surgeons to decide for the surgical intervention. . . . .	13
2.7	Cell sources in cartilage tissue engineering. . . . .	22
2.8	Progenitor and stem cells in cartilage tissue engineering. . . . .	25
3.1	Objectives and specific aims. . . . .	28
4.1	Zonal structure and indentation protocol. . . . .	33
4.2	Example of indentation measurement. . . . .	35
4.3	Relaxation response of human femoral condyle cartilage. . . . .	36
4.4	Two indentation curves of the initial phase of contact without and with offset to correct for tissue surface irregularities. . . . .	37
4.5	Depth-dependent elastic modulus of human femoral condyle cartilage. . . . .	44
4.6	Histological sections of human femoral condyle articular cartilage. . . . .	45
4.7	Zone-dependent elastic modulus of human femoral condyle cartilage. . . . .	46
5.1	Scheme of the decellularisation procedure. . . . .	51
5.2	Histological analysis of tissues before (control) and after decellularisation treatment. . . . .	57
5.3	Cell adhesion molecules retained in the ECM before (control) and after (cECM ,tECM, sECM) decellularisation. . . . .	58
5.4	DNA and GAG content before (control) and after treatment (decellularised). . . . .	59
5.5	Ultrastructure of cartilage, tendon and skin. . . . .	61

---

5.6	Elastic modulus of cartilage and tendon after the decellularisation treatment.	62
5.7	Biocompatibility of decellularised tissues. . . . .	63
5.8	Effect of scCO <sub>2</sub> and pre-treatment. . . . .	64
6.1	Scaffold fabrication and decellularisation protocols. . . . .	73
6.2	DNA and GAG content of the decellularised articular cartilage scaffold. . .	78
6.3	Ultrastructure of scaffolds after decellularisation treatment. . . . .	79
6.4	Ultrastructure of the decellularised articular cartilage based scaffolds depending on the digest and crosslinker concentration. . . . .	80
6.5	Elastic modulus of the scaffolds depending on decellularisation, digest concentration and crosslinker concentration. . . . .	81
6.6	Elastic modulus as a function of crosslinking in dense scaffolds increased over time when scaffolds were seeded with chondro-progenitors. . . . .	82
6.7	Immunohistochemistry before and after decellularisation. . . . .	83
6.8	ECM secretion in decellularised articular cartilage scaffolds after 14 days and 28 days (loose scaffold). . . . .	84
6.9	ECM secretion in decellularised articular cartilage scaffolds after 14 days and 28 days (dense scaffold). . . . .	85
6.10	Lubricin and collagen type II secretion in decellularised articular cartilage based scaffolds after 14 days and 28 days (loose and dense scaffold) compared to human articular cartilage. . . . .	86



# List of tables

2.1	Treatments for patients with cartilage lesions and osteoarthritis. . . . .	13
2.2	Clinical studies of materials for (M)ACI. . . . .	16
2.3	Decellularisation and processing of articular cartilage into a scaffold. . . . .	20
4.1	Human articular cartilage samples with donor's age and osteoarthritis grade (Collins grade). . . . .	34
4.2	Quantification of histological staining. . . . .	39
6.1	Terminology of scaffolds depending on digest and crosslinker concentration.	74



# Glossary

## Abbreviations

a.u.	arbitrary units
AB	Alcian Blue
ACI	Autologous Chondrocyte Implantation
AM	Additive Manufacturing
cECM	cartilage Extracellular Matrix
COL	Collagen
DAPI	4,6-diamidino-2-phenylindole
ECM	Extracellular Matrix
ECPs	Epiphyseal Chondroprogenitor Cells
FDM	Fused Deposition Molding
FFF	Fused Filament Fabrication
GAGs	Glycosaminoglycans
H&E	Hematoxylin and Eosin
MACI	Matrix Assisted Chondrocyte Implantation
MMPs	Matrix Metalloproteinases
MSCs	Mesenchymal Stem Cells
scCO <sub>2</sub>	supercritical Carbon Dioxide

SDS	Sodium Dodecyl Sulphate
sECM	skin Extracellular Matrix
SEM	Scanning Electron Microscopy
SR	Picrosirius Red
tECM	tendon Extracellular Matrix
TKA	Total Knee Arthroplasty
ZoI	Zone of Inhibition

# Chapter 1

## Motivation

As early as in 1742 William Hunter recognized that cartilage damage is very problematic by stating that “From Hippocrates to the present age, it is universally allowed that ulcerated cartilage is a troublesome thing and that, once destroyed, is never recovered” (Hunter, 1742). Even though his statement was more than 270 years ago, it still describes a recurrent problem for orthopaedic surgeons. Indeed, until the present date, a permanent repair of articular cartilage is virtually impossible. Articular cartilage has a very low intrinsic healing capacity due to its alymphatic and avascular character. Unfortunately, initial cartilage damage (caused by sport activities or pathologies) can induce a cascade of accelerated degeneration, which finally leads to severe diseases such as osteoarthritis. In Europe, it is estimated that 30% of the population between 65-85 suffer from clinical osteoarthritis (Castell et al., 2015). This degenerative joint disease causes immense socio-economic burdens, accounting for very high medical costs. The situation is further aggravated by the aging population and emerging risk factors such as obesity and sport-related injuries (Mithoefer et al., 2015). An implant (total knee arthroplasty) is currently the final treatment option in the case of advanced degeneration and osteoarthritis (Portocarrero and Livinston, 2013).

Early preventive measures, as well as cartilage lesion treatment, might delay or avoid the occurrence of osteoarthritis (Ding et al., 2010; Vanlauwe et al., 2011). Notably, cell-based therapies such as Autologous Chondrocyte Implantation (ACI) have shown promising results, producing repaired tissue which resemble mainly hyaline cartilage (Brittberg et al., 1994, 2018). However, the formed repaired tissue has not demonstrated to have the same complex zonal structure, which may be crucial for the long-term function of articular cartilage. Therefore, new bioactive materials might be able to guide chondrocytes to produce hyaline cartilage with the required zonal structure. Additionally, alternative off-the shelf cell sources should be used to simplify and reduce ACI to a single-step procedure. With these materials

and cell sources at hand, scientists and orthopedic surgeons will hopefully be able to prevent the occurrence of osteoarthritis and finally challenge the initial argument of William Hunter.

# Chapter 2

## State of the Art

### 2.1 Articular Cartilage

There are different kinds of cartilage tissues that can be distinguished: elastic, fibrous and hyaline cartilage. For elastic cartilage, it is present in the aorta and outer ear and provides elasticity by its matrix protein elastin (Gotte et al., 1963). Whereas, fibrocartilage is found in inter-vertebral discs, menisci and tendons. Consisting mostly of collagen type I, fibrocartilage provides tissues with mechanical strength (Harkness, 1961). Finally, hyaline cartilage can be found in the nose, bronchi, trachea, larynx and in the articulations. Due to its glass-like appearance (hyalos means glass in Greek), the name hyaline cartilage was coined. Articular cartilage is hyaline cartilage that lines the ends of the articulating bones (Figure 2.1). Even though articular cartilage is approximately 2-3 mm thick only, it can withstand the harsh loading environment in the joints of our body. In order to withstand this harsh environment, articular cartilage has a particular structure and a nearly frictionless surface to enable smooth gliding of the opposing cartilage surfaces in our knee joint (Forster and Fisher, 1996). Inside the joint capsule, articular cartilage is surrounded by synovial fluid, which enhances the lubrication inside the knee joint (Schmidt et al., 2007). In addition, the synovial fluid is the only source of nutrients for the chondrocytes since cartilage is an avascular tissue (i.e. not connected to the blood supply). Chondrocytes are specialized cells residing in articular cartilage (Strangeways, 1920). The properties of articular cartilage can be understood by its composition and zonal structure.

#### 2.1.1 Composition and Zonal Structure of Articular Cartilage

Articular cartilage contains a considerable amount of water (65-85%) (Maroudas et al., 1969). This water is stored in a dense extracellular matrix (ECM) with an average pore size of only

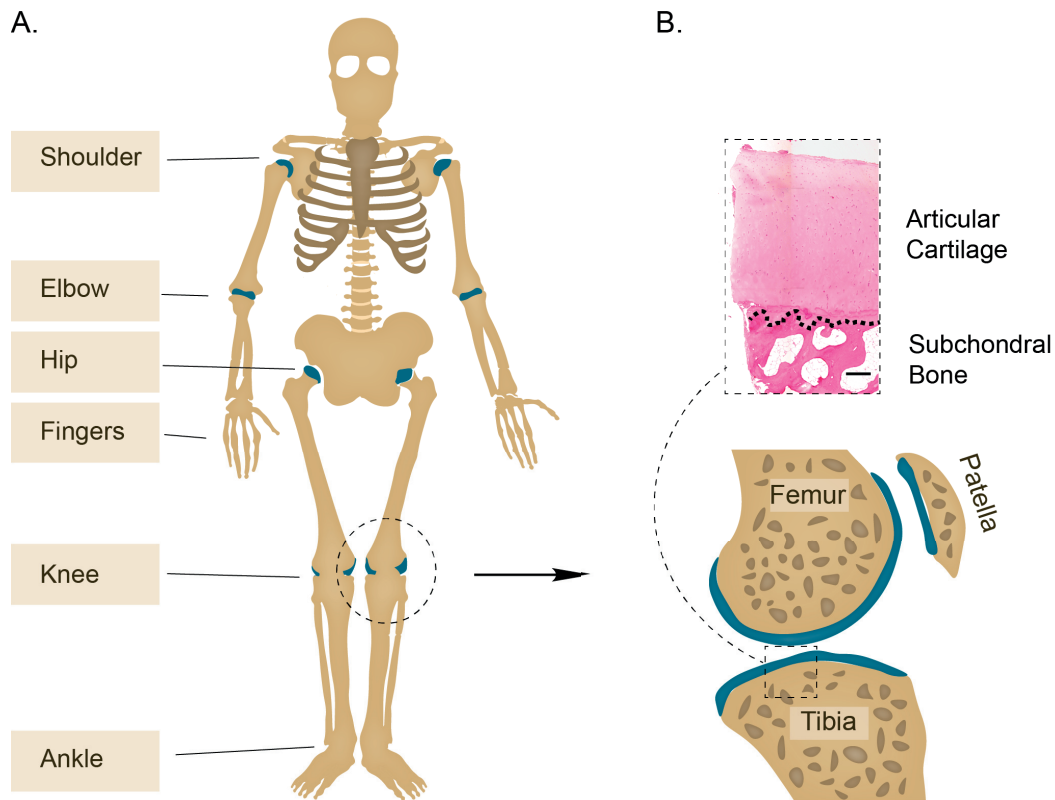


**Figure 2.1 Articular cartilage in humans.** A. Locations of articular cartilage in the human body. B. Side view of human knee with patella, femur and tibia indicating the position of the hyaline cartilage on the different bones. Histological section of articular cartilage stained by Haematoxylin and Eosin; upper part illustrates articular cartilage layer. Lower part (separated by a dashed line) indicates subchondral bone. Scale bar: 200  $\mu\text{m}$ .

6 nm (Maroudas, 1976). The ECM mainly consists of two different kinds of molecules: collagens (60-86% dry weight) and proteoglycans (15-40% dry weight) (Mow et al., 1992). Collagen type II is the most abundant collagen in articular cartilage (90-95%) (Miller and Lunde, 1973). Other collagens include type III, VI, IX and XI (Eyre et al., 2006). These collagen types aid to form and stabilize the type II collagen network.

Proteoglycans have a protein core to which glycosaminoglycan (GAG) chains are covalently attached. There are two GAGs in articular cartilage, keratan and chondroitin sulphate, which can be detected. Chondroitin sulphate is the predominant GAG type in cartilage (Mathews et al., 1958). GAG chains extend from the protein core and form brush-like structures (Figure 2.2). Due to charge repulsion, the GAG chains remain separated, which results in occupation of more space within the ECM. There are different types of proteoglycans in articular cartilage such as aggrecan, decorin, biglycan and fibromodulin (Aspberg, 2016). Aggrecan is the most abundant and largest proteoglycan. It is composed of a protein



backbone to which the polysaccharides chondroitin or keratin sulphate are attached. The important feature of aggrecan is its ability to form aggregates with hyaluronan (Hardingham and Muir, 1972). These aggregates form via link proteins between aggrecan and hyaluronan (Hardingham, 1979).

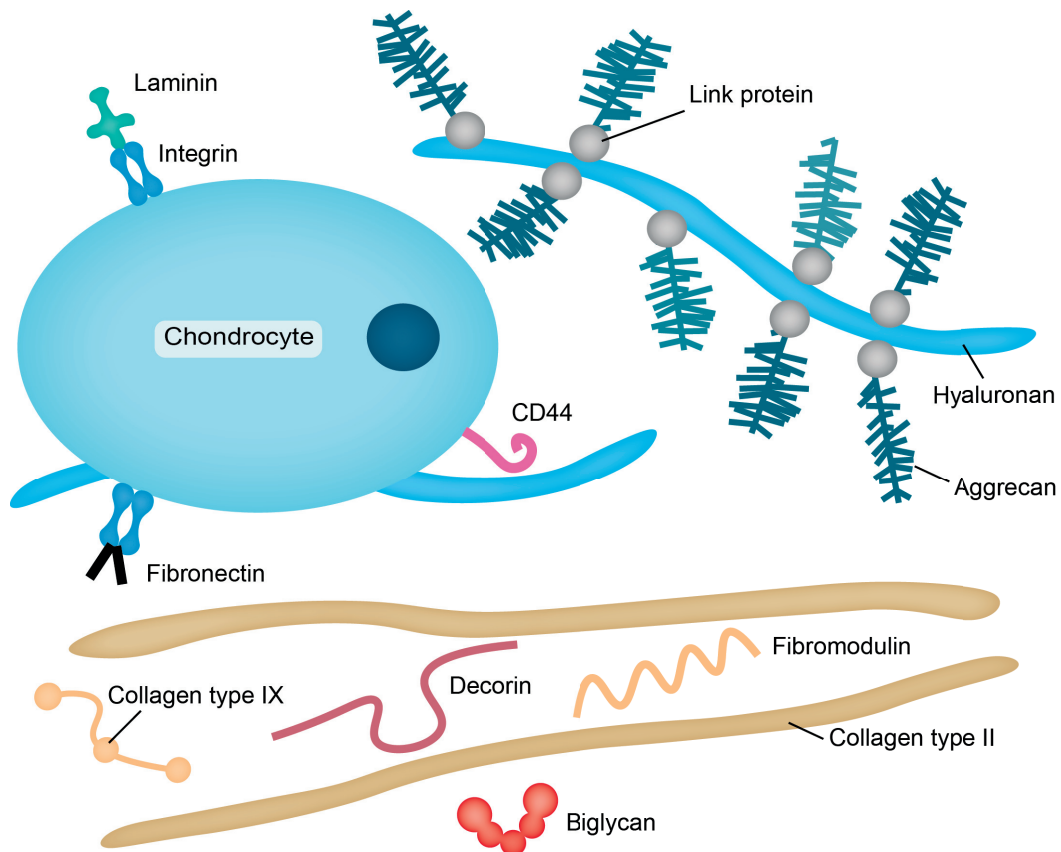


**Figure 2.2 Composition of extracellular matrix in articular cartilage.** Hyaluronan binds to the CD44 cell receptor and is connected with aggrecan via link proteins. Collagen type II fibrillation is influenced by collagen type IX, decorin, biglycan and fibromodulin. Integrin receptors bind to fibronectin and laminin.

The less abundant proteoglycans such as decorin, biglycan and fibromodulin interact with collagens (Aspberg, 2016). Apart from water and ECM, articular cartilage also contains very few chondrocytes, which occupy only 2% of the volume (Alford and Cole, 2005). Chondrocytes have a low metabolic activity and synthesize ECM molecules very slowly. For instance, the turnover of proteoglycans in articular cartilage can take up to 25 years and the collagen half-life is estimated to be between decades to 400 years (Eyre et al., 2006; Masuda et al., 2003).

The composition, structure and chondrocyte distribution are inhomogeneous and change dependent on depth from the cartilage surface towards the bone (Maroudas, 1973; Maroudas

et al., 1969). According to depth, four different cartilage zones can be distinguished: a) superficial zone, b) middle zone, c) deep zone and d) calcified zone (Figure 2.3).

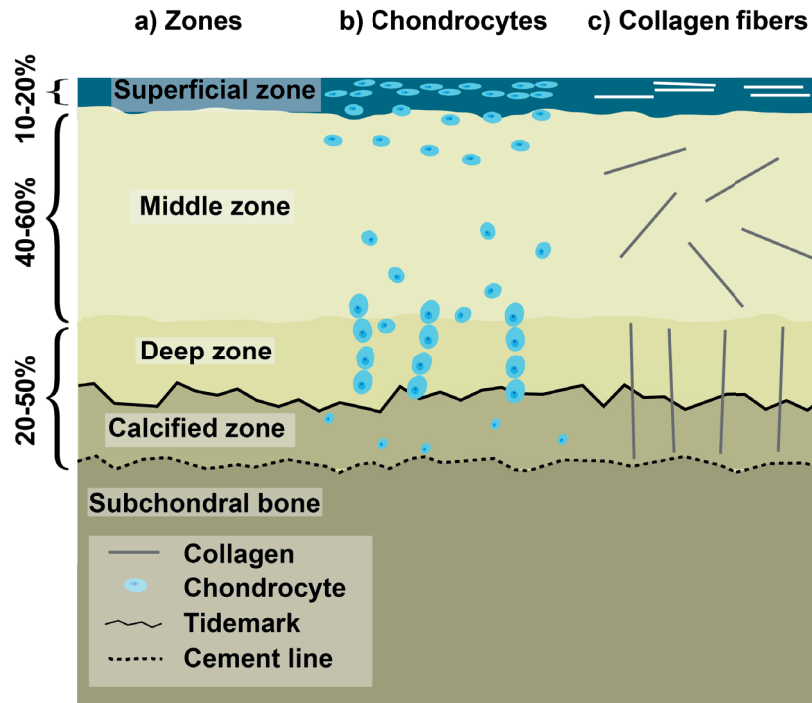


**Figure 2.3 Zones present in articular cartilage with chondrocyte and collagen fiber orientation/distribution.** a) Zonal structure: superficial (10-20% of cartilage volume), middle (40-60% of cartilage volume), deep zone (20-50% of cartilage volume), calcified zone and subchondral bone can be distinguished. The tidemark is the transition between deep zone and calcified zone, whereas the cement line is the transition between calcified layer and subchondral bone. b) Chondrocyte orientation/distribution. c) Zone-dependent collagen fiber orientation/distribution.

From the superficial zone towards the subchondral bone, the GAG content increases, whereas the collagen content diminishes (Muir et al., 1970). The superficial zone only makes up 10-20% of the cartilage volume. It is rich in small diameter collagen fibers, which are oriented in parallel to the cartilage surface (Maroudas and Bullough, 1968). This parallel orientation causes the high tensile strength and shear resistance of articular cartilage (Muir et al., 1970). In the superficial zone the chondrocytes are flatly oriented and express a protein called "lubricin" or "superficial zone protein" (Schumacher et al., 1994). Lubricin reduces friction on the cartilage surface and is thus essential for the function of articular cartilage (Rhee et al., 2005). The middle zone takes up 40-60% of cartilage volume and the collagen fibers are randomly oriented and have a larger diameter than in the superficial zone (Minns and Steven, 1977; Weiss et al., 1968). The chondrocytes have a spherical shape, are arbitrarily distributed and express the intermediate layer protein (Lorenzo et al., 1998).

The transition between the deep zone and the calcified zone is called tidemark (Redler et al., 1975). The deep zone and calcified zone occupy 20-50% of the total cartilage volume. In the deep zone towards the subchondral bone, the collagen fibers and chondrocytes are organized in columns (Trueta and Little, 1960). The transition between calcified zone and subchondral bone is called cement line. The cement line can be interpreted as a "viscous" interface between cartilage and bone (R Lakes, 1979).

All the aforementioned structural and biochemical features of articular cartilage play an important role for its biomechanical behavior (Chen et al., 2001b; Lu and Mow, 2008).

### 2.1.2 Biomechanical Properties of Articular Cartilage

There are three phases that contribute to the biomechanical properties of articular cartilage: i) a solid phase: the ECM, ii) a fluid phase: the synovial fluid produced by the synovial membrane and iii) an ion phase consisting of different ion species such as sodium ( $\text{Na}^+$ ), calcium ( $\text{Ca}_2^+$ ), chloride ( $\text{Cl}^-$ ), and potassium ( $\text{K}^+$ ) (Lai et al., 1991; Linn and Sokoloff, 1965; Lu and Mow, 2008; Maroudas, 1973).

In engineer terms, articular cartilage can thus be described as a "fluid-saturated, fiber-reinforced, porous and permeable composite matrix" (Mow et al., 1984) or in a simplified manner: a sponge with very low permeability. The negatively charged sulphate ( $\text{SO}_4^-$ ) and carboxylic groups ( $\text{COO}^-$ ) of the polysaccharides (chondroitin or keratin sulphate) give a high negative charge density (Maroudas et al., 1969). The high negative charge of the proteoglycan aggrecan attracts positively charged ions such as sodium ( $\text{Na}^+$ ) and calcium ( $\text{Ca}_2^+$ ). These positively charged ions attempt to neutralize the negative charge of the sulphate groups in aggrecan. As a result of the high ion concentration in the ECM of articular cartilage compared to the ion concentration in the surrounding synovial fluid, an osmotic pressure builds up in the ECM (Maroudas, 1976).

This osmotic pressure is maintained and absorbs load and mechanical shock during daily activities. The water cannot escape quickly from the ECM during load, due to two reasons: first, the water molecules are bound by the charged ECM molecules and ions and second, the very low permeability of its ECM (6 nm pore size on average (Maroudas, 1976)). The permeability of articular cartilage changes depth-dependently. The superficial zone is the most permeable and the deep zone the least permeable (Maroudas and Bullough, 1968).

During daily activities articular cartilage experiences different mechanical stimuli including tensile, compressive and shear stresses (Athanasίου et al., 2009). Compressive loading is the predominant type of loading in articular cartilage.

Due to the flow of synovial fluid inside the low-permeable matrix, articular cartilage possesses time- and rate- dependent deformation characteristics, which can generally be

described as visco-elastic (Hayes and Mockros, 1971). An important mechanical variable in articular cartilage is the aggregate modulus, which is between 0.5 and 0.9 MPa (Athanasίου et al., 1991). Apart from its compressive properties, articular cartilage also provides an almost frictionless surface with a friction coefficient of 0.05-0.015 (Forster and Fisher, 1996). The low friction coefficient is essential for the smooth gliding of opposing cartilage surfaces within the knee joint.

### **2.1.3 Articular Cartilage Defects and Osteoarthritis**

Articular cartilage defects can have a variety of causes ranging from strong impact, repeated loading and presence of foreign bodies to genetic causes such as osteochondritis dissecans (Clements et al., 2001; Jeffrey et al., 1995; Rosenthal et al., 1983). According to their size and depth, the defects can be classified as chondral (lesions are limited to superficial and middle zone), osteochondral (lesions that go down to the subchondral bone) and lesions that penetrate down to the bone marrow (Simon and Jackson, 2018). A classification for the different lesions is illustrated in Figure 2.4.

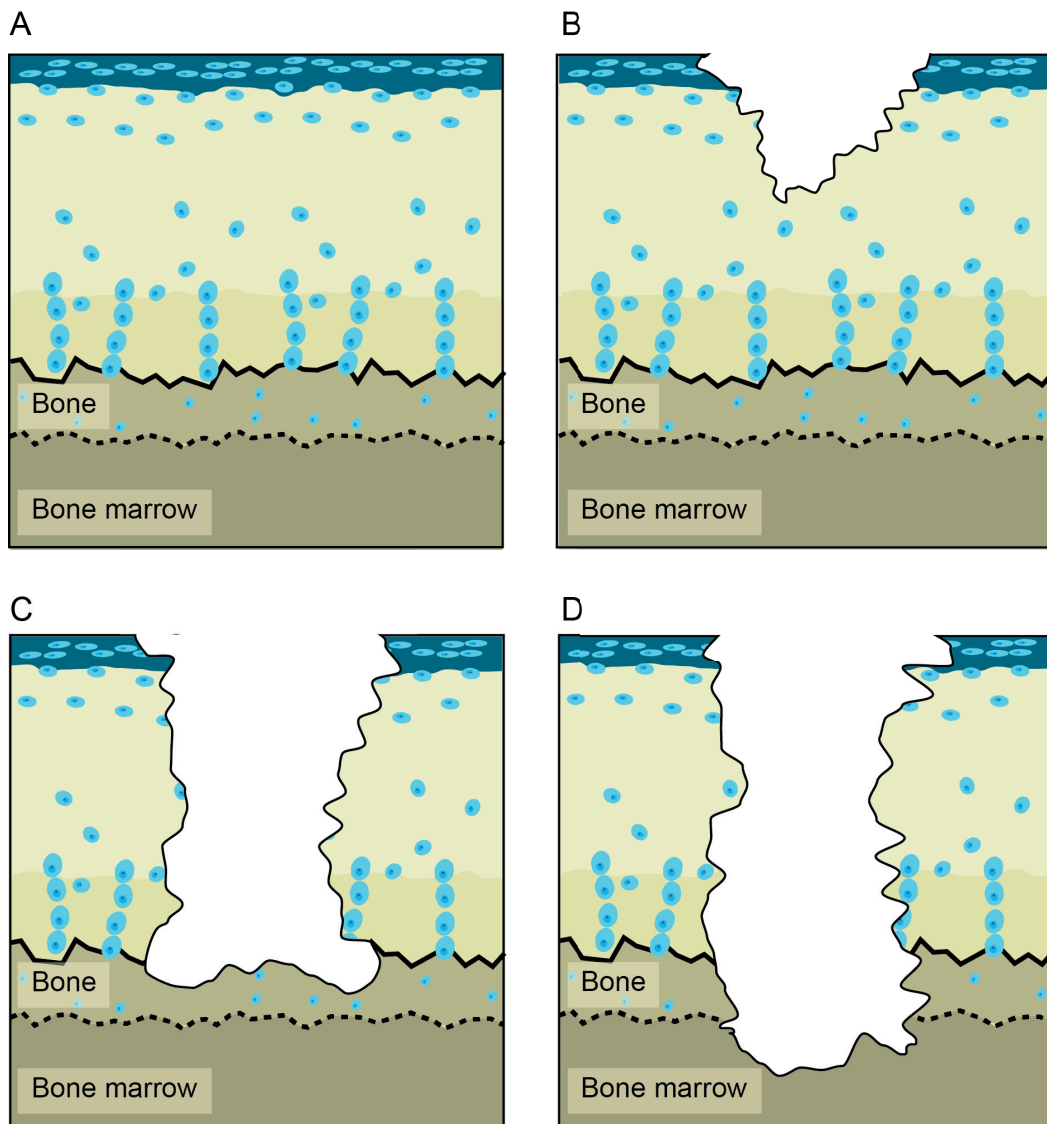


**Figure 2.4 Articular cartilage defect types.** A. Healthy cartilage. B. Chondral lesion. C; Osteochondral lesion. D. Osteochondral lesion with bone marrow defect.

If left untreated, cartilage lesions can progress in size and develop into osteoarthritis over time (Charalambous, 2014). Osteoarthritis is a degenerative disease affecting the entire joint (Loeser et al., 2012). To slow down degeneration and occurrence of osteoarthritis, it can be beneficial for the patient if cartilage lesions are detected and dealt with early (Vanlauwe et al., 2011).

## **2.2 Treatments for Cartilage Lesions and Osteoarthritis**

Depending on the disease state and physical condition of the patient, different treatment options are available. These treatment options are summarized in Table 2.1 and are visualized in Figure 2.5.

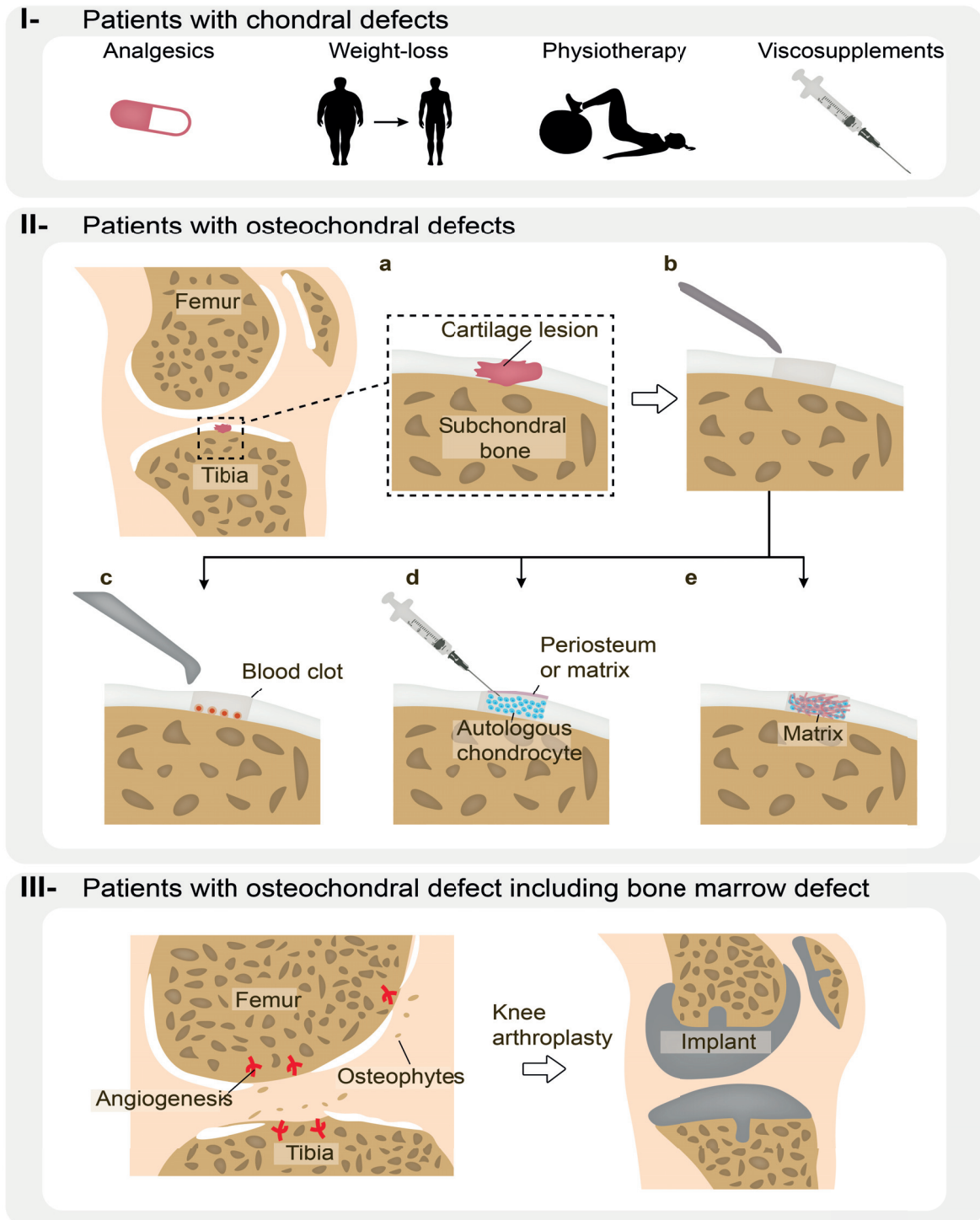


**Figure 2.5 Treatments for patients with cartilage lesions and osteoarthritis (knee as example).** I. Patients with chondral defects; II. Patients with osteochondral defects: a. Depiction of a full-thickness focal chondral lesion. b. The lesion is debrided (diseased tissue is removed) to ensure that newly forming tissue can integrate within the host tissue. c. Microfracture treatment. d. Autologous Chondrocyte Implantation (ACI). e. Matrix Assisted Autologous Chondrocytes Implantation. III. Patients with osteochondral defect including bone marrow defect: osteoarthritis and subsequent knee arthroplasty with implant.

### **2.2.1 Pain Alleviation and Prevention**

In the early stage (chondral lesions), analgesics, weight loss, physiotherapy or viscosupplements are possible treatments. Analgesics only alleviate the pain, whereas weight loss and physiotherapy might aid to slow down further cartilage degeneration. Viscosupplements such as hyaluronic acid have shown to mildly reduce pain when injected into the knee cavity (Petrella et al., 2002). However, a recent systematic review, which analyzed 12,667 adults receiving viscosupplements, has concluded that the reduction of pain was minimal to non-existent (Rutjes et al., 2013). On the contrary, a reduction of 56.5 % in osteoarthritis-inflicted pain according to the Likert scale was reported in another study (Heisel and Kipshoven, 2013). Furthermore, the authors of the review discourage the administration of viscosupplements, due to increased risk of adverse effects. For a more advanced disease stage (osteochondral defects), surgical procedures are recommended.

### **2.2.2 How To Choose the Surgical Intervention?**

In order to choose the appropriate surgical treatment for an individual patient, "treatment algorithms" were developed. These treatment algorithms help the surgeon to decide for the appropriate surgical intervention depending on defined criteria, which are summarized in Figure 2.6 (Cole et al., 2009; Oliver-Welsh et al., 2016). According to the treatment algorithm, assessment of need for surgery, lesion size and physical demand are the most important criteria for the surgeon. Before planning a surgery, the surgeon has to carefully consider the pain level, pathologies and the risk-benefit ratio for each individual patient. The lesion size and the activity level play important roles in the decision for the most suitable treatment. A summary of treatments currently applied in clinics is illustrated in Figure 2.5.



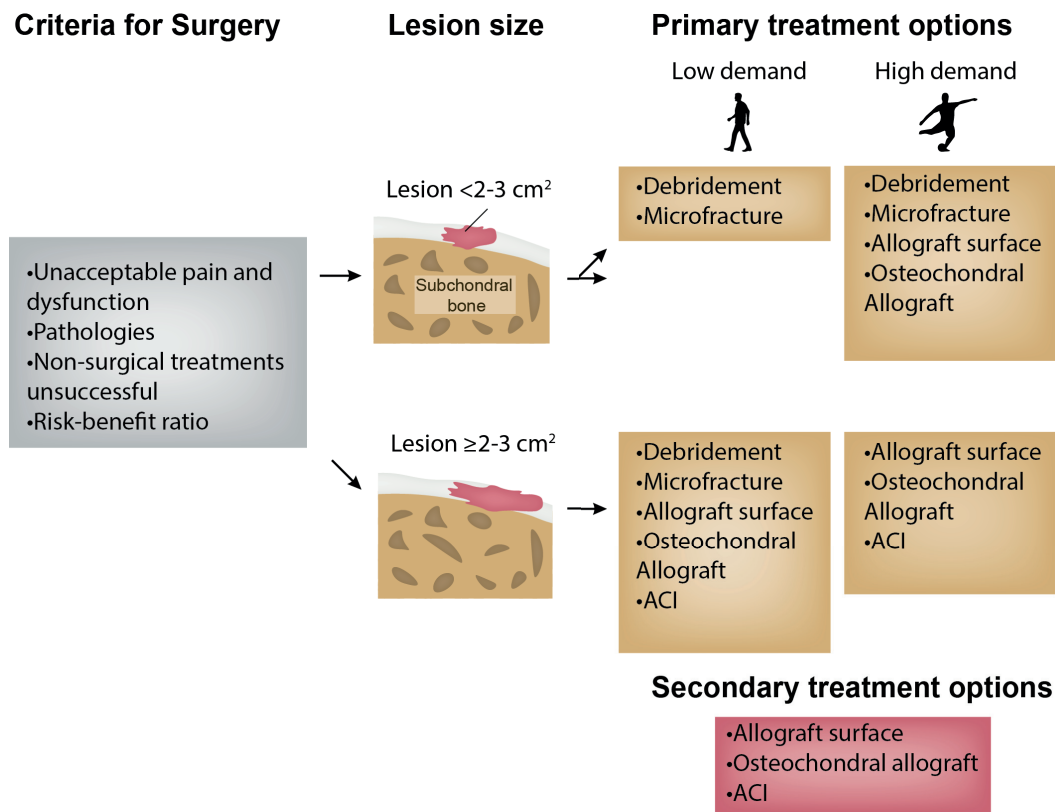


**Figure 2.6** Criteria for surgeons to decide for the surgical intervention. This figure was inspired by the work of (Cole et al., 2009).

**Table 2.1** Treatments for patients with cartilage lesions and osteoarthritis.

Treatment	Description	Benefits	Limitations	Patient group
Non-surgical	Viscosupplements Analgesics Weight-loss Physiotherapy	Relatively inexpensive No surgery	Palliative	All patient groups
Athroscopic-chondroplasty	Removal of detached Cartilage	Pain relief	Palliative No scientific proof	All patient groups
Microfracture	Puncturing of subchondral bone to release MSCs	Rapid recovery	Fibrocartilage Variable outcome	Young athletes
Joint arthroplasty	Implant to replace joint	Pain relief	Risk of infection Wear of implant (Reoperation)	Osteoarthritis patients at late stage
Autologous chondrocyte Implantation (ACI)	Autologous cells are extracted and harvested to be reinjected	Might induce hyaline cartilage	Expensive Repair tissue is variable	
Matrix-assisted Autologous chondrocyte Implantation (MACI)	Similar to ACI, but chondrocytes are cultured on a 3D matrix prior to implantation	Might induce hyaline cartilage	Expensive Repair tissue is variable	

### 2.2.3 Microfracture

Microfracture is a common technique used to treat full-thickness articular cartilage defects, which are smaller than 2-3  $cm^2$ . This surgical technique, which builds upon the body's own healing potential, was developed by Steadman and colleagues in the 1980s (Steadman et al., 2001). Briefly, in microfracture (Figure 2.5) the damaged cartilage tissue is debrided (removed down to the calcified zone). Channels are then punctured into the subchondral bone with an awl, spaced 3-4 mm apart and 2-4 mm deep, to expose the bone marrow. Subsequently, MSCs migrate from the bone marrow to the site of the cartilage defect and form a fibrin clot which over time develops into a tissue (Figure 2.5).

The drawback of microfracture is the fibrous character of the forming repaired tissue, which has demonstrated to have inferior biochemical and mechanical properties compared to hyaline cartilage (Mithoefer et al., 2009). The repaired tissue formed after microfracture, effectively provides short-term improvement of knee function (within the first 24 months), however there are few studies available that have investigated the long-term effectiveness of microfracture (Mithoefer et al., 2009). In one of these long-term studies, microfracture has demonstrated that five years after the treatment, early signs of osteoarthritis might appear regardless of the size of the lesion (Knutsen et al., 2007). To improve the control and outcome of microfracture, combination with covers such as periosteal flaps or natural and synthetic scaffold materials is an option (Dorotka et al., 2005; Siebold et al., 2003). Nevertheless, for the repair of larger cartilage lesions, other surgical techniques are more suitable.

### 2.2.4 Autologous Chondrocyte Implantation

For larger defects, exceeding 2-3  $cm^2$ , Autologous Chondrocyte Implantation (ACI) is recommended. ACI is a cell-based cartilage repair technique, which utilizes the patient's own chondrocytes to create a graft tissue (Figure 2.5).

ACI was first implemented by Brittberg in 1987 and has since been constantly modified (Brittberg et al., 1994). Currently, there are four different generations of the ACI procedure. Except for the latest generation, all ACI procedures entail a two-step protocol. First, a biopsy is taken from a non-load bearing area of articular cartilage to isolate and expand the chondrocytes *in vitro*. Once a sufficient cell number is reached (12-48 million cells, after approximately 4 weeks), the chondrocytes are reinjected into the defect site or cultured on biomaterials prior to implantation. The biomaterial has evolved during each ACI generation.

In the first generation of ACI, a periosteal flap was used to cover the defect site. Thus, the periosteal flap was fixed with fibrin glue on the cartilage defect to create a cavity. The

autologous chondrocytes were subsequently injected into this cavity. The first generation of ACI has already demonstrated a significant improvement in function, formation of hyaline-like cartilage tissue and a reduction of pain. For instance, comparing the improvement of clinical score to microfracture, ACI demonstrated a superior outcome 10 years post-surgery in case of cartilage defects exceeding  $3 \text{ cm}^2$  (Basad et al., 2010; Saris et al., 2014).

However, the major limitation of the first generation of ACI is the use of the periosteal flap. Firstly, harvesting the periosteum for the periosteal flap increases operating time and secondly the periosteal flap can induce hypertrophy (Peterson et al., 2000). To circumvent the problem of hypertrophy, bio-absorbable collagen membranes were used in the second generation of ACI to replace the periosteal flap. The clinical performance of these matrices was tested in numerous human clinical studies, with the common tendency of improving the clinical score.

The third generation of ACI is known as Matrix-Assisted Chondrocyte Implantation (MACI). In MACI, autologous chondrocytes are expanded *in vitro* and cultured on a chondro-inductive matrix during 3 days prior to implantation. Subsequently, the cell-seeded matrix is glued into the defect site with fibrin glue. In a recent randomized controlled study of 144 patients with a 5 years-follow up, MACI has demonstrated a statistically significant improvement with lesions bigger than  $3 \text{ cm}^2$  when compared to microfracture (Brittberg et al., 2018).

Finally, in the fourth generation, ACI is reduced to a single-step procedure by using non-expanded autologous chondrocytes or allogenic progenitor cells (Orth et al., 2014). Further success and improvement of ACI and MACI depend on the cell type and biomaterial that is used for the procedure. In the following section, different biomaterials currently used in clinics, development of biomaterials in research and information about the different cell sources and cell types will be given.

### **Commercial Matrices for (M)ACI**

Commonly applied, commercially available, bio-absorbable materials are listed in Table 2.2. Collagen is the predominant bio-absorbable material, with products derived from porcine collagen type I/type III (ACI-MAIX, Chondro-Gide and MACI) or from collagen type I only (CaRes, Neocart, Novocart 3D). The absorbable MACI membrane has two distinct sides. The upper side is engineered to have low friction (low porosity), whereas the lower side is engineered for cell infiltration (high porosity). Alternative matrix materials include hyaluronan (Hyalograft C, Anika Pharmaceuticals, USA), Polyglycolic acid (Bio-Seed C, Biotissue, Germany), fibrin gel (Chondron, Regrow, India) or cellular cartilage spheroids

(Chondrosphere, Co.don, Germany). Based on personal observation, all listed matrices commonly have relatively low initial mechanical properties.

**Table 2.2 Clinical studies of materials for (M)ACI.**

Product	Manufacturer	Natural material	Clinical studies (human)
ACI-MAIX	Matricel (Germany)	Porcine I-III collagen membrane	(Ebert et al., 2011; J.R. et al., 2014) (Bauer et al., 2012; Zheng et al., 2007)
Chondro-Gide	Geistlich Pharma (Switzerland)	Porcine I-III collagen membrane	(Marlovits et al., 2012; Ronga et al., 2004) (Haddo et al., 2004)
MACI	Vericel (USA)	Porcine I-III collagen membrane	(Anders et al., 2012; Zhang et al., 2014) (Aldrian et al., 2014)
CaRes	Atrho-Kinetics (Austria)	Rat collagen type I matrix	(Barthel et al., 2011; Steinhagen et al., 2010)
Neocart	Histogenics (USA)	Bovine collagen type I matrix	(Crawford et al., 2012, 2009)
Novocart 3D	TETEC (Germany)	Bovine sollagen biphasic membrane	(Niethammer et al., 2014; Zak et al., 2014) (Angele et al., 2015)
Hyalograft C	Anika Pharmaceuticals (USA)	Hyaluronan	(Brun et al., 2008; Wondrasch et al., 2009) (Clar et al., 2010; Kon et al., 2016)
Bio-seed C	Biotissue (Germany)	Polyglycolic acid	(Erggelet et al., 2010; Fontana et al., 2012) (Kreuz et al., 2013; Mancini and Fontana, 2014)
Chondron	Regrow (India)	Fibrin gel	(Fickert et al., 2014; Könst et al., 2012)
Chondrosphere	Co.don AG (Germany)	Spheroids in suspension from autologous chondrocytes	(Fickert et al., 2014)

## 2.2.5 Total Knee Arthroplasty

A total knee arthroplasty (TKA) is performed to alleviate the pain and regain function for patients suffering from advanced osteoarthritis (Ethgen et al., 2004). Briefly, the articular cartilage and part of the bone is removed by the orthopedic surgeon to replace the articulation with an implant (Figure 2.5). Although TKA has demonstrated high success rates, there is still some risk for revision surgeries due to prematurely failing implants. Failure of implants is usually attributed to loosening (39.9%), infection (27.4%), instability (7.5%), periprosthetic fracture (4.7%), and arthrofibrosis (4.5%) (Sharkey et al., 2013). Even though TKA is an efficient procedure to treat patients with advanced osteoarthritis, it is not intended for younger patients due to the need for revision. Cartilage tissue engineering might aid to repair or regenerate cartilage tissue.

## 2.3 Cartilage Tissue Engineering

Tissue engineering involves the de- novo formation of a tissue by the combination of a porous biomaterial (scaffold), cells and bioactive factors (Hollister, 2005; Hutmacher, 2000). The biomaterial or scaffold provides a three- dimensional mechanical support on which the cells can grow into a geometrically defined structure. In the case of cartilage tissue engineering, a scaffold typically has the following requirements: i) degradation synchronized with chondrocytes ECM production; ii) bioactivity for chondrocyte attachment, migration and signaling; iii) suitable mechanical properties to withstand the harsh mechanical environment within the knee joint; and, iv) possess an interconnected porous structure to enable chondrocyte ingrowth, nutrient-and waste exchange (Nuernberger et al., 2011). Scaffolds can be produced by synthetic or natural materials. Synthetic materials have the advantage of more easily modifiable properties and reproducibility, but they often lack bioactivity. In contrast, natural materials inherently provide bioactivity (Lutolf and Hubbell, 2005). In the following sections, the use of decellularised matrices will be discussed. Furthermore, potential cell types and cell sources for cartilage tissue engineering will be elucidated.

### 2.3.1 Decellularised Articular Cartilage

Decellularised tissues are a particularly attractive material in tissue engineering due to their tissue-specific composition and environment which is still unmatched by synthetic materials. With decellularisation, cellular components are removed from tissues to use the remaining acellular ECM as a scaffold. It is commonly agreed that successful decellularisation is defined by the following criteria: no visible cell nuclei in histology staining, less than 50 ng dsDNA/mg dry tissue and a DNA fragment size of less than 200 base pairs (Crapo et al., 2011). It is crucial that all cellular material is carefully removed to avoid adverse effects for the patient (Keane et al., 2012). Apart from DNA, the oligosaccharide Gal $\alpha$ 1,3-Gal $\beta$ 1-4GlcNAc-R, also known as "Gal epitope" can cause adverse effects (Badylak and Gilbert, 2008). The gal epitope is only present in animal tissues and commonly causes immune-reactions in humans. It can be argued that for articular cartilage due to its avascular and alymphatic character (relatively immuno-privileged), the Gal epitope is not likely to trigger a severe immune-reaction (Bedi et al., 2010; Revell and Athanasiou, 2009). Nevertheless, to circumvent this issue the gal epitope can be removed from animal tissues by treatment with  $\alpha$ -galactosidase, which has previously shown to minimize reactions (Kevin R. Stone et al., 1998).

Decellularisation of articular cartilage is especially demanding, due to its high ECM density (average pore size: 6 nm (Maroudas, 1976)). Likewise cell ingrowth into its dense

ECM is very challenging. It was shown that whole articular cartilage could be decellularised by applying harsh protocols which usually involve many time-consuming steps (Bautista et al., 2016; Luo et al., 2015; Schneider et al., 2016; Yang et al., 2010). For cell infiltration, however, the porosity of articular cartilage requires enhancement, for example by introducing channels or by removing GAGs through enzymatic digestion (Bautista et al., 2016; Luo et al., 2015). Using these measures, the cell infiltration was still mostly limited to the surface of the scaffolds. Further porosity enhancement was achieved when articular cartilage was processed into particles or hydrogels which enabled a good infiltration (Beck et al., 2016; Cheng et al., 2009; Gawlitta et al., 2015; Ghosh et al., 2018; Rowland et al., 2016; Sutherland et al., 2015; Visser et al., 2015; Yang et al., 2008, 2010). Despite that processing lead to the destruction of articular cartilage's zonal structure, its tissue-specific composition has shown to produce a chondrogenic effect (either alone or in synergy with growth factors) (Blacker et al., 2018; Cheng et al., 2009; Ghosh et al., 2018; Luo et al., 2015; Rowland et al., 2013; Sutherland et al., 2015; Visser et al., 2015). It should be noted that the chondrogenic effect is likely depending on the decellularisation protocol. Thus, a systematic comparison of decellularisation protocols for articular cartilage has revealed protocol-dependent effects on the ECM that can either be advantageous or disadvantageous for the bioactivity (Schneider et al., 2016).

A summary of present decellularisation methods for articular cartilage and the corresponding studies can be found in Table 2.3. In all listed studies, a high biocompatibility of the resulting decellularised articular cartilage was found *in vitro* (Bottagisio et al., 2016; Burk et al., 2014; Deeken et al., 2011; Dong et al., 2015; Farnebo et al., 2014; Fermor et al., 2015; Roth et al., 2017; Schneider et al., 2016; Tiziana Martinello, 2014; Yang et al., 2013, 2010; Youngstrom et al., 2013). Nonetheless, only a few studies have evaluated the *in vivo* effect of the decellularised cartilage tissues (Blacker et al., 2018; Dong et al., 2015; Liu et al., 2017; Yang et al., 2008, 2010). For instance, a good biocompatibility of decellularised cartilage was found in BALB/C mice (Blacker et al., 2018). Another study observed an enhanced histological score of the forming neotissue when decellularised articular cartilage was seeded with MSCs in rabbits (Yang et al., 2010). It was further demonstrated that cartilage-like tissue has formed in nude mice (Kang et al., 2014; Yang et al., 2008).

Regardless of these promising results, all studies listed in Table 2.3 have inherent limitations. First, there is no common protocol for the decellularisation of articular cartilage. As a result of the diverse protocols, likewise the structure, mechanical properties and biocompatibility can be affected to a different extent. Optimization of the decellularisation protocol would, thus, be essential to minimize any negative effect on the ECM.

Secondly, the sterilization of the decellularised tissues was performed with various techniques such as ethylene oxide, 70% ethanol, peracetic acid and UV irradiation. Similar to the decellularisation protocol also the sterilization method should be carefully chosen, due to its reported effect on the mechanical properties of biomaterials (Freytes et al., 2008; Rosario et al., 2008; Sun and Leung, 2008). Milder techniques such as supercritical carbon dioxide can minimize the negative impact of sterilization (Bernhardt et al., 2015).

Finally, the biological tests on the decellularised matrices lacked uniformity. When comparing the studies, different cell types and rarely the tissue-specific cell type were used to examine the biological response of the decellularised tissues. For instance, mouse 3T3-cells were seeded in decellularised bovine osteochondral plugs to investigate their biocompatibility (Fermor et al., 2015). Similarly, the *in vivo* tests were performed in diverse animal models and focused on a multitude of biological responses, which were not consistent among studies. Yet, mostly favorable responses like tissue remodeling, improvement of histological score and bone and fibrocartilage formation could be described (Dong et al., 2015; Farnebo et al., 2014; Gawlitta et al., 2015; Lin et al., 2018; Liu et al., 2017; Yang et al., 2008, 2010).

Even though decellularised articular cartilage shows great potential, there still remains much to be investigated to translate it into a clinical application. Novel approaches should be developed to simplify and standardize the decellularisation of articular cartilage.

Table 2.3 Decellularisation and processing of articular cartilage into a scaffold.

Processing	Decellularisation method	Sterilization technique	Biological response	Study
Powder	Trypsin, Triton-X-100	70% EtOH	<i>in vitro</i> : hMSCs- chondrogenesis	Ghosh2018
Whole tissue	Freeze-thaw, detergent	N/A	<i>in vivo</i> : rabbits- promotes tissue regeneration	Lin2018
Whole tissue	Nucleases, osmotic shock, freeze-thaw, detergent	N/A	<i>in vitro</i> : human chondrocytes-chondrogenesis	Blacker2018
Whole tissue	SDS, enzymes	N/A	<i>in vivo</i> : BALB/C mice- immune response	Bautista2016
Whole tissue	Freeze-thaw	Peracetic acid	<i>in vitro</i> : hMSCs- cell penetration-100 um after 28 days	Schneider2016
Whole tissue	Freeze-thaw, osmotic shock, enzymes, nucleases,	Antibiotics	<i>in vitro</i> : ASCs-cytocompatibility	Luo2015
Whole tissue	Freeze-thaw, osmotic shock, SDS, nucleases,	Peracetic acid	<i>in vitro</i> : FPSCs-chondrogenic differentiation	Femor2015
Powder	Nucleases	Dehydrothermal treatment	<i>in vitro</i> : 3T3 cells-cytocompatibility	Rowland2016
Powder	Mechanical, enzymatic	Ethylene oxide	<i>in vitro</i> : hMSCs	Gawliita2015
Powder	Freeze-thaw, osmotic shock, Triton-X-100	N/A	<i>in vivo</i> : bone formation- 8 wks with hMSCs in rats	Sutherland2015
Powder	No decellularisation	Ethylene oxide	<i>in vitro</i> : MSCS- chondrogenesis	Rowland2013
Powder	Enzymes, nucleases, Triton-X-100	Ethylene oxide	<i>in vitro</i> : rabbit MSCS- cytocompatibility	Yang2010
Powder	No decellularisation	Ethylene oxide	<i>in vivo</i> : rabbits- significant improvement of histological score	Cheng2009
Powder	TritonX-100, osmotic shock, enzymes	60Co g irradiation (at 5 mrad)	<i>in vitro</i> : hASCs- chondrogenic differentiation	Yang2008
Hydrogel	Osmotic shock, detergent, enzymes	Ethylene oxide	<i>in vitro</i> : BMSCs; <i>in vivo</i> : nude mice- cartilage like tissue formed	Beck2016
Hydrogel	Triton X-100, sonication, nucleases	N/A	<i>in vitro</i> : rBMSCs- chondrogenic expression, matrix synthesis	Visser2015
			<i>in vitro</i> : MSCs- chondrogenesis	



### 2.3.2 Commercial Products

As previously explained, decellularised tissue matrices are attractive materials due to their inherent bioactivity, structure and mechanical properties. According to the current knowledge, Chondrofix® (ZimmerBioMet, USA) is the only product derived from decellularised human hyaline cartilage currently on the market. Chondrofix® is intended for osteochondral cartilage repair. The regeneration of articular cartilage with Chondrofix® was observed in a case study during a 25-months period (Reynolds and Bishai, 2014). During that time the Chondrofix® plug was completely integrated within the host tissue and showed no visible borders. In another study with 58 patients (age range: 18-59) and a follow-up of up to 28 months, a satisfactory activity level and function was observed (Long et al., 2016). The favorable healing response with Chondrofix® might be due to relevant mechanical properties (e.g., bone and cartilage compressive moduli), coefficient of friction and a comparable water content in regards to native articular cartilage (Gomoll, 2013). Despite these encouraging results, there is also evidence of delamination in several cases with the Chondrofix® implant (Degen et al., 2016). Furthermore, there are several limitations for the other two aforementioned Chondrofix® studies. First, the patient population was too small to draw statistically significant conclusions. Secondly, both studies were isolated case studies and lacked the confidence level of a randomized control study. Finally, the patient follow-up was too short (only 28 months) and should be increased to at least 5 years. Future studies with decellularised articular cartilage are necessary to evaluate the potential of those materials.

### 2.3.3 Cell Sources

The cell source plays a critical role for the success of cell-based therapies in cartilage repair. An ideal cell type for articular cartilage repair should produce a dense cartilage-specific ECM, be easily acquired, available in high numbers and be inducible towards the desired phenotype. The most frequently used cell source in cell-based cartilage repair are autologous chondrocytes (Martin et al., 2015). However alternative cell sources such as nasal septum, auricular and polydactyly chondrocytes have likewise shown promising results (Maehara et al., 2017; Mortazavi et al., 2017; Mumme et al., 2016; Wong et al., 2018). These cell types are illustrated in Figure 2.7. Furthermore, chondro-progenitor and stem cells have demonstrated their potential in cartilage repair. All aforementioned cell sources will be discussed in the sections below.

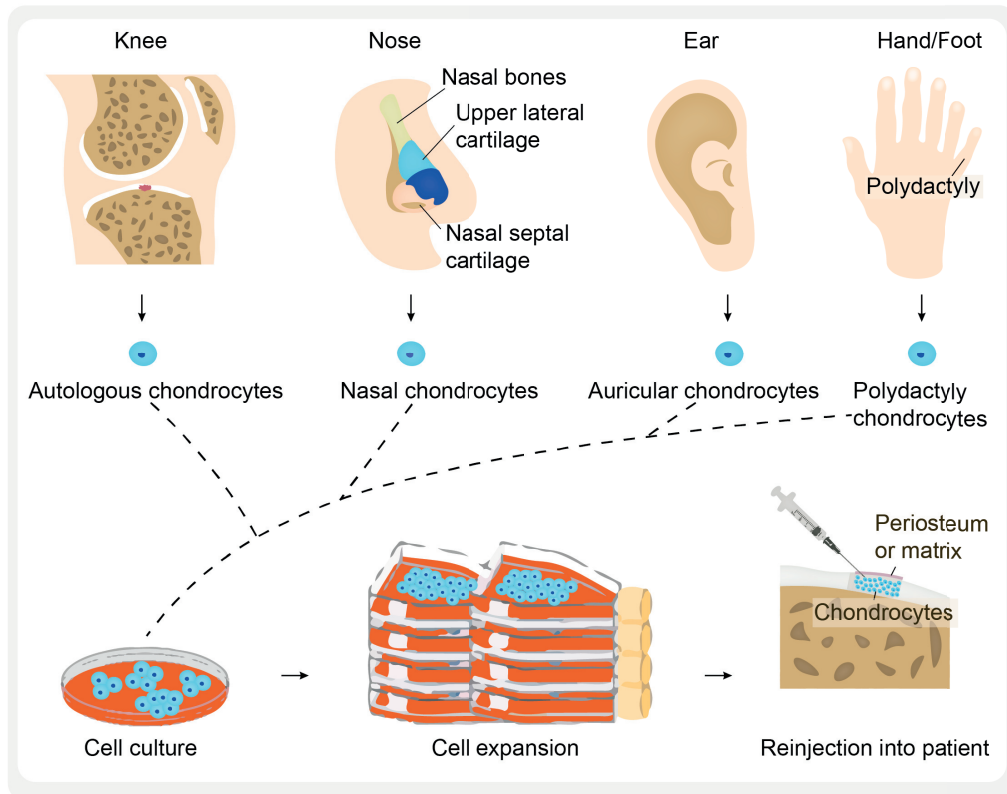


**Figure 2.7 Cell sources in cartilage tissue engineering.** Chondrocytes are commonly extracted from the knee, but recent alternatives also investigated nose-septum, chondral and polydactyly chondrocytes for articular cartilage repair.

### Autologous Knee Chondrocytes

Autologous knee chondrocytes are the most common cell type applied in present cartilage repair strategies. As previously described for the ACI procedure, autologous chondrocytes are extracted from a biopsy in a non-load bearing area of the patient's knee. Autologous chondrocytes minimize adverse immune reactions that might occur when using allogenic or xenogenic cell sources. However, it should be noted that articular cartilage is considered relatively immuno-privileged due to its avascularity and dense ECM (Bedi et al., 2010; Revell and Athanasiou, 2009). This low immunogenicity implies that allogenic or xenogenic cells might not induce an immune response in articular cartilage. The use of autologous chondrocytes has the advantage of their fully differentiated state, inherent ECM production and phenotypic stability. Their drawback is the low cell yield and the long culture time (up to several weeks) to produce a clinically relevant number of chondrocytes. Simultaneously,

the monolayer culture, required for cell expansion, causes de-differentiation into a more fibroblastic phenotype with more collagen type I and less collagen type II expression over time (Von Der Mark et al., 1977). Although, autologous chondrocytes can be re-differentiated when cultured in 3D, this would further complicate the procedure (Benya and Shaffer, 1982). Additionally, the extraction of autologous chondrocytes requires two surgical interventions, which increase the risk of adverse effects for the patient and make autologous cells less economically viable. Hence, there is an ongoing search for alternative cell sources.

### **Nasal Septum Chondrocytes**

Recently, very encouraging results were obtained by nasal septum chondrocytes in a clinical trial with 10 patients, showing significantly improved life-quality after 24-months (Mumme et al., 2016). Indeed, previous *in vitro* and *in vivo* experiments have emphasized the capacity of nasal septum chondrocytes. Thus, their chondrogenic potential was greater than the one of the frequently used knee-derived autologous chondrocytes (Kafienah et al., 2002). Additionally, nasal septum chondrocytes have the significant advantage to be independent of the donor's age (Rotter et al., 2002). When seeded in scaffolds *in vitro*, nasal septum chondrocytes increased the mechanical properties of the constructs after 2 weeks by producing GAGs and collagen type II (Farhadi et al., 2006). Moreover, nasal septum chondrocytes are mechano-responsive and thus increased the secretion of ECM molecules under physiological loading, even promoting the expression of lubricin (Candrian et al., 2008). Likewise, in past *in vivo* experiments in rabbits and mice, nasal septum chondrocytes produced ECM molecules and formed cartilage-like tissue (Vinatier et al., 2009). Even though the results are very encouraging, the aforementioned clinical study was performed in only 10 young patients with small defects. However, another study involving 108 patients is currently being performed, which will further evaluate the potential of these cells in articular cartilage repair (Onuora, 2016).

### **Auricular Chondrocytes**

Auricular chondrocytes have previously shown their potential in craniofacial and nasal augmentation and repair (Yanaga et al., 2006). Indeed, auricular chondrocytes, when seeded in biodegradable matrices, have produced mechanical properties which approach those of native auricular cartilage (Park et al., 2004). Lately, the potential of auricular chondrocytes for articular cartilage repair was evaluated. Thus, in a recent study, these cells demonstrated to produce molecules which are associated to articular chondrocytes (Wong et al.,

2018). Nonetheless, the available publications on articular cartilage repair with auricular chondrocytes are limited and future work is required to fully evaluate their potential.

### **Polydactyly Chondrocytes**

Another appealing cell source are polydactyly chondrocytes. Polydactyly patients have supernumerary fingers or toes, which are routinely removed at a young age. Their accessible extraction and derivation from young patients give them a huge potential. Compared to articular chondrocytes, polydactyly chondrocytes demonstrated a more rapid proliferation and produced thicker cell sheets (Maehara et al., 2017; Mortazavi et al., 2017). However, to date, there is still little published work on their use in articular cartilage repair. It would be interesting to evaluate their efficacy in future studies.

### **Stem Cells**

Besides the aforementioned, already differentiated cell types, stem cells offer a promising cell source in cartilage tissue engineering and regenerative medicine. Primarily, bone marrow derived mesenchymal stem cells have been investigated for articular cartilage repair (Martin et al., 2015; Nam et al., 2018). However, also adipose stem cells bear a great potential due to their assessibility (Zuk et al., 2002). In general, stem cells can be distinguished by their potency (totipotent, pluripotent, multipotent) as illustrated in Figure 2.8. For instance, embryonic stem cells are derived from the zygote or early Morula stage (3-4 days) and are totipotent. A cell is considered totipotent when it can develop any tissue type. Pluripotent cells are derived from the blastocyst stage (after 5-7 days) and can differentiate into any of the three germ-layers (ectoderm, mesoderm, endoderm). A multipotent cell can form specific types of cells. For example, mesenchymal stem cells are derived from the bone marrow, are multipotent and can form osteoblasts (bone cells), chondrocytes (cartilage cells), myocytes (muscle cells) and adipocytes (fat cells which give rise to adipose tissue). The following paragraphs will focus on the potential of bone marrow derived mesenchymal stem cells (MSCs) and adipose stem cells in articular cartilage repair.

Bone marrow derived MSCs are a promising cell source for clinical use in articular cartilage regeneration. The extraction of MSCs from the bone marrow is relatively simple and following extraction, MSCs can be readily expanded and stored in cell banks (Koga et al., 2009; Pittenger, 1999; Simonsen et al., 2002). Bone marrow derived MSCs have also demonstrated potential in osteochondral repair, due to their ability to differentiate into cartilage and bone (de Vries-van Melle et al., 2014; Quarto et al., 2001; Wakitani et al., 2002). However, the chondro-differentiation leads to a hypertrophic and fibrous phenotype (Pelttari

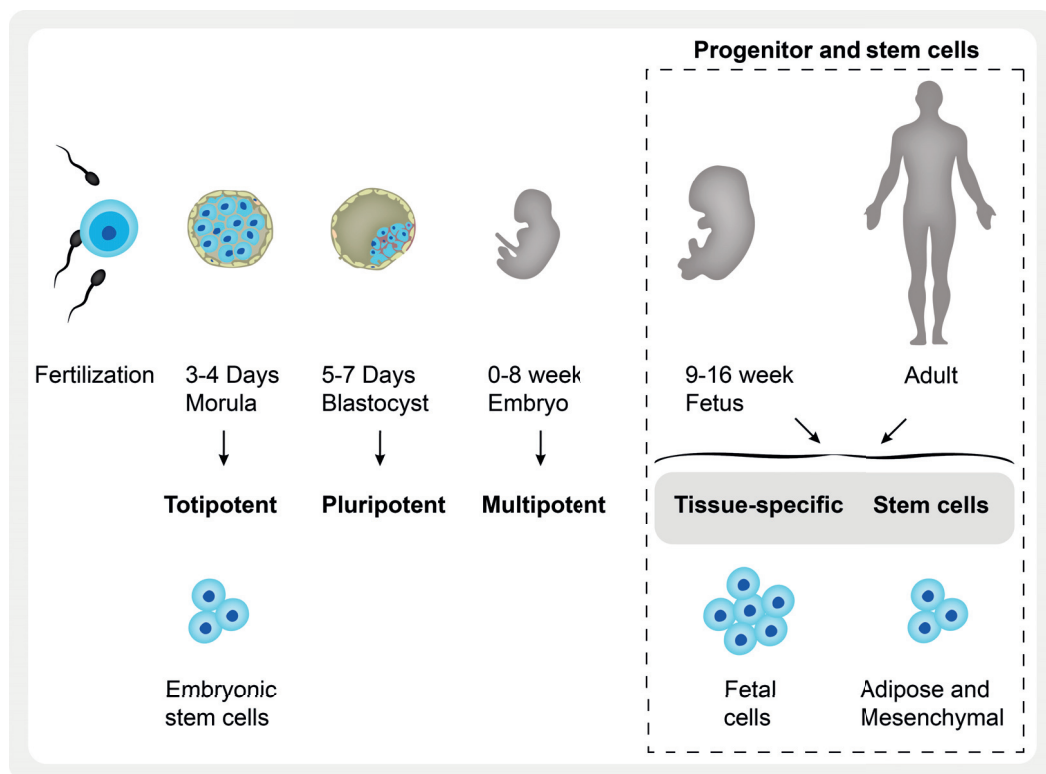


**Figure 2.8 Progenitor and stem cells in cartilage tissue engineering.** Time line and explanation for the extraction of stem and progenitor cells. Stem cells are usually pluripotent or multipotent, whereas progenitor and adult cells are tissue-specific. In articular cartilage repair commonly bone-marrow derived mesenchymal and adipose stem cells are used. Embryonic stem cells are illustrated to explain the relation of cell potency.

et al., 2006). Despite the presence of this issue, the regeneration of articular cartilage with bone marrow derived MSCs has been demonstrated in several human case studies. In a study with 72 patients, autologous chondrocytes were compared to MSCs in ACI treatment (Nejadnik et al., 2010). There was no significant difference between the repair with the autologous chondrocytes or the MSCs. However, the use of MSCs as cell source is less expensive than autologous chondrocytes since the surgery can be performed in a single-step procedure. The cost-effectiveness and reduction of surgical interventions make MSCs a valuable cell source for cartilage tissue engineering. Nonetheless, the extraction of bone marrow has an inherent risk for the patient and is very painful.

Therefore, deriving multipotent stem cells from adipose tissues would be a good alternative (Zuk et al., 2002). Adipose stem cells can simply be extracted from human lipoaspirates and thus provide minimally invasive access to multipotent stem cells. Just like bone marrow-derived MSCs, adipose stem cells can differentiate toward the osteogenic, adipogenic, myo-

genic, and chondrogenic lineages, but with the advantage of simple assessability and omitting the more invasive procedure for the patient compared to bone marrow extraction.

However, regarding articular cartilage repair, a variety of results with adipose derived stem cells ranging from good to mediocre were obtained. For instance, in a study of Park and colleagues performed in rats, superior formation of hyaline cartilage was observed with bone marrow and synovium derived stem cells compared to adipose stem cells (Park et al., 2006). The same effect was confirmed by a study of Koga and colleagues, which demonstrated that synovium and bone marrow derived stem cells induced a superior healing response compared to MSCs derived from skeletal muscle or adipose tissue (Koga et al., 2008). At the same time, there are concerns about the safety of bone marrow derived MSCs and adipose stem cells due their multipotency. Future studies, thus, have to demonstrate the safety of these cells and systematically compare the clinical outcome to autologous chondrocytes.

### **Chondro-Progenitor Cells**

Chondro-progenitor cells have proven to be a stable cell source for articular cartilage repair with less concerns about safety than for bone marrow derived MSCs or adipose stem cells. Indeed, fetal progenitor cells in cartilage, also called "epiphyseal chondro-progenitor cells (ECPs)", have demonstrated a high proliferation rate and remarkable phenotypic stability (Darwiche et al., 2012; Studer et al., 2017). The advantage of ECPs in cartilage repair is their predefined differentiation potential, which omits the use of specific growth factors or culture conditions to direct differentiation. Furthermore, a cell bank of ECPs was established in Switzerland, making ECPs a readily available off-the-shelf cell source (Applegate et al., 2009, 2013; Quintin et al., 2007). This cell bank has a significant clinical advantage due to its single-donor origin, thus, ensuring safety and reproducibility. Future clinical studies should further evaluate the potential of ECPs in articular cartilage repair.

# Chapter 3

## Research Question

### 3.1 Background

The major drawback of current clinical treatments for articular cartilage such as ACI and MACI is that they can only create fibrocartilage or a mixture of fibro- and hyaline cartilage (Brun et al., 2008; Oussedik et al., 2015). Fibrocartilage, in contrast to native hyaline cartilage, presents inferior mechanical properties and therefore degrades much faster than hyaline cartilage (Mankin, 1974). This is in agreement with the observation that pure hyaline cartilage is correlated to good to excellent clinical results (mainly collagen type II) compared to fibrocartilage (Peterson et al., 2000). For successful and long-lasting cartilage regeneration, it would be essential to have a treatment that can create hyaline cartilage. It was previously hypothesized that one possibility to engineer pure hyaline cartilage is the production of scaffolds which mimic the mechanical properties and zonal structure of native cartilage (Klein et al., 2009; Levett et al., 2014; Tatman et al., 2015). An attractive material for the fabrication of those scaffolds would be decellularised articular cartilage that is able to support chondrogenesis even without additional growth factors (Cheng et al., 2009, 2011; Ghosh et al., 2018).

### 3.2 Objectives

This project aims at developing scaffolds based on decellularised articular cartilage with tailorable mechanical properties that can induce zonal lineage commitment in chondroprogenitors without the use of other stimuli. The mechanical properties of the scaffolds should be adapted to match those of the cartilage zones and induce zone specific cell behavior. The four specific aims to realize the overall goal are summarized in Figure 3.1.

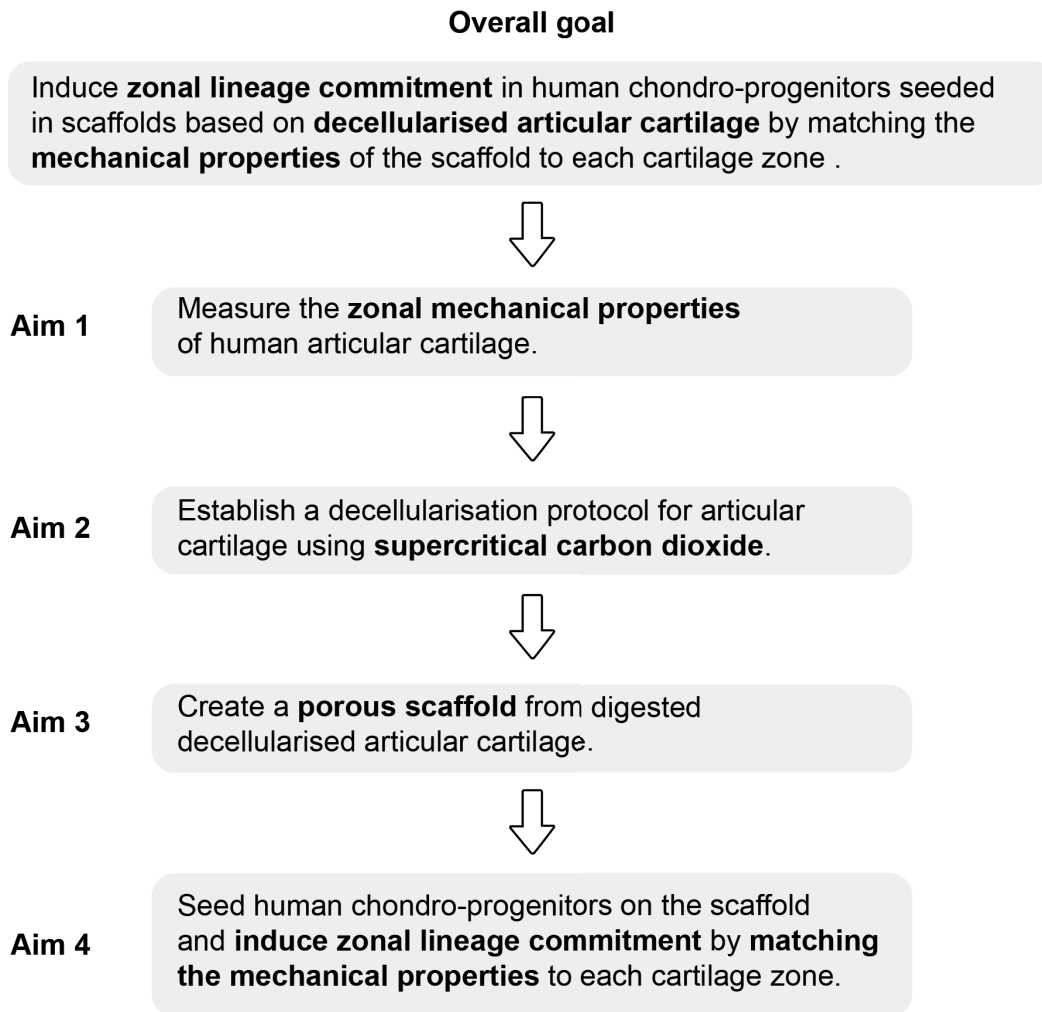


**Figure 3.1 Objectives and specific aims.**

### 3.2.1 Aim 1

As no reliable data for human tissues is available in the literature, the first aim is to measure the mechanical properties of the zones in human articular cartilage by instrumented indentation (**chapter four**). Histology will be used to carefully validate the quality of the human tissues, which are derived from surgical procedures. The information of this study will later be important to define the mechanical properties of the developed scaffold.

### 3.2.2 Aim 2

The second aim is the development of an alternative decellularisation technique for bovine articular cartilage intending to overcome the limitations of existing complex and time-



consuming protocols (**chapter five**). Common decellularisation protocols consist of lengthy tissue-specific protocols combining chemical and physical methods which can negatively influence the bioactivity of the decellularised tissue (Crapo et al., 2011). Thus, a novel decellularisation technique based on supercritical carbon dioxide and a CO<sub>2</sub>-philic detergent should be developed. Supercritical carbon dioxide has liquid-like density and gas-like transport properties and could therefore enhance both diffusion and cell removal in articular cartilage compared to existing decellularisation protocols (Schneider, 1978). Further, due to its reported application as sterilization technique, supercritical carbon dioxide has the potential to include decellularisation and sterilization in a single-step procedure (Bernhardt et al., 2015).

### 3.2.3 Aim 3+4

The third aim is to fabricate porous scaffolds from the dense decellularised articular cartilage with tailorable mechanical properties (**chapter six**). Enhancing the porosity of articular cartilage is necessary to enable cell ingrowth. This is important for aim four, the seeding with human chondro-progenitors, which should induce a zone-specific cell behavior in the scaffolds without additional growth factors. Therefore, the mechanical properties of the scaffold material will be adjusted by changing the digest and EDC/NHS crosslinker concentrations. Implementing a scaffold based on decellularised cartilage with zone-specific mechanical properties might lead to the formation of a more functional and hyaline-like neotissue together with ACI and MACI treatments.

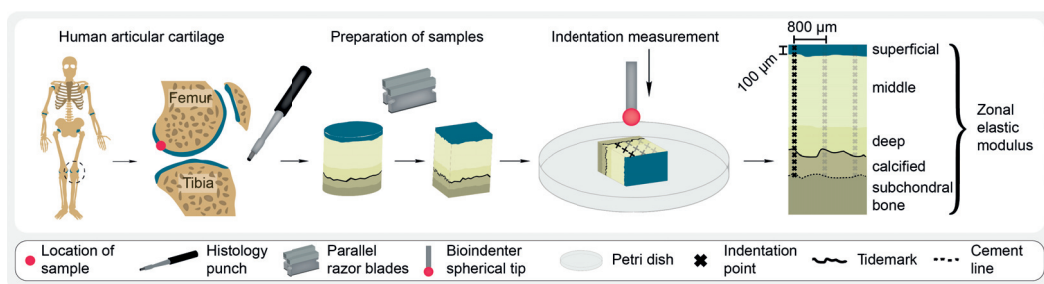


# Chapter 4

## Zonal Mechanical Properties of Human Articular Cartilage

*This chapter is based on the following publication: Antons, J., Marascio, M.G.M., Nohava, J., Martin, R., Applegate, L.A., Bourban, P.E. and Pioletti, D.P., 2018. Zone-dependent mechanical properties of human articular cartilage obtained by indentation measurements. Journal of Materials Science: Materials in Medicine, 29(5), p.57. The first author contributed to the writing of the manuscript, measurements and histological analysis.*

### 4.1 Graphical Abstract



### 4.2 Abstract

Emerging 3D printing technology permits innovative approaches to manufacture cartilage scaffolds associated with layer-by-layer mechanical property adaptation. However, information about gradients of mechanical properties in human articular cartilage is limited.

In this study, we quantified a zone-dependent change of local elastic modulus of human femoral condyle cartilage by using an instrumented indentation technique. From the cartilage superficial zone towards the calcified layer, a gradient of elastic modulus values between  $0.020 \pm 0.003$  MPa and  $6.44 \pm 1.02$  MPa was measured. To validate the tissue quality, the histological tissue composition was visualized by glycosaminoglycan and collagen staining. This work aims to introduce a new protocol to investigate the zone-dependent mechanical properties of graded structures, such as human articular cartilage. From this knowledge, better cartilage repair strategies could be tailored in the future.

**Keywords:** instrumented indentation, bioindentation, articular cartilage, mechanical property gradient

### 4.3 Introduction

For functional tissue engineering, scaffolds should present appropriate mechanical strength to support loading after implantation (Guilak et al., 2001) and therefore the mechanical properties of the scaffold need to match the target tissue (Hutmacher, 2000). Fabrication of such a scaffold can be complex because most tissues are not homogeneous and possess varying mechanical properties throughout their structure. With the emerging 3D printing technologies, such as biofabrication (Mouser et al., 2016; Visser et al., 2013; Zadpoor and Malda, 2016), melt electrospinning writing (Brown et al., 2011, 2015; Dalton et al., 2008) and fused deposition moulding (Chia and Wu, 2015; Zein et al., 2002), scaffolds could be produced with local mechanical properties mimicking those of tissues to be replaced.

Articular cartilage is one of these inhomogeneous tissues in which mechanical properties change steeply depending on tissue depth. The gradient of elastic modulus in cartilage is caused by the variation of tissue composition (Jeon et al., 2010; Mow et al., 1991). Depending on depth, four cartilage zones are distinguished (Temenoff and Mikos, 2000): a) superficial zone (10-20%); b) middle zone (40-60%); c) deep zone (20-50%); and d) calcified zone (schematic found in Fig. 4.1). The interface between deep zone and calcified zone is the tidemark, whereas the interface between calcified zone and subchondral bone is called cement line. The zones can be described as their proportion of the overall tissue depth in percentage (Athanasίου et al., 2009).

The zones differ on the one hand by their composition with glycosaminoglycan (GAG) and collagen (COL) content and on the other hand by collagen fiber orientation and cell density (Kempson et al., 1968; Muir et al., 1970; Stockwell, 1967).

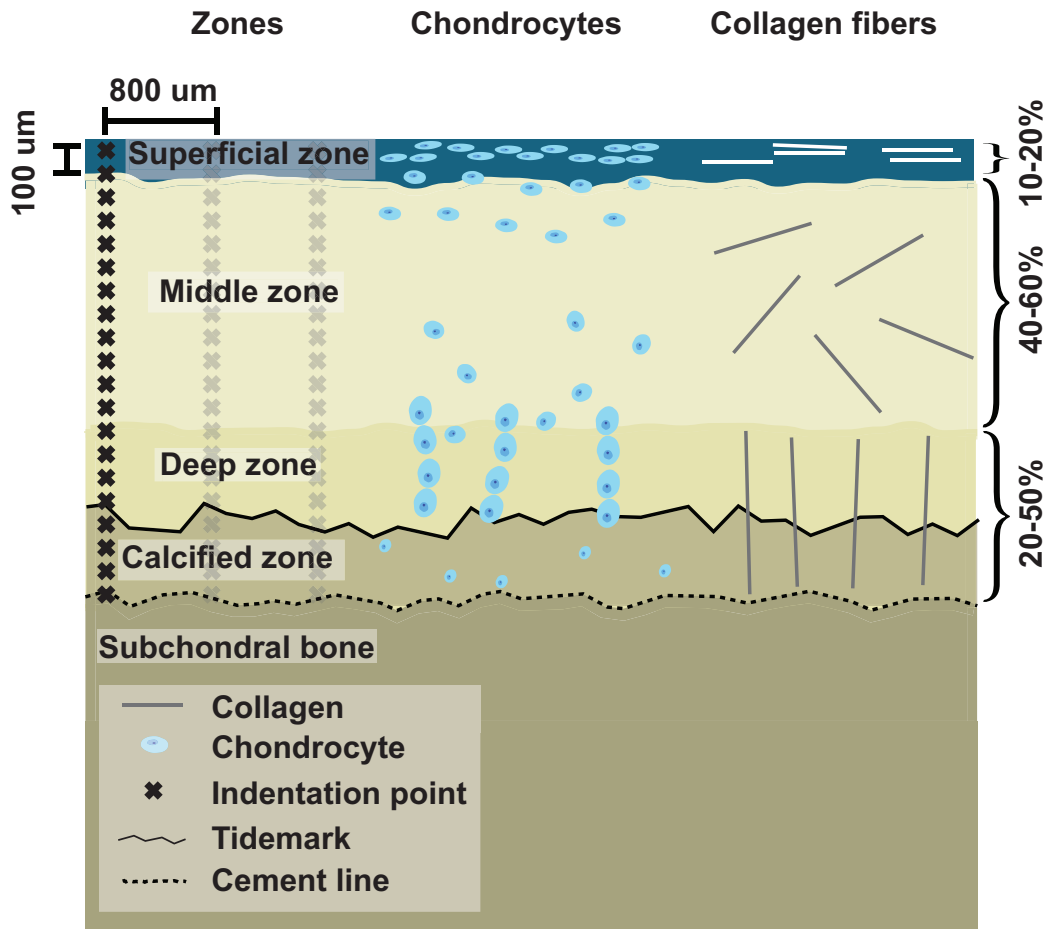


**Figure 4.1 Zonal structure and indentation protocol.**

Although the mechanical properties of cartilage have been extensively studied, the majority of the studies focussed on the bulk properties measured from the top of the tissue (i.e. (Armstrong and Mow, 1982; Laasanen et al., 2003; Mow et al., 1984)). Only a few studies have characterized the local mechanical properties in the different zones of articular cartilage (Ebenstein et al., 2011; Franke et al., 2007, 2011). In other studies different techniques were used including atomic force microscopy (Tomkoria et al., 2004) or specialized compression setups (Chen et al., 2001b) to determine the zonal properties. However, the stress applied was averaged on full thickness specimens, producing only a partial estimation of zonal cartilage mechanic response.

The scarcity of data on zonal mechanical properties in human cartilage could be explained by the technical difficulty of these kinds of measurements. To overcome this difficulty, nanoindenters exploiting a small tip to perform local indentations were adapted to measure mechanical properties of soft materials (Eberwein et al., 2014; Swain et al., 2017). Compared to atomic force microscopy, nanoindentation offers a quicker way to estimate the local

mesoproperties (e.g. the local mechanical properties of the indented layer). This allows us collecting a larger ensemble of measurements in a larger area, describing more efficiently the zonal stiffness dependency.

The objective of the present study was to measure the zone-dependent elastic modulus of human cartilage tissue with a newly developed instrumented indentation technique to provide target values for future scaffold designs in tissue engineering. The meso-scale measurements (every 100  $\mu\text{m}$ ) are within the resolution of modern 3D printers, which can then adapt the scaffold properties layer-by-layer.

## 4.4 Materials and Methods

### 4.4.1 Human cartilage origin and preparation

Osteochondral plugs (diameter 8 mm) were harvested from the medial posterior femoral condyle of six donors (Table 4.1).

**Table 4.1 Human articular cartilage samples with donor's age and osteoarthritis grade (Collins grade).**

Donor	Age	Sex	Condition	Collins grade (I-IV)
1	62	f	osteoarthritis	II
2	63	m	osteoarthritis	II
3	58	m	osteoarthritis	II
4	50	f	osteoarthritis	II
5	19	m	osteoochondritis dissecans	-
6	20	m	osteoochondritis dissecans	-

Tissues were obtained from the DAL/CHUV biobank (Lausanne), under anonymous donation, in accordance with its regulation and approval by the Institutional Biobank. Donors 1-4 had an osteoarthritis severity grade II according to the Collins grade (Collins, 1949), whereas donors 5-6 were young patients having osteochondritis dissecans. The osteoarthritis stage and disease evaluations were performed by an experienced knee surgeon. Plugs were taken from visually intact regions without damage from the surgical procedure. The cartilage plugs were cut with a cutting guide using two parallel razor blades with an inter-blade distance of 3 mm to obtain flat cartilage surfaces. The remaining tissue was used for histological analysis. For the instrumented indentation measurements, the sample was glued onto a 35 mm petri dish with the cross-section facing the indenter using a small drop of instant adhesive (Loctite 401, Henkel, Germany). Samples were frozen at  $-20^{\circ}\text{C}$  and stored until

further use. Before the measurement, the sample was thawed for 2 hours in phosphate buffered saline solution at 22°C. The sample was completely immersed in saline solution supplemented with 1% pentamycin/streptomycin to preserve hydration of the tissue and to avoid degradation during the measurements. Under these conditions it was previously demonstrated that the mechanical properties of articular cartilage are not influenced by one freeze/ thaw cycle (Szarko et al., 2010).

#### 4.4.2 Indentation measurements

The indentation tests were performed by a specifically developed indenter (Bioindenter™, Anton Paar, Peseux, Switzerland). This indenter was adapted to measure the mechanical properties of soft materials. All indentation tests were implemented in displacement control mode using a spherical indenter tip (diameter 500  $\mu\text{m}$ ) made of ruby. The maximum depth of 20  $\mu\text{m}$  was attained at a displacement rate of 120  $\mu\text{m}/\text{min}$ . The loading was followed by a 30 s hold-time and 120  $\mu\text{m}/\text{min}$  unloading rate leading to a relaxation response (Fig. 4.2).

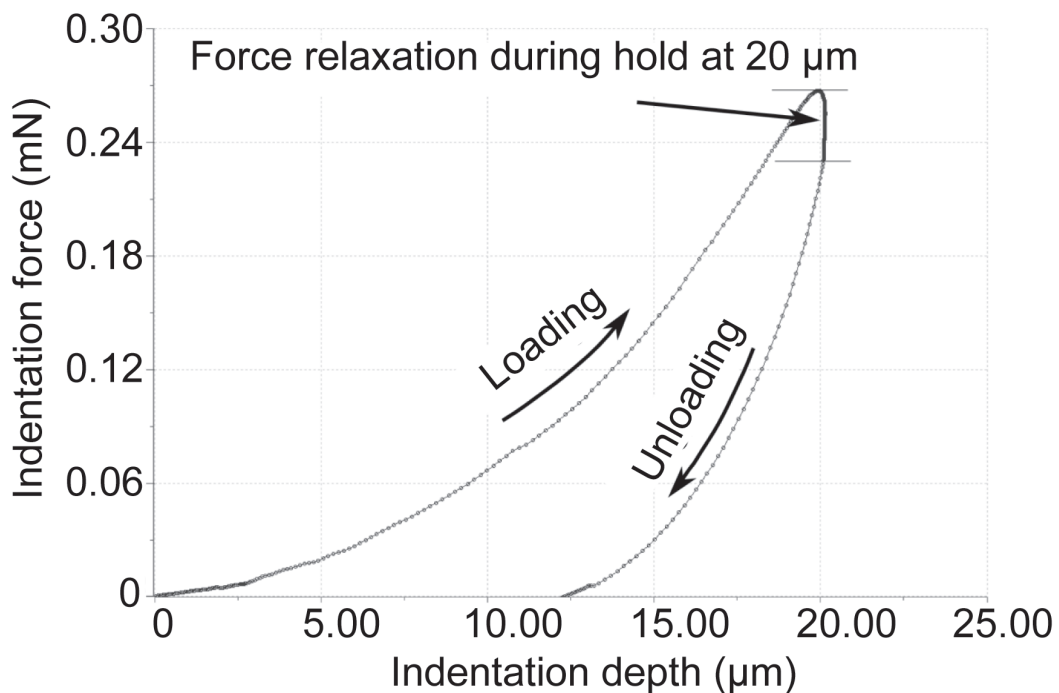


**Figure 4.2 Example of indentation measurement.** Indentation was performed on donor 4, Indentation 17.

The final objective of such measurements is to reproduce the progressive stiffening by additive manufacturing (AM). In particular, Fused Deposition Modelling / Fused Filament Fabrication (FDM/FFF) was selected as method of choice among the AM technologies. By

FDM/FFF, features up to 50-200  $\mu\text{m}$  can be reproduced in z-direction (Wang et al., 2017b). Therefore, an indentation pace of 100  $\mu\text{m}$  was defined to match the manufacturing limits. The first indentation was performed 100  $\mu\text{m}$  from the superficial zone towards the bone as indicated in Fig. 4.1. Subsequently, a line consisting of 11-40 indentations, spaced by 100  $\mu\text{m}$  was performed on cross-sectioned cartilage towards the bone. Three parallel indentation lines with a gap of 800  $\mu\text{m}$  were measured. A typical indentation measurement on articular cartilage is illustrated in Fig. 4.2. The relaxation behaviour of articular cartilage during the 30 s hold-time is shown in Fig. 4.3.

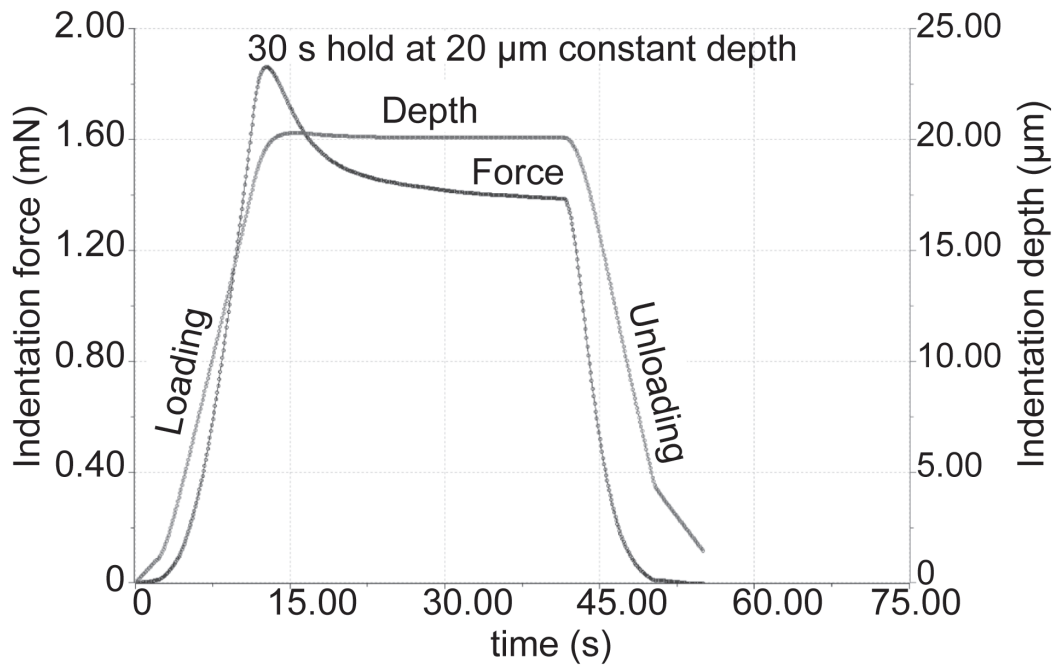


**Figure 4.3 Relaxation response of human femoral condyle cartilage.** Example of indentation at 120  $\mu\text{m/s}$  loading rate, 30 s hold and 120  $\mu\text{m/s}$  unloading rate.

The elastic modulus was calculated according to Hertz's model for contact of a sphere with a flat surface by fitting the loading curve (Fig. 4.4) by Eq. 4.1 (modified from (Last et al., 2009)):

$$F = \frac{4}{3} \times E_r \sqrt{R} \times (h_{offset})^{\frac{3}{2}} \quad (4.1)$$

In Eq. 4.1  $h$  is the indentation depth,  $R$  is the radius of the indenter,  $E_r$  is the reduced elastic modulus and  $F$  is the maximum load during the indentation. The  $h_{offset}$  accounts for the initial establishment of “soft” contact that resulted from small local irregularities (unevenness) of the surface. An example of this initial phase of contact establishment is shown in Fig. 4.4.



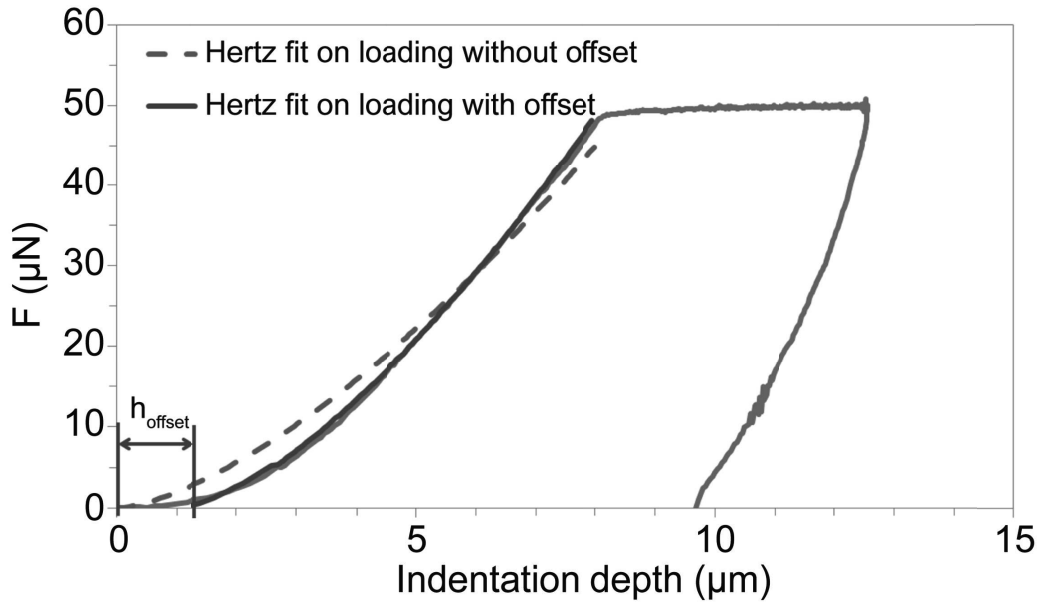


**Figure 4.4** Two indentation curves of the initial phase of contact without and with offset to correct for tissue surface irregularities.

Since this initial phase of contact is not representing the properties of the cartilage tissue, it was decided to fit the loading portion of the indentation curve after the correction  $h_{offset}$ .  $H_{offset}$  is the distance required by the indenter to establish reliable “soft” contact and can be indicated by rapid increase in the force-distance curve.

Linearized fit of the loading portion of the indentation curve was done using Eq. 4.1 with proprietary Indentation software (Anton Paar, Indentation V7.3.9, Peseux, Switzerland), where  $h_{offset}$  is representing the initial phase of ‘soft’ contact (i.e. not representing the tested tissue).

### 4.4.3 Relative depth

The relative depth of the cartilage was determined by normalizing the cartilage thickness of the sample to the indentation point. The start of the cartilage superficial layer is 0% and the start of the tidemark is 100%. The cartilage thickness was measured from the histological section at five randomly chosen points from the cartilage surface to the tidemark with Image J (version 1.48v) and subsequently averaged. Zones are defined according to their relative proportion as stated in the literature (Athanasίου et al., 2009). The superficial zone has a relative proportion between 10-20%, the middle zone with 40-60% and the deep zone at

20-50%. The precise localization of the cartilage zones is therefore challenging and the indication in Fig. 4.5 serves as an estimate.

#### 4.4.4 Histology

The samples were fixed in 4% paraformaldehyde at 22°C overnight. Thereafter, the bone was decalcified by a solution consisting of 20% Tri-sodium citrate in acetic acid for 48 hours at 22°C. This was followed by dehydration in ethanol and embedding into paraffin following standard histological protocols. Sections with a thickness of 5  $\mu\text{m}$  were cut with a microtome and stained for standard Hematoxylin and Eosin (H&E), for sulphated GAGs with Alcian Blue staining (Sigma-Aldrich, Buchs, Switzerland) and for COL with Picrosirius Red staining (Sigma-Aldrich, Buchs, Switzerland). The histological sections were analysed with a Leica DM5500 (Wetzlar, Germany) microscope. A tile scan for measurements and images was performed with the 5x magnification including an automatic stitching of the images. The close up image was taken at 20x magnification.

#### 4.4.5 Quantification of histology sections

The cell count was determined by acquiring images in 10 randomly selected regions of each sample in 20x magnification (539.35 x 404.51  $\mu\text{m}$ ), counting the cells manually supported by ImageJ (version 1.48v) and its plugin CellCounter.

### 4.5 Results

#### 4.5.1 Indentation measurements

In all cartilage samples, the indentation measurements highlighted a gradient of elastic modulus with an increase of values from  $0.020 \pm 0.003$  MPa at the cartilage superficial zone to  $6.44 \pm 1.02$  MPa at the calcified layer (Fig. 4.5). The gradient intensity deviated between the six donors, but showed the same common tendency.

All samples were normalized to their relative depth (distance between cartilage superficial layer and tidemark) to account for different thicknesses. Donor one and three were not measured up to the tidemark due to a fixed number of indentations in the indentation protocol.

**Table 4.2 Quantification of histological staining.**

	<b>Patient 1</b>	<b>Patient 2</b>	<b>Patient 3</b>	<b>Patient 4</b>	<b>Patient 5</b>	<b>Patient 6</b>
<b>Thickness (<math>\mu\text{m}</math>)</b>	2512.80 $\pm$ 48.29	1966.40 $\pm$ 58.3	2593.00 $\pm$ 74.64	1484.00 $\pm$ 75.23	2686.00 $\pm$ 65.34	3624.40 $\pm$ 164.11
<b>Cell count</b>	36.90 $\pm$ 5.41	47.20 $\pm$ 10.51	40.20 $\pm$ 10.02	44.70 $\pm$ 11.19	32.70 $\pm$ 7.53	26.77 $\pm$ 9.27

### 4.5.2 Histological evaluation

The cell distribution and cell shape in the human cartilage tissue visually corresponded to healthy cartilage and thus confirmed the quality within the harvesting site (Fig. 4.6 A). The intensity of Alcian Blue (AB) staining and thus the GAG content increased with depth from the cartilage superficial layer towards the tidemark (Fig. 4.6 B). A low intensity (L) AB staining was observed at the cartilage surface, whereas towards the calcified layer the staining intensity increased (H). The GAG content was in general lower in the superficial zone, increased with depth in the middle layer and decreased in the deep layer towards the tidemark. High GAG content was additionally visible in close contact to the chondrocytes themselves (Fig. 4.6 F), interpreted as continuous GAG synthesis of intact chondrocytes in the osteoarthritis affected cartilage. In Picrosirius Red staining (SR), the staining for collagen, the trend was inversed indicating a high (H) intensity staining at the surface and lower intensity (L) towards the calcified layer. For SR the staining intensity was high at the surface and decreased towards the calcified layer (Fig. 4.6 C). Concerning the collagen content, the superficial layer showed a mild fibrillation and degeneration of collagen fibres (Fig. 4.6 G), but a stable portion of the cartilage matrix in the middle layer and a decrease in the deep layer towards the tidemark. The collagen fiber orientation was visualized under polarized light. The parallel orientation of the collagen fibers in the superficial layer was evidenced by the different color under polarized light (Fig. 4.6 D,H). Moreover, the thickness of the articular cartilage layer and cell count was measured (Table 4.2). The average cell count was very similar for all samples ranging from  $32.70 \pm 7.53$  to  $47.2 \pm 10.51$  cells. The thickness of the articular cartilage ranged from  $1484.00 \pm 75.23 \mu\text{m}$  to  $3624.40 \pm 164.11 \mu\text{m}$  between patients.

## 4.6 Discussion

Only a few studies have characterized the mechanical properties in the different zones of articular cartilage and most of these studies focus on animal samples (Chen et al., 2001b;

Tomkoria et al., 2004). In addition, the limitations in previous studies are pre-treatments of the samples by paraformaldehyde (fixation), ethanol (dehydration) or embedding (PMMA) before the measurement (Campbell et al., 2012; Gupta et al., 2005). These pre-treatments change the mechanical properties of the samples. The novelty of the present work is the zonal measurement of six human articular cartilage samples by instrumented indentation in wet condition without any pre-treatment. The measured local elastic modulus was then compared to the local tissue composition obtained by histological staining.

We successfully measured zonal elastic modulus of human femoral condyle cartilage using nanoindentation and found that elastic modulus increased with depth. This work compares well to previous work of other studies where the zonal properties of human articular cartilage were inferred from bulk compression measurements (Chen et al., 2001b). Indeed, in this mentioned study, an increasing gradient of elastic modulus with increasing depth was also found. Moreover, although their measurements were performed on the cartilage of the femoral head, the range of elastic modulus was comparable to our results. They reported an equilibrium confined compression modulus between  $1.16 \pm 0.20$  MPa in the cartilage superficial layer to  $7.75 \pm 1.45$  MPa in the deep layer while we measured between  $0.020 \pm 0.003$  MPa and  $6.44 \pm 1.02$  MPa from cartilage superficial zone towards the calcified layer by nanoindentation. Even though our measurements were performed on the cartilage cross-section we hypothesize that the elastic modulus should be very similar to measurements from the top. Our hypothesis is based on a previous study which discovered that measuring local mechanical properties by atomic force microscopy from the cross-section or the top of porcine articular cartilage samples made a difference of up to 20% in elastic modulus (superficial: 20% lower, middle: 14% lower, deep: no difference) (McLeod et al., 2013). In contrast to our study, they observed a decreasing elastic modulus towards the deeper zones of articular cartilage. This could be due to the different length scale in which they measured since indentations were performed with a diameter of  $5 \mu\text{m}$  tip in small regions of  $20 \mu\text{m} \times 20 \mu\text{m}$ , whereas our measurements were in the meso-scale performed with  $500 \mu\text{m}$  diameter tip and  $100 \mu\text{m}$  distance between indentations. Another reason for the gradient difference could be that they measured on porcine instead of human articular cartilage.

To validate the quality of the human cartilage tissue, we assessed the zone-dependent GAG and COL content by histochemical analysis (Fig. 4.6) (Alcian Blue and Picrosirius Red). The GAG and COL content of the samples changed according to depth. The collagen portion of the matrix remained stable in all samples while the GAG content varied from low in the superficial layer to high in the middle layer and lowered again towards the calcified layer.

The collagen fibers are responsible for the tensile properties of cartilage (Kempson et al., 1968) and have shown to only have little effect on the compressive properties. Nevertheless, it has been demonstrated that collagen fibers could indicate tissue quality and onset of osteoarthritis (Hollander et al., 1995). Since we have observed a mild fibrillation of collagen in the superficial layer, this might indicate a degeneration in the samples, but mostly in the superficial layer.

We observed that GAG content increased from the superficial zone towards the middle zone and diminished between middle and deep zone, whereas at the same time elastic modulus increased from the superficial zone towards the subchondral bone. The increase in elastic modulus between middle and deep zone was thus not solely caused by the GAG content. We assume that the elastic modulus increase in the deep zone might have been due to a higher collagen content and collagen fiber diameter in the deep zone (Muir et al., 1970). The same assumption for the deep layer of articular cartilage has already been made in another study in which zonal mechanical properties were measured (Chen et al., 2001b). In general, special care should be taken when measuring heterogeneous materials with significant modulus heterogeneity with indentation (such as at the cartilage-bone interface). It has previously been demonstrated that in the case of a significant material heterogeneity the indenter size should be less than 10% of the expected length scale of modulus changes in order to obtain correct results (Armitage and Oyen, 2017). The measurements in the present work were focussed on the articular cartilage zones and not on the subchondral bone. Thus, the criterion of having an indenter size of less than 10% of the expected length scale of modulus does not necessarily have to be followed for our measurements since a difference in the order of 2 in magnitude of elastic modulus is not given.

Even though the mechanical gradient was comparable to existing measurements, some aspects and limitations of the technique used here should be considered. Due to its nature of testing relatively small areas (around 200  $\mu\text{m}$  diameter) instrumented indentation is quite sensitive to local differences and hence to sample degradation, sample preparation, and the surrounding environment. An approximation of the area involved in the indentation response can be done via contact radius. For elastic spherical indentation the contact radius  $a$  is  $\approx R\sqrt{h}$  where  $R$  is the radius of the indenter and  $h$  is the indentation depth. For this study this corresponds to a contact radius of  $\approx 100 \mu\text{m}$ . We chose a contact area of 100  $\mu\text{m}$  and a space between indentation points of 100  $\mu\text{m}$  to get a full coverage of all zones and a maximum of information about the zonal properties. We assume that the cartilage deformation is only elastic (i.e. it fully recovers after unloading) as we found very similar results when performing two consecutive measurements on the same spot.

The measurement of the superficial zone is particularly challenging since the indentation is near the edge and edge-effects could introduce artifacts into the measurements (Jakes et al., 2009; Jakes and Stone, 2011). This can be partially overcome by indentation from the top surface. However, indenting from the top surface would only help measuring the local bulk properties of the tissue (e.g. the average properties of all the layers). Separate measurements of previously dissected layers should be difficult, because according to the Mow model (Mow et al., 1989), the measured cartilage properties are dependent on the cartilage thickness and the underlying substrate. The local character of the instrumented indentation method used in this work might explain the standard deviation for the measurements in supplemental data (Fig. 4.7). For each patient three indentation lines were performed and averaged. These parallel lines were spaced by 800  $\mu\text{m}$ . It is possible that the chosen distance between the indentation lines was too large and the elastic modulus in the adjacent lines already changed due to different structure or composition. For a better comparison between samples we normalized the depth to the distance between cartilage surface layer and calcified layer. Unfortunately, not all samples were measured up to the calcified layer. This was due to the fixed indentation procedure which did not account for different thicknesses of the cartilage. However, the same common trend (i.e. increase of elastic modulus towards the bone) can be observed in all samples. The sample degradation, the age of the donor, the disease state or the site in which the sample was harvested could also influence the measurement. Although we took care to include only visually intact cartilage in this study, it is virtually impossible to exclude degradation of the microstructure especially on the surface. It was also difficult to harvest the samples from precisely the same region of the femoral condyle. This was caused by the degeneration state of the tissue and the surgical procedure which left regions damaged by cuts and burns. In addition to the aforementioned issues, it was technically difficult to measure the sample in precise depths from the top surface, which led us to measure the sample from the cross-section.

Instrumented indentation would enable engineers to obtain local mechanical data about their target tissue to better match the properties of their scaffold design to the target tissue. The local elastic modulus of human femoral condyle articular cartilage measured in this work could thus be useful to provide target values for future scaffold designs. The values can be registered in a 3D printer which adapts the scaffold properties layer-by-layer. This approach would not only be limited to articular cartilage, but has the potential to improve the scaffold design for several organs that possess defined local mechanical properties.

## **4.7 Acknowledgements**

The authors would like to thank the Swiss National Science Foundation (#200021-143413) for their financial support. Furthermore, the authors would like to thank Dr. Nadine Stokar for her help with histology interpretation, and Mme Sandra Jaccoud and Dr. Virginie Philippe for assistance with the DAL Biobank.

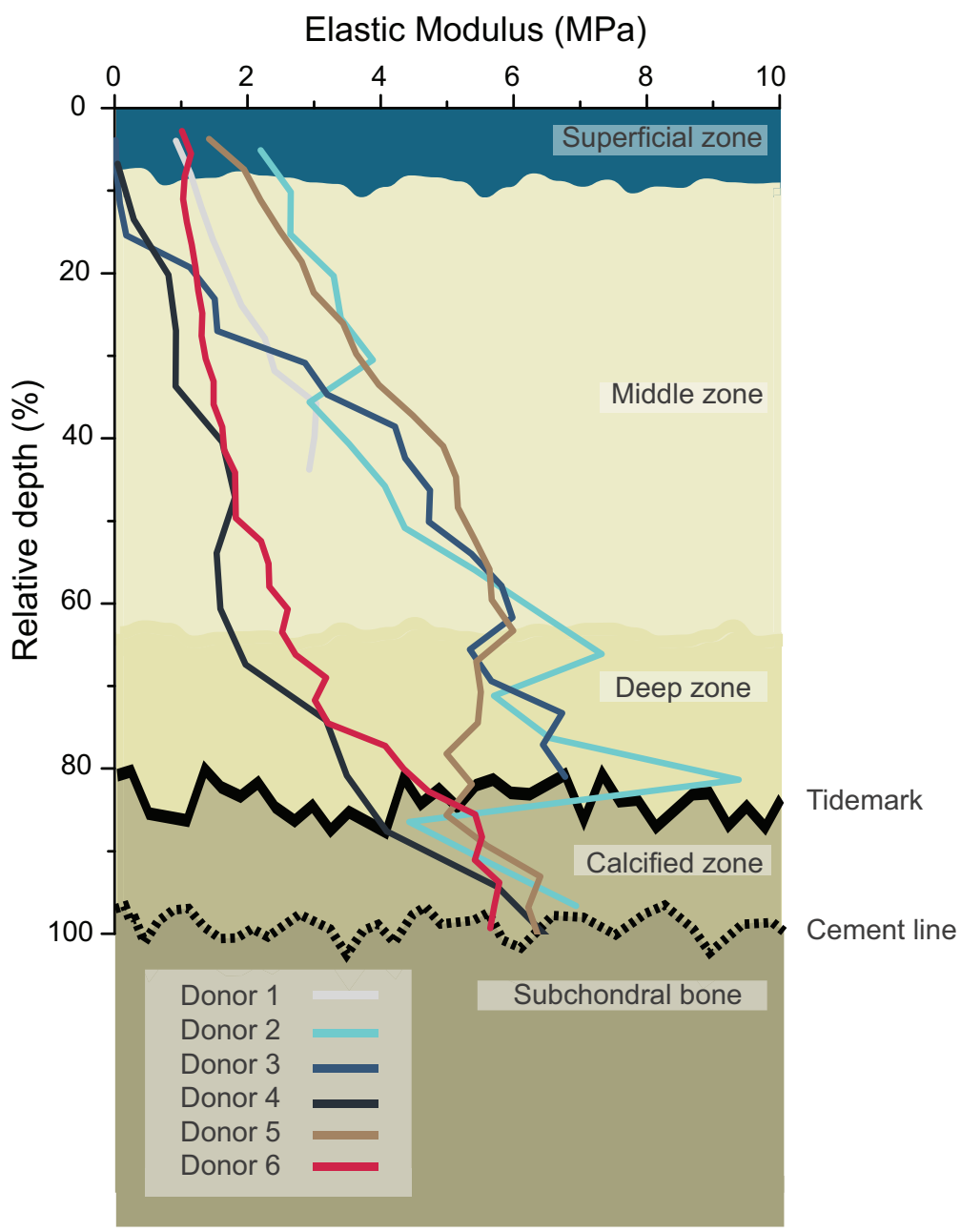


**Figure 4.5 Depth-dependent elastic modulus of human femoral condyle cartilage.** The relative depth corresponds to the distance between the superficial layer (0%) and subchondral bone (100%) and was normalized for each sample. Donor 1 and 3 were not measured to 100% since the fixed number of indentations did not reach to the bone. Donor 2 was not considered for elastic modulus values, but kept to show gradient; n=3; standard deviation was omitted to visualize trend (displayed in supplementary Fig. 4.7).



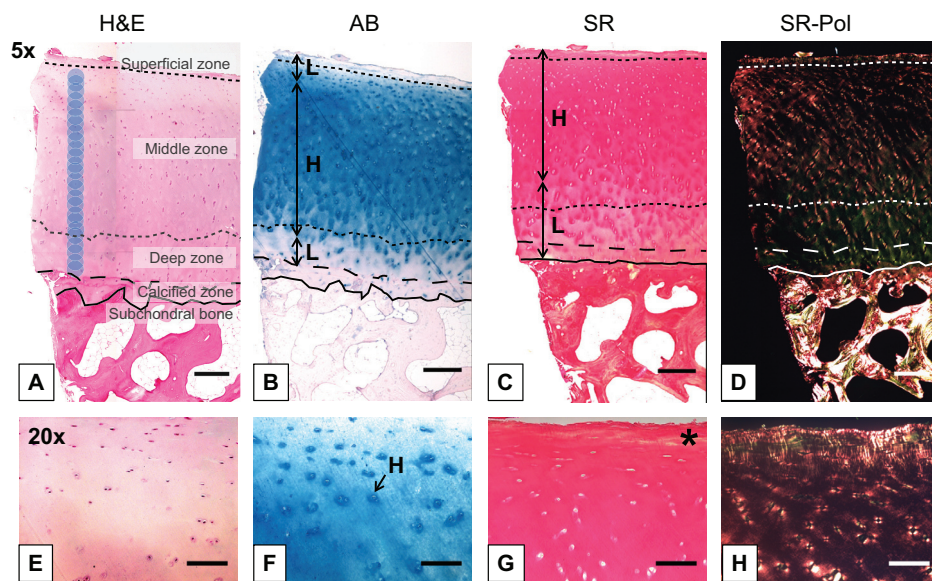


**Figure 4.6** Histological sections of human femoral condyle articular cartilage. A+E. Hematoxylin and Eosin (H&E) staining to visualize tissue morphology; B+F. Alcian Blue (AB) to stain sulphated GAG content; C+G. Picosirius Red (SR) to stain collagen; D+H. SR under polarized light to visualize COL fiber orientation; low (L) and high (H) staining intensity; G. surface area with loose collagen (degeneration) (\*). Dashed lines indicate different cartilage zones; A+B+C+D, 5 x magnification, scale bar: 400  $\mu\text{m}$ ; E+F+G+H 20x magnification, scale bar: 100  $\mu\text{m}$ . Images acquired with a Leica DM5500; sections were taken from patient 3.

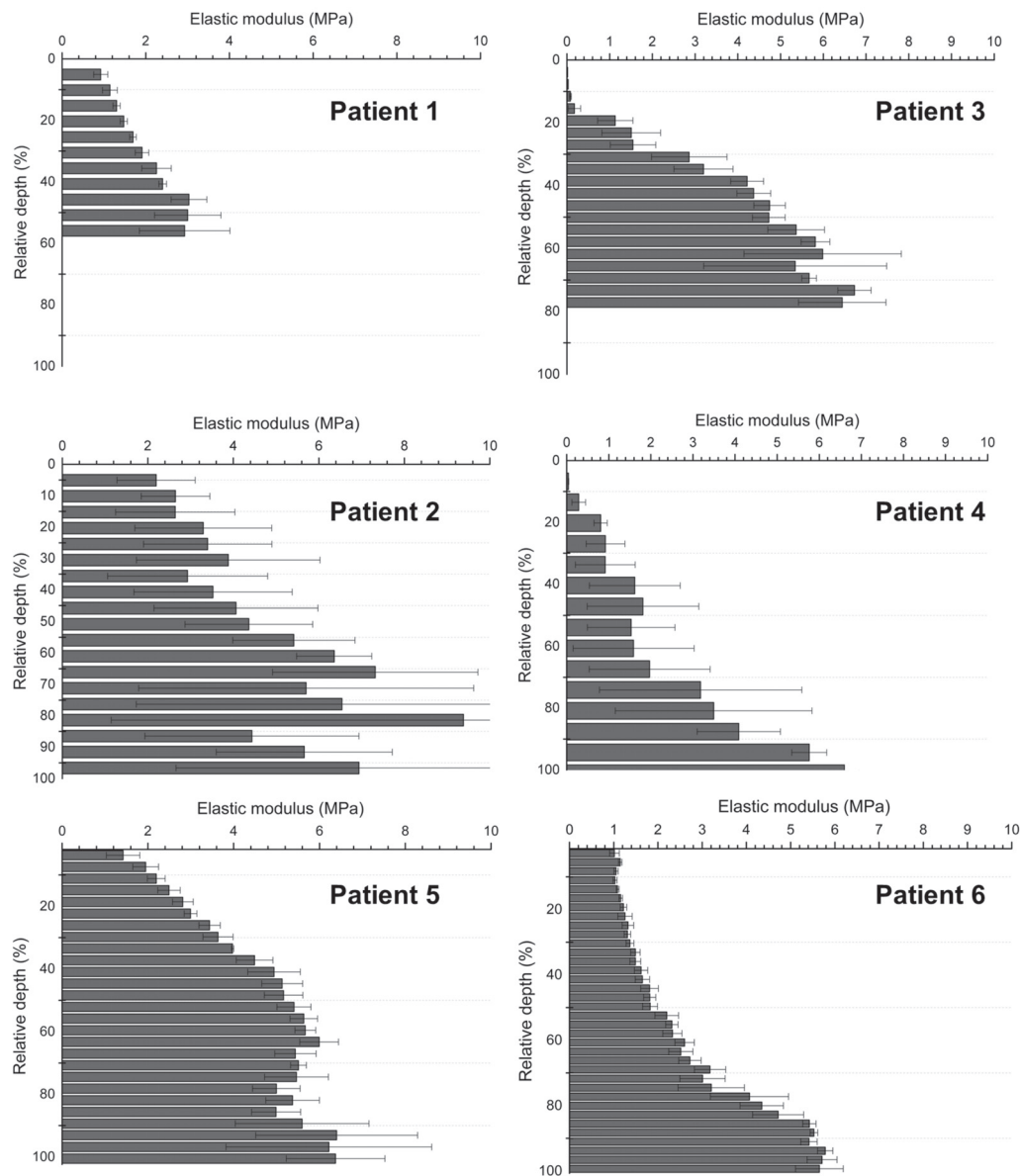


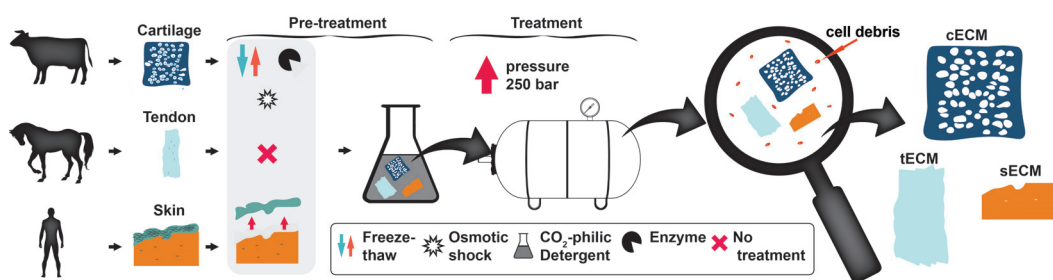
**Figure 4.7 Zone-dependent elastic modulus of human femoral condyle cartilage.** The relative depth corresponds to the distance between the superficial layer (0%) and bone (100%) and was normalized to the thickness of each sample; Donor 1 and 3 were not measured up to 100% since the fixed number of indentations did not reach completely to the bone;  $n=3$ .

# Chapter 5

## Decellularised Tissues obtained by a CO<sub>2</sub>-philic Detergent and Supercritical CO<sub>2</sub>

*This chapter is based on the following publication: Antons, J., Marascio, M.G.M., Aeberhard, P., Weissenberger, G., Hirt-Burri, N., Applegate, L.A., Bourban, P.E. and Pioletti, D.P., 2018. Decellularised tissues obtained by a CO<sub>2</sub>-philic detergent and supercritical CO<sub>2</sub>. European cells & materials, 36, pp.81-95. The first author contributed to the writing of the manuscript, development of the decellularisation protocol and experimental design.*

### 5.1 Graphical Abstract



### 5.2 Abstract

Tissue decellularisation has gained much attention in regenerative medicine as an alternative to synthetic materials. In decellularised tissues, biological cues can be maintained and

provide cellular environments still unmet by synthetic materials. Supercritical CO<sub>2</sub> (scCO<sub>2</sub>) has recently emerged as a promising alternative decellularisation technique to aggressive detergents; in addition, scCO<sub>2</sub> provides innate sterilisation. However, to date, decellularisation with scCO<sub>2</sub> is limited to only a few tissue types with low cellular density.

In the current study, a scCO<sub>2</sub> technique to decellularise high density tissues, including articular cartilage, tendon and skin, was developed. Results showed that most of the cellular material was removed, while the sample structure and biocompatibility was preserved. The DNA content was reduced in cartilage, tendon and skin as compared to the native tissue. The treatment did not affect the initial tendon elastic modulus [reduced from 126.35±9.79 MPa to 113.48±8.48 MPa ( $p > 0.05$ )], while it reduced the cartilage one [from 12.06±2.14 MPa to 1.17±0.34 MPa ( $p < 0.0001$ )]. Interestingly, cell adhesion molecules such as fibronectin and laminin were still present in the tissues after decellularisation. Bovine chondrocytes were metabolically active and adhered to the surface of all decellularised tissues after 1 week of cell culture. The developed method has the potential to become a cost-effective, one-step procedure for the decellularisation of dense tissues.

**Keywords:** Decellularisation, supercritical carbon dioxide, extracellular matrix, articular cartilage, tendon, skin

### 5.3 Introduction

Decellularised tissue matrices closely mimic their 3D native structures and, thus, have a substantial advantage when compared to synthetic materials. The potential of decellularised matrices is well recognised for the replacement of different tissue types (Badylak et al., 2011; Caione et al., 2012; Macchiarini et al., 2008; Patton et al., 2007). Remarkable success is demonstrated in *in vitro* experiments in which the tissue function of porcine heart (Ott et al., 2008; Wainwright et al., 2010), rat and human kidney (Song et al., 2013) and rat lung (Ott et al., 2010; Petersen et al., 2010) can partly be restored after recellularisation of previously decellularised tissues. Moreover, decellularised matrices are attractive scaffolds for the repair of tendons (Nourissat et al., 2015; Raghavan et al., 2012; Xu et al., 2017).

A tissue is considered as decellularised if no visible nuclei remain, less than 50 ng double-stranded DNA per mg extracellular matrix (ECM) dry weight is detected and the DNA fragment length is less than 200 bp (Crapo et al., 2011). Decellularised matrices are produced by a multistep tissue-specific decellularisation process including lysis of the cell membranes, separation of the cellular components from the ECM, solubilisation of the cytoplasmic and nuclear components and removal of the cellular debris (Aubin et al., 2013).

However, this decellularisation process is time-consuming and can compromise the structure and mechanical properties of the tissue (Crapo et al., 2011).

One of the currently most effective decellularisation methods uses perfusion of detergents, such as sodium dodecyl sulphate (SDS), to facilitate removal of cellular material (Ott et al., 2010, 2008; Petersen et al., 2010; Uygun et al., 2010; Wainwright et al., 2010). However, this is limited to vascularised tissues. To decellularise denser tissues, e.g. articular cartilage, many steps, such as freeze-thaw, osmotic shock and enzymatic treatment, are required to make the ECM accessible to decellularisation agents. One of the reasons for the long procedure is that this process still relies on the relatively slow diffusion of detergents inside non- or poorly vascularised tissues. Consequently, traces of these detergents might remain inside the tissue and may cause cytotoxicity and adverse effects (Ott et al., 2008). Moreover, at the end of the treatment, the decellularised tissues still have to be sterilised, thus introducing an additional step in the protocol. Sterilisation can be achieved by soaking the decellularised tissues in acids or alcohols (Hodde and Hiles, 2002), ethylene oxide, gamma irradiation (Freytes et al., 2008) or other methods that can further alter the ECM and its mechanical properties (Freytes et al., 2008; Rosario et al., 2008; Sun and Leung, 2008).

One possibility for integrating both sterilisation and decellularisation in one step while simultaneously overcoming diffusion limitations would be the use of a supercritical fluid as a rinsing agent. A supercritical fluid is a substance at a temperature and pressure higher than its critical point, in which liquid and gas phases cannot be distinguished. Supercritical fluids can diffuse through solids as a gas and dissolve substances as a liquid. This unique behaviour could potentially widely reduce decellularisation time by enhancing the diffusion kinetics. A suitable supercritical fluid for decellularisation is supercritical carbon dioxide (scCO<sub>2</sub>) since its supercritical point is reached at relatively mild conditions (7.2 MPa/37 °C). Furthermore, scCO<sub>2</sub> can sterilise the sample, having a minor to negligible influence on the tissue structure (Bernhardt et al., 2015). Nevertheless, scCO<sub>2</sub> itself is apolar, thus, the addition of an entrainer, e.g. ethanol, is necessary to eliminate or counteract charged molecules such as phospholipids (Dunford and Temelli, 1995; Montanari et al., 1999; Tanaka et al., 2004). Using scCO<sub>2</sub> with ethanol already provides successful decellularisation for aorta, cornea, oesophagus and adipose tissues (Casali et al., 2018; Guler et al., 2017; Halfwerk et al., 2018; Huang et al., 2017; Sawada et al., 2008; Wang et al., 2017a; Zambon et al., 2016). However, when dealing with denser tissues, ethanol does not have the required counteractive solvent strength. Instead of ethanol, CO<sub>2</sub>-philic detergents, such as the commercially available and low-cost Dehypon® LS-54 (BASF, Ludwigshafen, Germany), could provide the required solvent strength. LS-54 can dissolve bio-macromolecules within scCO<sub>2</sub> and has a solvability as high as 4 weight % due to its four CO<sub>2</sub>-philic propylene oxide groups (Liu et al., 2002).

This study hypothesis was that the detergent LS- 54, in combination with scCO<sub>2</sub> , might be beneficial for decellularisation of dense tissues. Thus, the purpose of the study was to determine whether the treatment of high density tissues, including articular cartilage, tendon and skin, with a CO<sub>2</sub>-philic detergent and a rinsing step in scCO<sub>2</sub> might create a decellularised tissue showing: (i) effective removal of immunological material (visual cell nuclei and DNA), (ii) mechanical and structural properties in the range of the native tissues (control) and (iii) the ability to support cellular growth.

## 5.4 Materials and Methods

Each of the tissues was treated according to the decellularisation procedure summarised in Fig. 5.1. The tissue-specific protocol and all characterisation techniques are detailed in this section. All products used in the experiments were purchased from Sigma-Aldrich (Buchs, Switzerland) unless mentioned otherwise.

### 5.4.1 Pre-treatment

#### Cartilage

Bovine articular cartilage was obtained from a local slaughterhouse and immediately processed on ice to avoid degradation. The cartilage was carefully harvested from the femoral condyles using an 8 mm biopsy punch and a scalpel to create a cylindrical shape. The bone-facing part of the cartilage was removed with a razor blade and a custom-made guide, leaving a uniform 3 mm-thick cylindrical sample. Afterwards, the cartilage cylinders were thoroughly rinsed in phosphate-buffered saline (PBS), dried with a paper towel and stored at - 80 °C until further use. As the first tests revealed that it was impossible to completely decellularise cartilage and skin with scCO<sub>2</sub> and detergent only in the autoclave available for the study, additional pre-treatment steps were introduced.

The pre-treatment of cartilage consisted of several steps (Fig. 5.1). First, 6 freeze-thaw cycles at - 80 °C for 2 h (including the initial storage at - 80 °C) and, then, at 37 °C for 1 h were performed. Next, the samples were treated with 0.05% trypsin-EDTA (25300062; Life Technologies) at 37 °C for 24 h. Subsequently, the samples were exposed to an osmotic shock by placing them in hypertonic buffer solution (1.5 M NaCl in 10 mM Tris-HCL, pH 8) for 4 h followed by a hypotonic solution (10 mM Tris-HCL, pH 7.6) for 20 h. Then, the cartilage was immediately treated according to the section “scCO<sub>2</sub> treatment”.

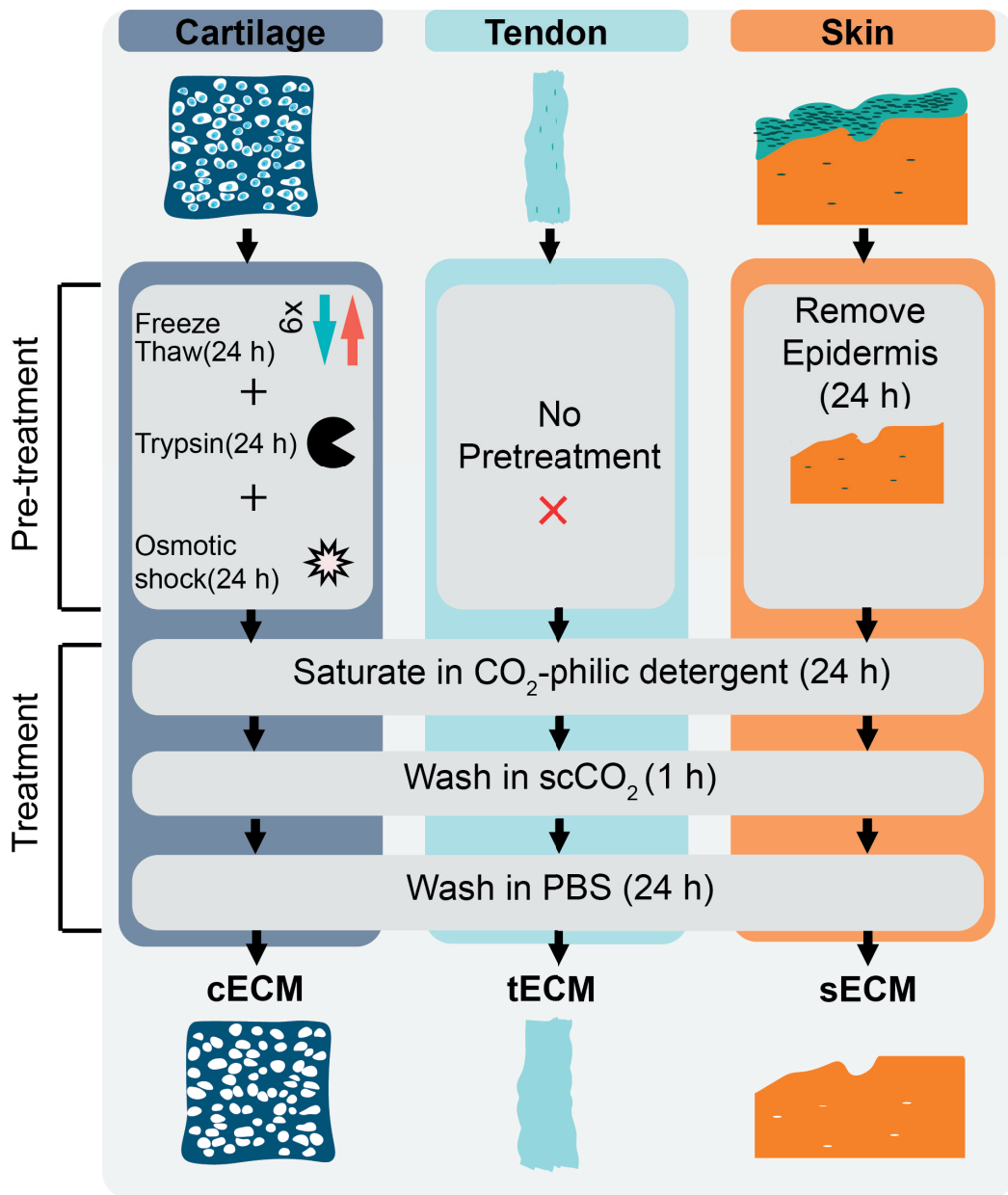


**Figure 5.1** Scheme of the decellularisation procedure.

### Tendons

Horse superficial digital flexor tendons were purchased from a local slaughterhouse and processed frozen, to avoid degradation, into 2 mm-thick slices using a diamond band saw (Exakt Technologies, Oklahoma City, Oklahoma, USA). Then, tendons were dried with a paper towel and stored at - 80 °C until further use.

## Skin

Human skin was obtained from the DAL/CHUV biobank (Lausanne, Switzerland), under anonymous donation, in accordance with its regulation and approval by the Institutional Biobank (Lausanne, Switzerland). The human skin was immediately cut into pieces of approximately 15 × 15 mm, dried with a paper towel and stored at - 80 °C until further use. To start the decellularisation procedure, skin was pre-treated with 1 M NaCl for 24 h prior to careful removal of the epidermis with forceps. Then, the skin was immediately treated according to the section “scCO<sub>2</sub> treatment”.

### 5.4.2 Treatment

#### scCO<sub>2</sub> treatment

Based on the protocols described by others (Guler et al., 2017; Huang et al., 2017; Sawada et al., 2008; Wang et al., 2017a), scCO<sub>2</sub> was used to eliminate cellular components from the tissues (Fig. 5.1). A modification of these protocols was carried out by pre-saturating the tissues in a CO<sub>2</sub>-philic detergent instead of using ethanol as entrainer to add polarity to CO<sub>2</sub>. Briefly, all tissues were washed for 24 h in a solution of 2% LS-54 (Dehypon®, BASF, Ludwigshafen, Germany) under vigorous shaking at 37 °C. Then, the detergent-saturated tissues were individually sealed inside sterilisation bags (Medline Industries, Northfield, Illinois, USA) and placed in an autoclave (SITEC AG, Maur, Switzerland) for 1 h. 99.9% pure CO<sub>2</sub> was introduced into the pressure vessel (volume of vessel: 4 L), then, pressure was increased to 25 MPa using a high-pressure pump. The temperature was adjusted to 37 °C, but the temperature fluctuated between 31-37 °C due to an imprecise temperature controller, which was conceived for higher temperatures (up to 350 °C). Later, the pressure vessel was rapidly depressurised using a manual valve at a depressurisation rate of approximately ≈ 10 MPa/ min. To remove residual detergent, the samples were washed in PBS under vigorous agitation for 24 h while changing the PBS every 8 h.

### 5.4.3 Biological Characterization

#### Histology and immunohistochemistry

To qualitatively assess the removal of cellular material and ECM components, histological sections of native (control) and decellularised tissues (cartilage: cECM; tendon: tECM; skin: sECM) were compared. Briefly, all samples were fixed in 4% paraformaldehyde and dehydrated in a graded series of ethanol. Samples were embedded in paraffin, sectioned with



a microtome to a thickness of 5  $\mu\text{m}$  and stained following standard histology protocols. To stain and visualise any possible remaining cell nuclei, a haematoxylin and eosin dye (H&E) and 4,6-diamidino-2-phenylindole (DAPI) staining was used. Glycosaminoglycans (GAG) and collagen (COL) were visualised with alcian blue and picosirius red dyes, respectively.

To evaluate the preservation of cell adhesion molecules after decellularisation, immunohistochemistry for fibronectin and laminin was performed. Briefly, 5  $\mu\text{m}$  sections of paraffin-embedded samples were de-paraffinised, rehydrated in PBS and permeabilised with a solution of 0.25% Tween-20 in PBS for 10 min. To expose the ECM molecule's epitopes, samples were digested for 10 min at 37 °C with 4 mg/mL pepsin in 0.01 M HCl. Fibronectin was detected by immunofluorescence, whereas laminin was detected by a peroxidase reaction. Thus, to detect laminin, an additional step to block endogenous peroxidases by Bloxall solution for 10 min was introduced (Bloxall, SP-6000, Vectorlabs, Burlingame, California, USA). To block non-specific antigens, sections prepared for both fibronectin and laminin labelling were treated with 1% bovine serum albumin solution in PBS at room temperature for 30 min. Laminin was detected by a peroxidase reaction using a polyclonal primary antibody against laminin (1 : 200; L9393) overnight at 4 °C. This was followed by incubation with one drop per section of the horseradish peroxidase (HRP) labelled secondary goat anti-rabbit antibody (ImmPRESS™ HRP anti- rabbit, MP-7401, Vectorlabs). Subsequently, laminin was detected by adding ImmPACT DAB peroxidase (HRP) substrate (SK-4105, Vectorlabs).

Fibronectin was detected by immunofluorescence by using a monoclonal primary antibody against fibronectin (1 : 200; 610077, BD Biosciences) overnight at 4 °C. This was followed by incubation with Alexa Fluor 568 labelled secondary donkey anti-mouse antibody (1 : 100; A10037, Invitrogen) at ambient temperature for 2 h. Tissue sections were examined under a widefield microscope (DM 5500, Leica) (n = 3 for control and LS-54).

### **DNA quantification**

To assess total DNA content, samples were dried overnight in an oven at 65 °C and the dry weight was recorded. Then, the samples were thoroughly digested in papain buffer [100 mM  $\text{Na}_2\text{HPO}_4$ , 100 mM ethylenediaminetetraacetic acid (EDTA), 10 mM cysteine-HCl, 250  $\mu\text{g}$  papain/mL, pH 6.5] at 65 °C under agitation at 750 rpm overnight or until no visible tissue material remained. The resulting digest was purified by phenol : chloroform : isoamylalcohol (25 : 24 : 1, v/v). The aqueous phase was ethanol- precipitated on ice for 30 min. After centrifugation (16,000  $\times\text{g}$ , 10 min, 4 °C), the DNA pellet was washed and reconstituted in nuclease-free water. Subsequently, the DNA content was quantified using a NanoDrop spectrophotometer (Thermo Fisher Scientific, Waltham, MA, USA). Each sample condition (control and LS-54) was measured in quadruplicate.

### **GAG quantification**

Sulphated GAGs were quantified by 1,9-dimethylmethylene blue dye (DMMB) assay. Chondroitin sulphate dilutions from 0 to 100  $\mu\text{g}$  were used to create a standard curve. 100  $\mu\text{L}$  per well of papain-digested tissues at 6 mg dry tissue/ mL were pipetted into a 96-well plate in triplicates. Then, the absorbance was measured on a microplate reader (Wallac 1420 Victor2, PerkinElmer) at a wavelength of 595 nm. Afterwards, chondroitin sulphate concentrations were plotted against absorbance creating a standard curve to determine the GAG concentration in the tissue samples. Each sample condition (control and LS-54) was measured in triplicate.

## **5.4.4 Mechanical and Structural Characterization**

### **Scanning Electron Microscopy (SEM)**

To compare the ultrastructure of the tissue before and after the decellularisation treatment, SEM images were acquired. First, the tissues were fixed for 1 h with 1.25% glutaraldehyde and 1% tannic acid in a 0.1 M phosphate buffer, pH 7.4. Then, they were washed in PBS and fixed again in 1.0% osmium tetroxide in PBS for 30 min. Next, tissues were dehydrated in a graded alcohol series followed by critical point drying (CPD300, Leica Microsystems). Subsequently, the samples were coated with a 4 nm- thick layer of osmium using an osmium plasma coater (OPC60, Filgen, Japan). SEM sample preparation and imaging were performed at the EPFL BioEM facility, Lausanne, Switzerland. Images were acquired on a scanning electron microscope (Merlin SEM, Zeiss) at two magnifications, 5,000 $\times$  and 43,800 $\times$ , with an accelerating voltage of 1.5 and 1.2 kV, respectively. Articular cartilage was imaged from the superficial layer (top view), tendons from the top and skin from the cross-section. Each sample condition (control and LS-54) was imaged in triplicate.

### **Compression and Tension Tests: Cartilage**

To assess the difference in elastic modulus between native (control) and decellularised samples (cECM), an unconfined compression test was performed on a uniaxial test system (Instron E3000, Norwood, Massachusetts, USA; load cell: 3 kN). Briefly, each cartilage cylinder (8 mm diameter, 3 mm height) was compressed to 20% strain at a compression rate of 200  $\mu\text{m/s}$ . The elastic modulus was determined from the stress-strain curve between 5 and 15 % of strain. The control cartilage was taken from the - 80 °C freezer prior to the compression test and equilibrated to ambient temperature in PBS for 4 h. Each sample condition (control and LS-54) was measured in quadruplicate.

### **Compression and Tension Tests: Tendon**

Biomechanical testing of tendons was performed on a uniaxial test system (Instron E3000, Norwood, Massachusetts, USA; load cell: 3 kN). The samples (2 mm thickness, 50 mm length, 12 mm width) were placed between two standard tensile test clamps: one portion was attached to the upper clamp and the other end to the lower clamp with an initial tendon free length of 20 mm. An elongation rate of 0.1 mm/s was applied. The control tendon was taken from the - 80 °C freezer prior to the tension test and equilibrated to ambient temperature in PBS for 4 h. Each sample condition (control and LS-54) was measured in quadruplicate.

### **Compression and Tension Tests: Skin**

Skin was not mechanically characterised due to its limited load-bearing function.

### **Biocompatibility**

#### *Zone of inhibition assay*

To evaluate the biocompatibility of the decellularised tissues, a Zone of Inhibition (ZoI) assay was performed. Thus, the decellularised samples were tightly fixed into a 35 mm cell culture dish using a custom-made stainless-steel clamp. The size of the samples were 8 mm diameter and 3 mm depth for the cartilage plugs, 15 × 12 × 2 mm for tendon and 15 × 15 × 2 mm for skin. The bovine chondrocytes used for the biocompatibility tests were previously extracted from fresh bovine articular cartilage tissue using collagenase extraction. Briefly, the cell extraction was conducted for 24 h with 0.6% collagenase II (Life Technologies) in Dulbecco's modified Eagle's medium (DMEM) in a humidified atmosphere at 37 °C and 5% CO<sub>2</sub>. Subsequently, DMEM (10 % foetal bovine serum, 2 mM L-glutamine, 100 units/mL penicillin-streptomycin) containing 300,000 bovine chondrocytes (passage 5) was added to the cell culture dish. The cells were cultured in a humidified atmosphere at 37 °C and 5 % CO<sub>2</sub> until full confluence (i.e. 100%) was reached. A Giemsa dye was applied to stain and visualise the chondrocytes surrounding the material and any possible ZoI. Microscopy images for the Giemsa staining were acquired by a Leica DM5500 microscope and overview images were taken by an iPhone 5s (Apple). Each sample condition (control and scCO<sub>2</sub>/LS-54) was tested in triplicate.

#### *Cell viability*

To determine the cell viability, a PrestoBlue™ assay (PrestoBlue™, A13261, Life Technologies) was performed at day 1 and day 7 following the manufacturer's instructions. Briefly, 1 million bovine chondrocytes (passage 5) in 50 µL DMEM were evenly pipetted on top of the tissues and left to attach for 1 h in a humidified atmosphere at 37 °C and 5% CO<sub>2</sub>.

Then, DMEM was added to fully immerse the sample. The medium was changed every other day and at day 1 and day 7 a PrestoBlue™ assay was performed. Therefore, a 10% mixture of PrestoBlue™ reagent in DMEM was prepared and added to the chondrocytes. After 2 h incubation time, 100  $\mu$ L supernatant per well was distributed in triplicate in a black 96-well plate. Then, the fluorescence at 595 nm was measured using a microplate reader (Wallac 1420 Victor2, PerkinElmer).

To visualise metabolically active cells on the acellular tissues, a MTT assay (MTT, M6494, Thermo Fisher Scientific) was carried out following the manufacturer's protocol. Thus, 1 million bovine chondrocytes (passage 5) in 50  $\mu$ L DMEM were evenly pipetted on top of the tissues and left to attach for 1 h in a humidified atmosphere at 37 °C and 5% CO<sub>2</sub>. Then, DMEM was carefully added to fully immerse the tissues. The medium was changed every other day. At day 7, a MTT assay was performed for 4 h at 37 °C in a humidified atmosphere containing 5 % CO<sub>2</sub> using a 10 % mixture of MTT reagent and DMEM. Next, cell penetration was evaluated by histology, following fixing in 4% paraformaldehyde and embedding in paraffin. 5  $\mu$ m-thick sections of the tissues were prepared by a microtome and stained by H&E to visualise cell penetration by staining of cell nuclei. Microscopy images for the MTT assay and cell penetration were acquired by a Leica DM5500 microscope and the overview images were taken by an Iphone 5s (Apple). Each sample condition (control and scCO<sub>2</sub>/LS-54) was tested in triplicate.

### 5.4.5 Statistics

Statistical analysis was performed using GraphPad Prism (La Jolla, CA, USA) software. Means and standard errors were provided for DNA, GAG quantification and mechanical properties. An unpaired two-tailed student's t-test was used to compare differences between native (control) and decellularised tissues (cECM, tECM, sECM).  $p \leq 0.05$  was considered statistically significant.

## 5.5 Results

### 5.5.1 Biological Characterization

#### Histology

H&E staining showed complete visual removal of cell nuclei in articular cartilage, tendon and skin, whereas trace amounts of broken cell nuclei were detected by DAPI staining (Fig. 5.2 a-c). Picrosirius Red staining (SR) showed the conservation of collagen (COL), with

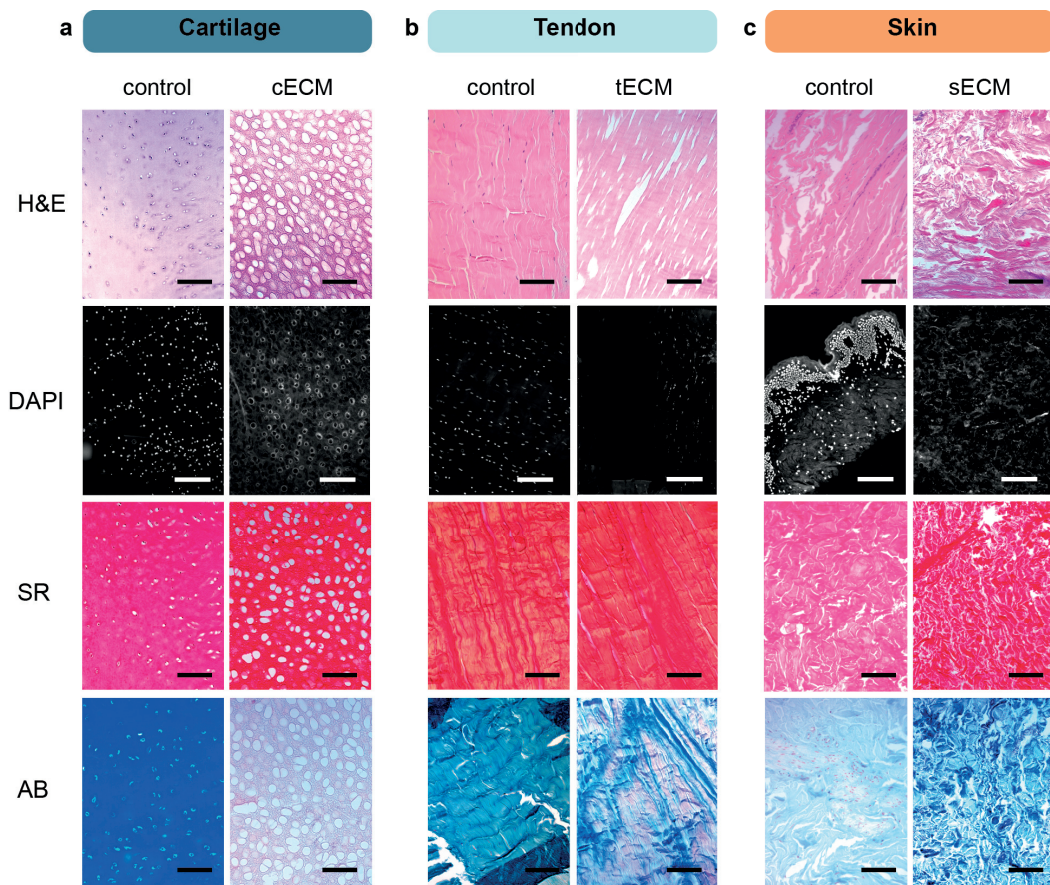


**Figure 5.2 Histological analysis of tissues before (control) and after decellularisation treatment.** Histological sections of a) bovine cartilage, b) horse tendon, c) human skin tissues stained with (H&E), DAPI, , picosirius Red (SR) and alcian blue (AB) dyes; scale bar: 200  $\mu\text{m}$  (cartilage: cECM; tendon: tECM; skin: sECM)

no visual difference between the control and decellularised tissues. In contrast, GAG content was severely reduced, as evidenced by alcian blue staining.

The preservation of important cell adhesion molecules (fibronectin, laminin) was evaluated by immunohistochemistry. Fibronectin and laminin were still present after the decellularisation procedure (Fig. 5.3). Articular cartilage was positive for fibronectin in the superficial layer (Fig. 5.3 a, white arrow), however, after decellularisation, fibronectin was distributed in the entire ECM. In both tendons and skin, fibronectin was abundant around the blood vessels (Fig. 5.3 b,c). Laminin was present in the pericellular space (Fig. 5.3 a, black arrow) and around the blood vessels (Fig. 5.3 b,c) and in the basal lamina of native (control) skin (Fig. 5.3 c, red arrow). For the skin (Fig. 5.3 c), it should be emphasised that the epidermis was removed during the decellularisation procedure and, thus, the basal lamina was not present.

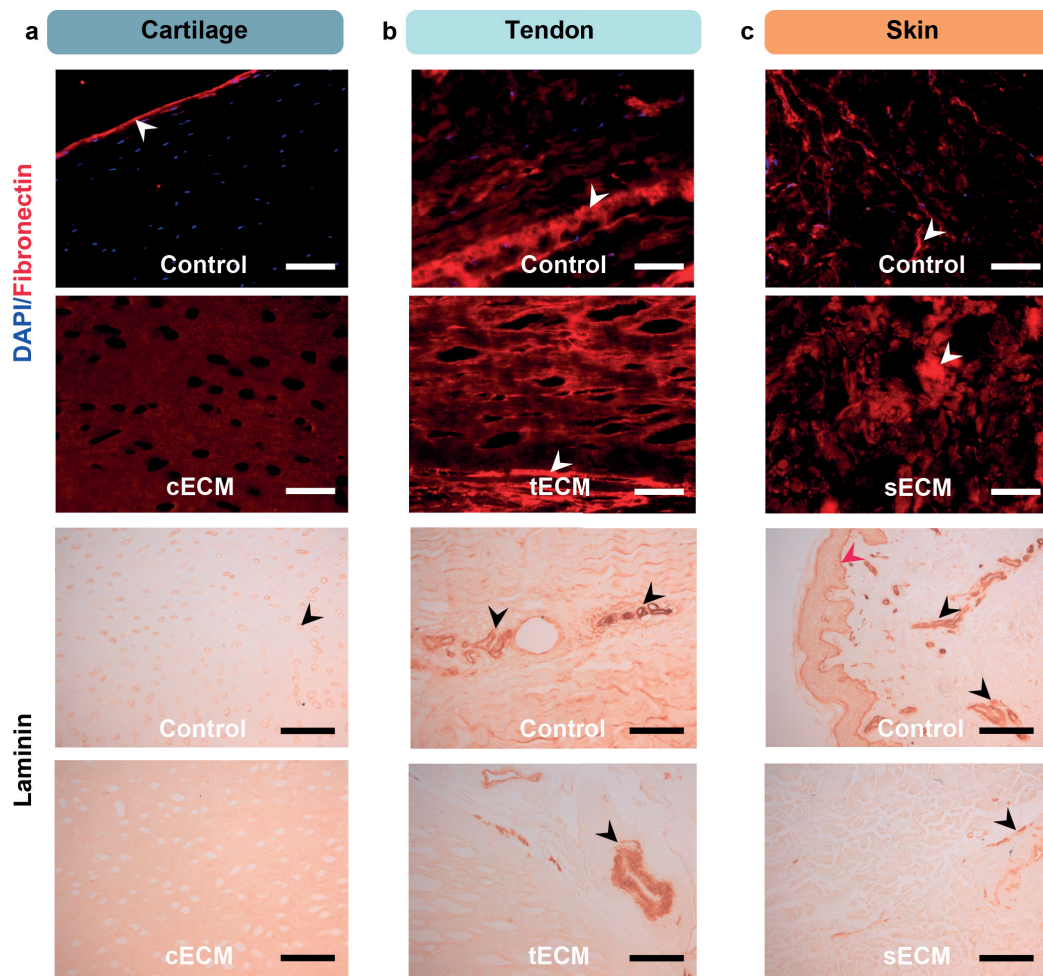


**Figure 5.3 Cell adhesion molecules retained in the ECM before (control) and after (cECM, tECM, sECM) decellularisation.** Histological sections of a) bovine cartilage, b) horse tendon, c) human skin tissue; fibronectin was visualized by fluorescence whereas laminin was detected by a peroxidase reaction; Arrows indicate regions of high staining intensity mostly around blood vessels and in the pericellular space; scale bar: 200  $\mu$ m.

### DNA and GAG content

DNA content was significantly ( $*p < 0.05$ ) reduced from  $1321 \pm 210$  ng to  $241 \pm 45$  ng dsDNA/mg dry tissue in cartilage (reduced by  $82 \pm 3$  %), from  $1135 \pm 262$  ng to  $378 \pm 68$  ng dsDNA/mg dry tissue in tendons (reduced by  $67 \pm 6$  %) and from  $554 \pm 34$  ng to  $29 \pm 0.05$  ng dsDNA/mg dry tissue in skin (reduced by  $95 \pm 0.004$  %), compared to the native tissue (Fig. 5.4 a,b). GAG content was also severely reduced ( $*p < 0.05$ ) as evidenced by alcian blue staining and quantitative analysis. In cartilage, GAG content was reduced from  $294 \pm 19$   $\mu$ g to  $68 \pm 31$   $\mu$ g/mg dry tissue (reduced by  $87 \pm 6$  %). In tendons, GAG content was reduced

from  $21 \pm 3 \mu\text{g}$  to  $6 \pm 3 \mu\text{g}/\text{mg}$  dry tissue (reduced by  $70 \pm 6 \%$ ) and in skin from  $4 \pm 2 \mu\text{g}$  to  $2 \pm 0.03 \mu\text{g}/\text{mg}$  dry tissue (reduced by  $66 \pm 0.4 \%$ ), compared to the native tissue (Fig. 5.4 a,b).

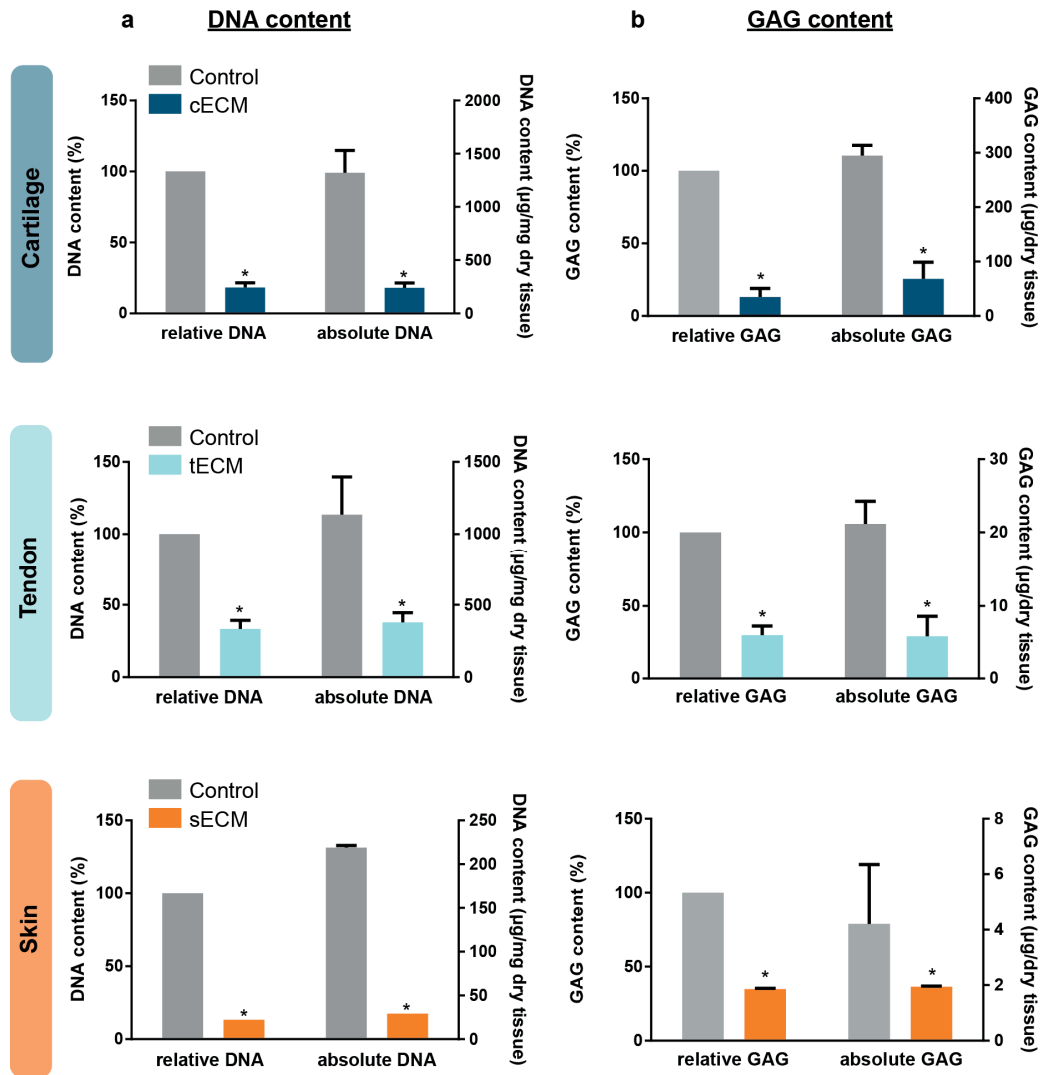


**Figure 5.4** DNA and GAG content before (control) and after treatment (decellularised). a) relative (normalized) and absolute DNA content; b) relative (normalized) and absolute GAG content. \* $p < 0.05$ .

#### Effect of pre-treatment and $\text{scCO}_2$ only

Fig. 5.8 displays the effects of  $\text{scCO}_2$  only and of pre-treatment on the DNA content of cartilage, tendons and skin. Using  $\text{scCO}_2$  only did not show any DNA reduction in cartilage ( $1453 \pm 463 \text{ ng DNA}/\text{mg}$  dry tissue), tendon ( $1117 \pm 34 \text{ ng DNA}/\text{mg}$  dry tissue) and skin

(637±19 ng DNA/mg dry tissue). Likewise, no visual removal of cell nuclei could be detected by histology (H&E staining). Without a pre-treatment, the DNA content of cartilage was not reduced (1363±87 ng DNA/mg dry tissue), whereas it was significantly reduced in tendons (378±68 ng DNA/mg dry tissue, \* p < 0.05) and skin (219±13 ng/mg dry tissue, \*p < 0.05). However, removing the epidermis prior to decellularisation could further reduce the DNA content of the skin (29±0.05 ng DNA/mg dry tissue, Fig. 5.4 a,b) and the number of cell nuclei at a visual analysis.

## 5.5.2 Mechanical and Structural Characterization

### SEM

The ultrastructure of the tissues was modified by the decellularisation treatment (Fig. 5.5). For cartilage (cECM), ECM density appeared particularly low as compared to native tissue (Fig. 5.5 a). This was evident from the decrease in mass surrounding the collagen network. No visual changes in density were observed for tendons and skin. For all tissues, the orientation and size of the collagen fibres themselves matched the control sample almost identically but showed a somewhat looser arrangement.

### Compression and tension test

The decellularisation procedure reduced significantly the elastic modulus of articular cartilage (p < 0.0001) from 12.06±2.14 MPa to 1.17±0.34 MPa (maintaining 14.44±2.81 % of the original elastic modulus) (Fig. 5.6 a). In contrast, tendon elastic modulus (Fig. 5.6 b) was reduced (p > 0.05) from 126.35±9.79 MPa to 113.48±8.48 MPa (maintaining 88.93±7.47% of its original elastic modulus) after decellularisation.

### Biocompatibility

Consistent growth of bovine chondrocytes in direct proximity to the decellularised tissues indicated no ZoI (Fig. 5.7, top). Other specific cells, including tenocytes and skin fibroblasts, showed similar results for each tissue (data not shown).

Chondrocytes were metabolically active and adhered to the surface of all decellularised tissues after 1 week of cell culture, as evidenced by MTT assay (Fig. 5.7, middle). The cell penetration of bovine chondrocytes was limited to the surface of all decellularised tissues types (Fig. 5.7, middle). Furthermore, chondrocytes remained viable after 1 week, as seen by a constant fluorescent signal in the PrestoBlue™ assay (Fig. 5.7, bottom).



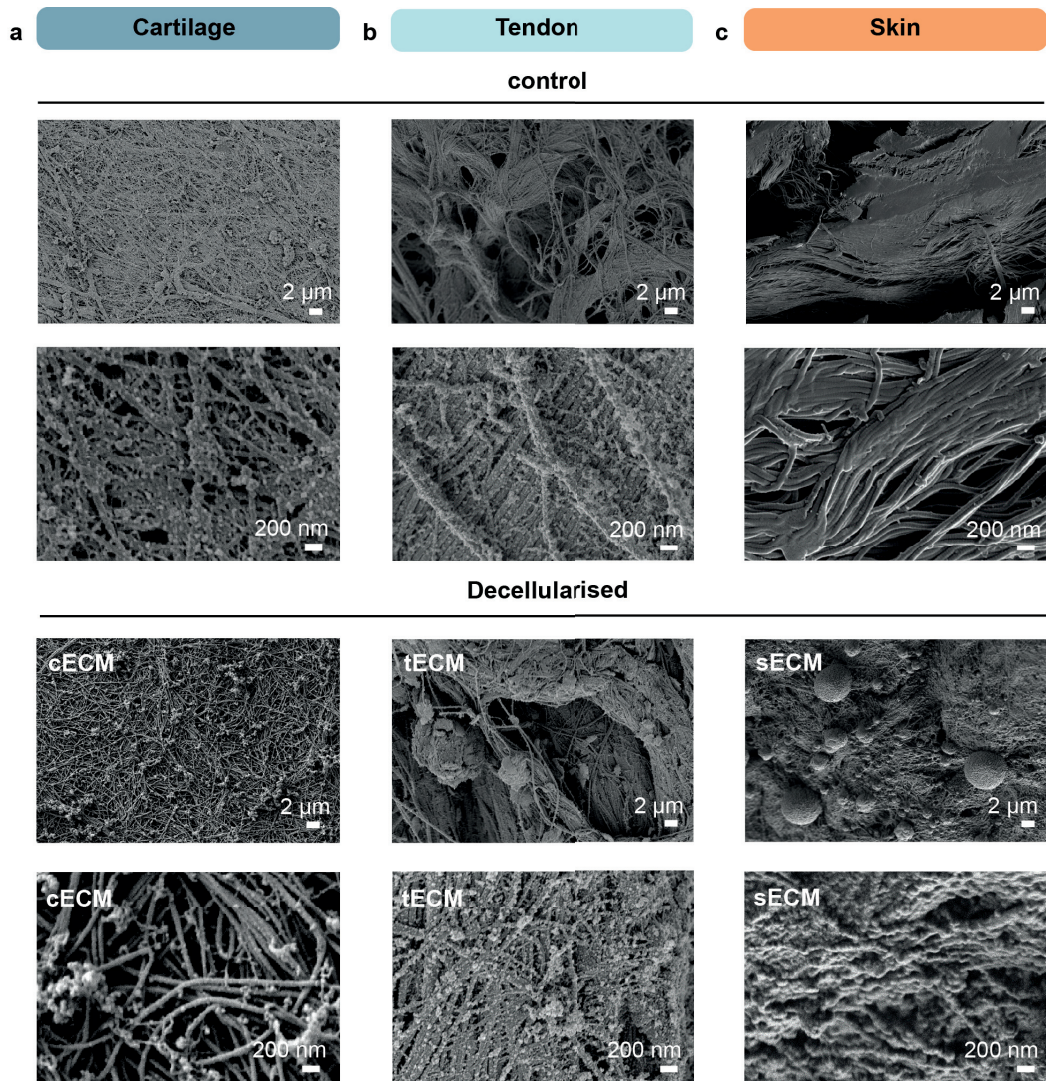


**Figure 5.5 Ultrastructure of cartilage, tendon and skin.** a) bovine cartilage (top view-superficial layer), b) horse tendon (top view), c) human skin (cross-section); DNA and GAG content of a) cartilage, b) tendon and c) human skin; scale bar : 2  $\mu\text{m}$  and 200 nm, respectively.

## 5.6 Discussion

The working hypothesis of the present study was that  $\text{scCO}_2$  might be optimised to decellularise dense tissues in combination with a  $\text{CO}_2$ -philic detergent. To verify this hypothesis, experiments with  $\text{scCO}_2$  on articular cartilage, tendons and skin were performed.

Decellularisation with  $\text{scCO}_2$  and a  $\text{CO}_2$ -philic detergent only, could not achieve a complete decellularisation of cartilage and skin. Thus, additional steps were introduced. For cartilage, an extensive pre-treatment involving freeze-thaw, osmotic shock and enzymatic

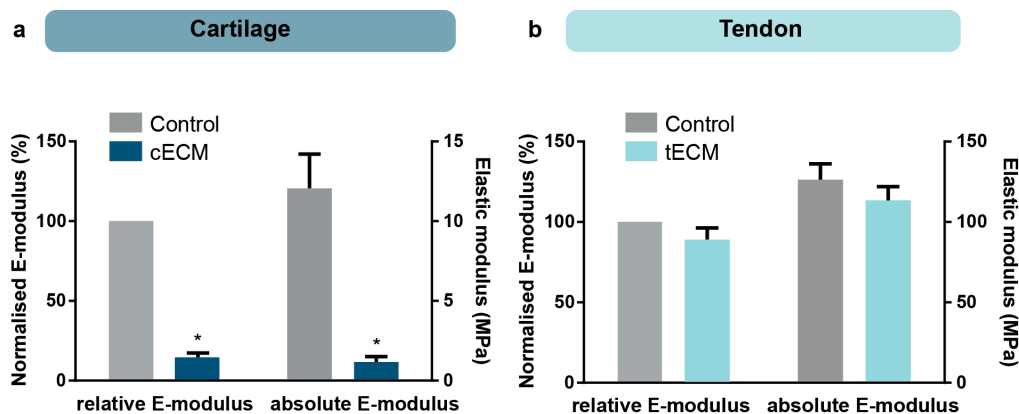


**Figure 5.6 Elastic modulus of cartilage and tendon after the decellularisation treatment.** a) Compression test of bovine cartilage at 200  $\mu\text{m/s}$  loading rate (elastic modulus normalized to the native tissue in percent and absolute values in MPa),  $n=4$  samples per condition; b) tension test of horse tendon at 0.1 mm/s (elastic modulus normalized to the native tissue in percent and absolute values in MPa),  $n=4$  samples per condition,  $*p<0.0001$ .

digestion was needed to achieve effective decellularisation. For skin, the pre-treatment consisted of removing the epidermis prior to decellularisation.

The described method substantially reduced the cellular material in all dense tissue types tested (Fig. 5.2 a-c). From a visual inspection, there were virtually no cell nuclei in the H&E staining as compared to the native tissue, which was confirmed by the significantly reduced DNA content ( $*p < 0.05$ ) (Fig. 5.4 a). There were only trace amounts of broken cell nuclei visible in the DAPI staining.

For cartilage, a DNA reduction from  $1321 \pm 210$  ng to  $241 \pm 45$  ng dsDNA/mg dry tissue (reduced by  $82 \pm 3\%$ ) was achieved (Fig. 5.4 a), compared to the 47.6 ng dsDNA/mg dry tissue (reduced by 94%) achieved by Bautista et al. (Bautista et al., 2016). In tendons, the DNA content was reduced from  $1135 \pm 262$  ng to  $378 \pm 68$  ng dsDNA/mg dry tissue (reduced by  $67 \pm 6\%$ ) (Fig. 5.4 a) as compared to the  $\approx 100$  ng/mg dry tissue (reduced by 90%) achieved by Xu et al. (Xu et al., 2017). For skin, a reduction from  $554 \pm 34$  ng to  $29 \pm 0.05$  ng dsDNA/mg dry tissue (reduced by  $95 \pm 0.004\%$ ) was observed (Fig. 5.4 a), compared to 40 ng dsDNA/mg dry tissue obtained by Zhang et al. (Zhang et al., 2016). It should be noted that the DNA content in the native tissues was higher per mg dry tissue than in the cited studies. This could be due to batch-to-batch variation and differences in the DNA extraction method.

Comparing the absolute DNA content achieved with the technique here described to the threshold defined by Crapo and et al. (Crapo et al., 2011), only skin was below the limit of 50 ng dsDNA/mg dry tissue, whereas cartilage and tendons contained substantially more DNA. GAG content was significantly reduced ( $p < 0.05$ ) in cartilage, in tendons and in

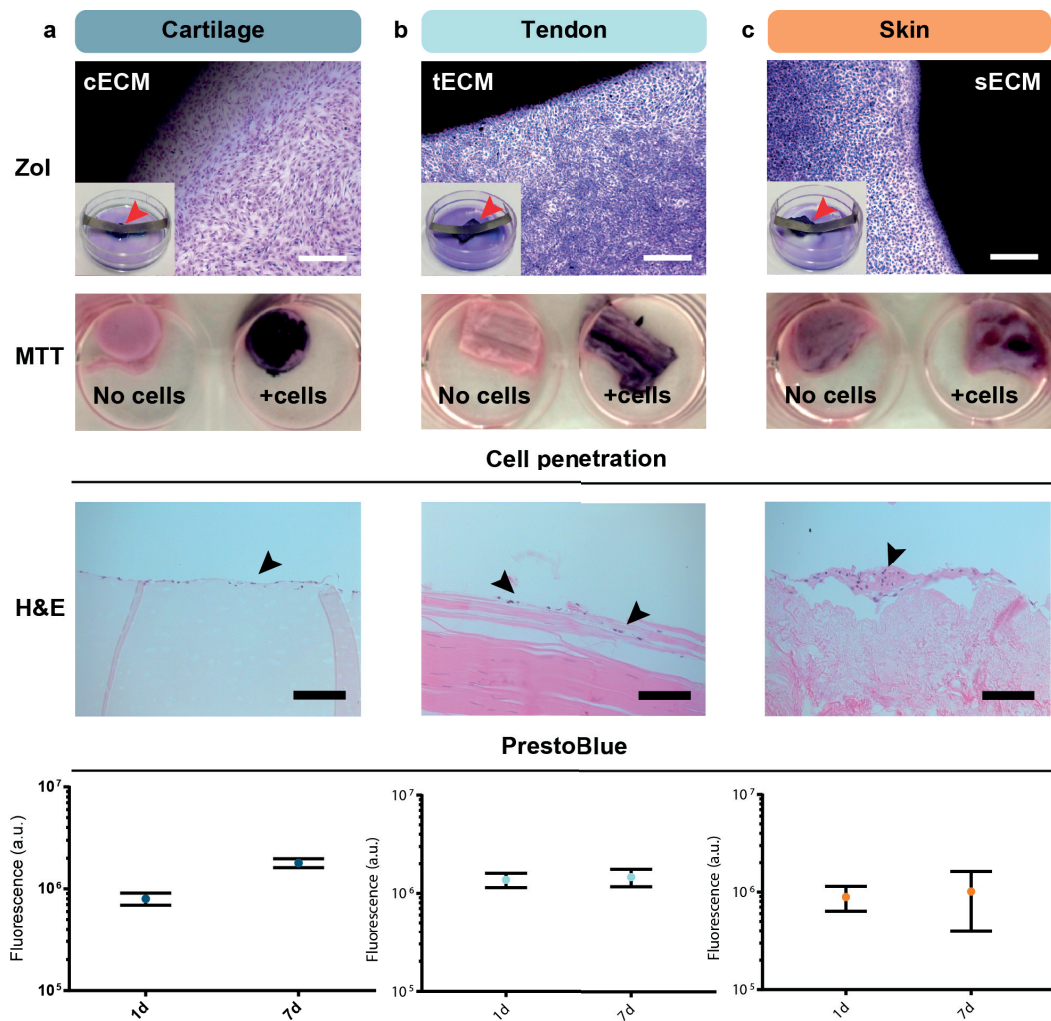


**Figure 5.7 Biocompatibility of decellularised tissues.** (Top) ZoI of a) bovine cartilage, b) horse tendon, c) human skin after 1 d, red arrows indicate location of decellularised tissue; scale bar: 400  $\mu\text{m}$ ; (Middle) MTT assay after 7 d of cell culture-(control without seeded cells); (Bottom); PrestoBlue assay shows constant fluorescent signal in arbitrary units (a.u.) after 7 d of cell culture; (in each test  $n=3$  samples per condition).

skin (Fig. 5.4 b). This was consistent with previous studies reporting a GAG reduction by  $71.0 \pm 6.10\%$  in cartilage (Bautista et al., 2016) and  $67\%$  in tendons (Youngstrom et al., 2013) using a SDS-based decellularisation protocol. For skin,  $1.56 \pm 0.42 \mu\text{g}/\text{mg}$  GAG/dry weight are retained in the decellularised dermis according to Zhang et al. (2016), being less than what was retained using the here presented protocol. However, Zhang et al. (2016) do not perform any comparison with the native tissue (Zhang et al., 2016).

It should be noted that decellularisation does not always remove a significant amount of GAGs. For instance, decellularisation of rat hearts with SDS in pulsatile flow retains most

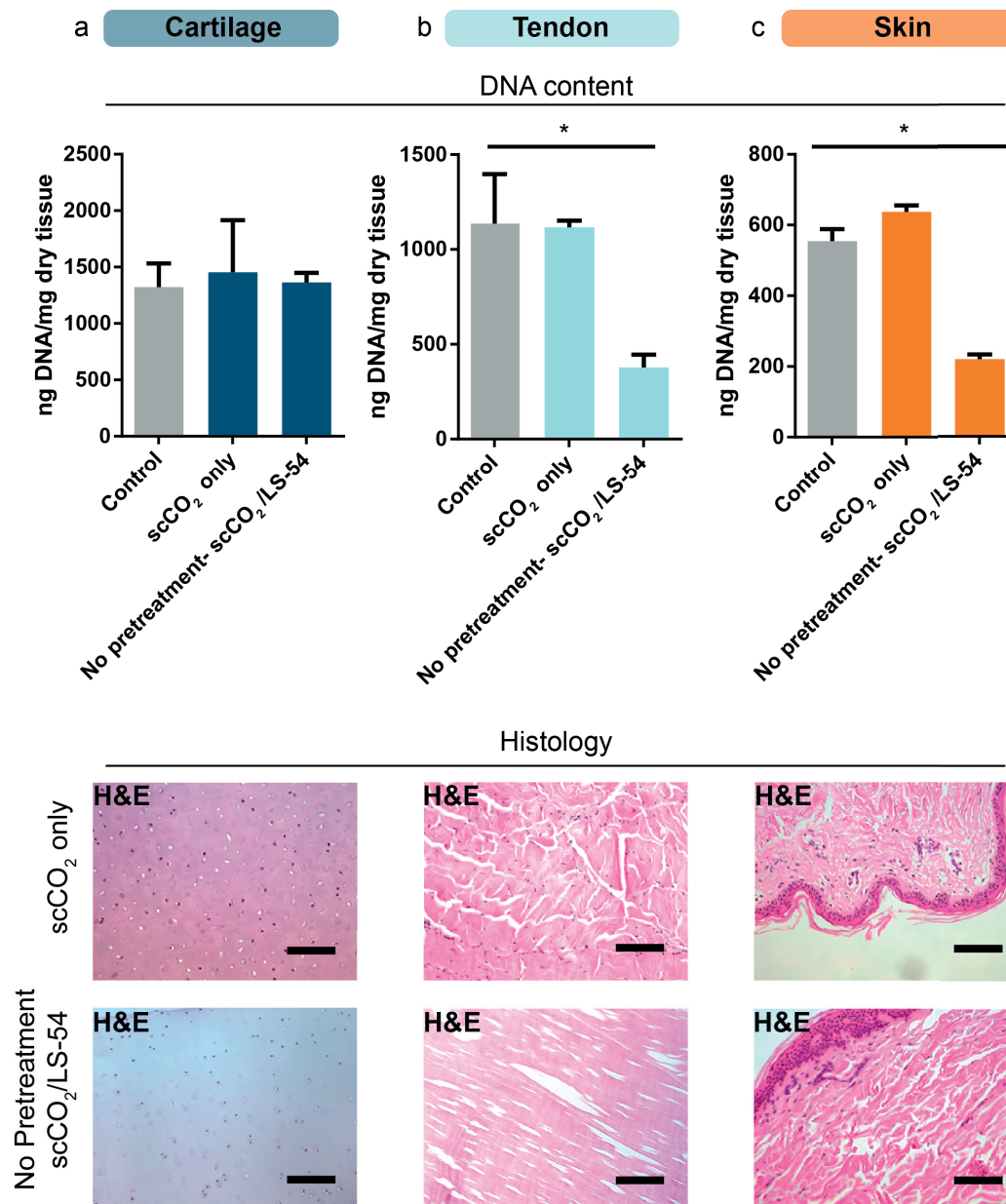


**Figure 5.8 Effect of scCO<sub>2</sub> and pre-treatment.** Upper part indicates DNA content in ng/mg dry tissue whereas lower part illustrates visual cell nuclei by H&E staining; a) cartilage; b) tendon; c) skin; \* $p < 0.05$ ; scale bar: 200  $\mu\text{m}$ .

of the GAGs in the ECM (Park et al., 2018). Likewise, optimisation of the decellularisation protocol can significantly enhance the remaining GAG content in a decellularised nucleus pulposus (Illien-Jünger et al., 2016). GAGs are important for the visco-elastic properties of tissues (Lovekamp et al., 2006). The GAG reduction was a possible explanation for the looser arrangement of collagen fibres in the ultrastructure of articular cartilage after

decellularisation (Fig. 5.5 a). Therefore, the present study supported the results of Schneider et al. (2016), who show a looser collagen fibre arrangement in articular cartilage after decellularisation (Schneider et al., 2016). Moreover, the less dense fibre arrangement results in a higher porosity, which is a potential advantage for the recellularisation of decellularised tissues (Nasrollahzadeh et al., 2017).

The cell adhesion molecules, fibronectin and laminin, were still present in the tissues after the decellularisation procedure (Fig. 5.3). Although, it should be noted that laminin was mostly present in close vicinity to blood vessels and in the pericellular space. A comparison of the results of this study with the previously cited decellularisation studies of articular cartilage (Bautista et al., 2016; Schneider et al., 2016) and tendons (Xu et al., 2017; Youngstrom et al., 2013) was not possible, since no immunohistochemistry was performed in these studies. Only in case of the Zhang et al. (2016) study, immunohistochemistry was performed and, similar to the observations of the present study, laminin was detected around the blood vessels (Zhang et al., 2016). The conservation of cell adhesion molecules after the decellularisation process was a positive result, since cell adhesion molecules are crucial for the bioactivity of the decellularised tissue. For this reason, cell adhesion molecules (fibronectin, laminin, arginylglycylaspartic-acid-containing molecules and others) are often added to synthetic materials to enhance their bioactivity (Lutolf and Hubbell, 2005; Shin et al., 2003).

Mechanical tests showed that the stiffness of the decellularised tissues was not affected by the treatment in case of tendons but dropped significantly ( $*p < 0.0001$ ) in articular cartilage (Fig. 5.6). These results compared well with other studies in which equine tendons and porcine articular cartilage are decellularised by SDS. For equine tendons, the elastic modulus decreases from  $76.13 \pm 4.12$  MPa to  $70.31 \pm 5.91$  MPa [ $92.35 \pm 8.41\%$  of the native tendons elastic modulus is maintained (Youngstrom et al., 2013)]; for porcine articular cartilage, the equilibrium modulus is reduced from 0.145 MPa to 0.035 MPa [maintaining  $24.8 \pm 2.2\%$  of the native cartilage properties (Bautista et al., 2016)]. In the described protocol, the reduction in elastic modulus of the articular cartilage could be caused by the extensive pre-treatment, which removed most GAG molecules from the ECM. A loss of GAGs, which attracts water into the ECM, affects the mechanical properties of tissues through a loss of hydrostatic pressure (Bautista et al., 2016; Maroudas et al., 1969; Maroudas, 1976). For tendons, the effect of a lower GAG content is less pronounced since tendons only contain between 0.2% and 5% GAGs in the tensional zone and in the dry mass at the bone insertion area, respectively (Merrilees and Flint, 1980). Since tendons mostly work in tension and not in compression, GAG content is less important than in articular cartilage, where 11% of GAGs in dry mass can be detected (Yu et al., 1997).

The decellularised tissues were non-cytotoxic to bovine chondrocytes (Fig. 5.7) and human tenocytes and fibroblasts (data not shown). The biocompatibility was further evidenced by ZoI, MTT and PrestoBlue™ assays after 1 week of culture. The cell penetration of bovine chondrocytes into the decellularised tissues was mostly limited to the surface of the tissue (Fig. 5.7, middle) after 1 week of cell culture. However, these tests are only a first indicator for a favourable biocompatibility. More extensive studies attempting to recellularise the obtained decellularised tissues should also be performed for a final confirmation of biocompatibility.

The effect of scCO<sub>2</sub> only and of pre-treatment on the DNA content of cartilage, tendons and skin are displayed in Fig. 5.8. scCO<sub>2</sub> only did not reduce the DNA content in any of the three tissues. This was expected since scCO<sub>2</sub> itself is apolar and needs a co-solvent such as ethanol or a CO<sub>2</sub>-philic detergent to remove polar molecules such as phospholipids (cell membrane) or DNA (Dunford and Temelli, 1995; Montanari et al., 1999; Tanaka et al., 2004). Without pre-treatment, scCO<sub>2</sub>/LS-54 could significantly reduce the DNA content of tendons ( $p < 0.05$ ). However, to effectively remove DNA content and visual cell nuclei, cartilage and skin required a pre-treatment prior to treatment with scCO<sub>2</sub>/LS-54. It is possible that a pre-treatment of articular cartilage was necessary due to the high density of its ECM with an average pore size of only 6 nm (Maroudas, 1976). Hence, to effectively remove phospholipids and DNA, a pre-treatment to loosen the ECM structure was required for cartilage. Without a pre-treatment, the DNA content of skin was significantly reduced ( $p < 0.05$ ), but visual cell nuclei remained as displayed in Fig. 5.8 c. Thus, the epidermis was removed prior to treatment with scCO<sub>2</sub>/LS-54.

The present study had also several inherent limitations. Decellularisation of cartilage and skin required a pre-treatment since scCO<sub>2</sub> and CO<sub>2</sub>-philic detergent could not completely decellularise these tissues. The pre-treatment significantly reduced the mechanical properties of articular cartilage. One possible solution to enhance the efficiency of the scCO<sub>2</sub> and CO<sub>2</sub>-philic detergent decellularisation and to avoid these aggressive pre-treatment steps is a modification of the process parameters such as pressure, treatment time, temperature and concentration of detergent. A higher process pressure (not possible with the autoclave used) could help to entirely remove the CO<sub>2</sub>-philic detergent LS-54 by simple rinsing with scCO<sub>2</sub>. With the current protocol, decellularised tissues still contained residual detergent and required an additional washing step in PBS to obtain a high biocompatibility. The detergent Dehypon® LS-54 is a common household and industrial surfactant, which has a high toxicity for aquatic organisms according to its safety data sheet. Hence, when used for decellularisation, LS-54 should be completely removed to avoid cytotoxicity. In preliminary tests of different doses of LS-54 in DMEM, a concentration as low as 0.01% demonstrated

toxicity on bovine chondrocytes. Living chondrocytes were observed at a concentration of 0.002% (data not shown). Thus, a complete removal of LS-54 is paramount. Trace amounts of this detergent can be detected by analytical methods such as nuclear magnetic resonance (NMR) (Juanssilfero et al., 2011). Thus, it would be possible to use NMR to evaluate the successful removal of the detergent LS-54 from the decellularised tissues. The size of the diverse decellularised tissues was different. This was due to the distinct processing steps of each tissue and different available tissue sources. However, the use of a supercritical fluid should also enable the use of bigger samples since diffusion is largely enhanced.

One aspect that was not verified completely during this study was the sterility of the decellularised tissues after scCO<sub>2</sub> treatment. scCO<sub>2</sub> can be used as a gentle sterilisation technique for tissues (Bernhardt et al., 2015). For instance, scCO<sub>2</sub> is used to sterilise tendons whereby mechanical properties are maintained (Nichols et al., 2009). However, if sterility was also achievable with the used protocol was not tested. This should ideally be done after a further optimisation of the protocol. However, the fact that cells were cultured with the treated matrix for the biocompatibility assay and no contamination was observed would indicate that the matrix was sterile. Despite these limitations, the scCO<sub>2</sub> and CO<sub>2</sub>-philic detergent decellularisation protocol worked well for tendons that were decellularised without any pre-treatment, while maintaining most of their mechanical properties. The protocols for skin and cartilage were not perfected yet as additional treatment steps were still necessary for decellularisation; however, there is still room for improvement by using a more powerful autoclave. Also, important cell adhesion molecules such as fibronectin and laminin were preserved in the ECM of all tested tissues after the procedure, an important aspect that was widely neglected in earlier publications. The focus of future experiments should be a further optimisation of the process parameters for all tissues, a substantial reduction of pre- and post-treatment steps for skin and cartilage and complete sterility testing. Taken together, the use of scCO<sub>2</sub> and CO<sub>2</sub>-philic detergent had advantages when compared to established methods for the decellularisation of tendons. With further optimisation of the process parameters, it could also become a true alternative for other dense tissues, including skin and cartilage.

## 5.7 Acknowledgements

We would like to thank the Swiss National Science Foundation (#200021-150190 and #IZLCZ3-156126) and the Lausanne Orthopaedic Research Foundation (LORF) for their financial support. P.A. was supported by a MD-PhD Leenaards grant. Additionally, we thank Sandra Jaccoud and Dr Virginie Philippe for assistance with the DAL Biobank and Maxence

Volz and Cédric Peneverye for their work on the skin decellularisation. Furthermore, we would like to thank Valérie Malfroy Camine for her precious help with the data visualisation.

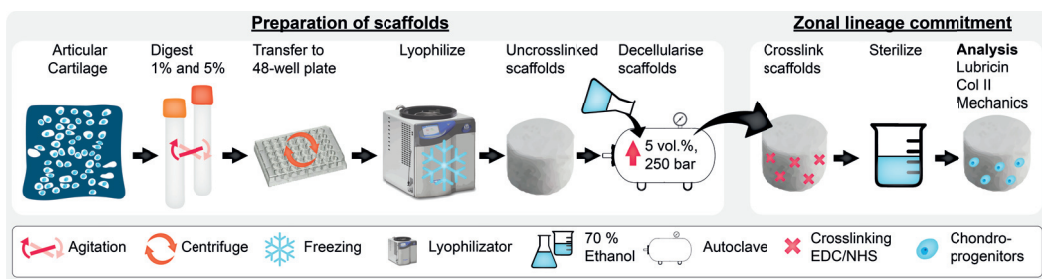


# Chapter 6

## Engineering the Superficial Zone in Cartilage Scaffolds based on Decellularised Bovine Articular Cartilage

*J. Antons, P.E. Bourban, D.P. Pioletti, L.A. Applegate. Manuscript submitted to The Journal of Tissue Engineering and Regenerative Medicine*

### 6.1 Graphical Abstract



### 6.2 Abstract

A novel strategy to enhance the functional properties of cartilage tissue engineering scaffolds is to mimic the zonal characteristics of articular cartilage. Notably, the superficial zone at the cartilage-cartilage interface fulfills a key function by providing lubrication and resistance to

shear stress. To implement the superficial zone, current research has focused on discerning the impact of biomaterial design and distinct external cues on zonal lineage commitment. However, most of the current approaches make use of synthetic materials, which commonly possess a lower bioactivity than natural materials. The higher bioactivity of natural materials has the advantage of potentially avoiding additional growth factors. Thus, the present work has focused on producing scaffolds based on decellularised articular cartilage to induce the superficial zone. To manufacture these scaffolds, bovine articular cartilage was first pepsin-digested, transferred into molds and lyophilized. Subsequently, a decellularisation protocol based on supercritical carbon dioxide and ethanol was adapted to remove remaining cell material from the scaffolds. Secondly, the scaffolds were crosslinked with different concentrations of EDC/NHS. It was demonstrated that the mechanical properties of the scaffolds could be tailored by changing the digest concentration prior to lyophilization. Interestingly, without using growth factors, human chondro-progenitors cultured within these scaffolds have shown signs of zonal lineage commitment towards the superficial zone by producing lubricin on the scaffold surface after 28 days of culture. These encouraging results could aid to implement the superficial zone with zone-specific cellular activity in future cartilage tissue engineering scaffolds.

**Keywords:** decellularisation, differentiation, extracellular matrix, human chondro-progenitors, superficial zone, zonal mechanical properties

### 6.3 Introduction

Articular cartilage consists of different zones depending on tissue depth, namely: superficial, middle, deep and calcified zone (Temenoff and Mikos, 2000). Each of these zones has a distinct purpose and contributes to the overall function of articular cartilage. Thus, to enhance the functional properties of scaffolds in cartilage tissue engineering, recent approaches have focused on mimicking the zonal characteristics of articular cartilage (Klein et al., 2009; Moutos et al., 2007; Tatman et al., 2015). Particularly, the superficial zone at the cartilage-cartilage interface fulfills a key function by providing lubrication and resistance to shear stress (Minns and Steven, 1977; Rhee et al., 2005; Schumacher et al., 1994). The low friction at the surface can mainly be attributed to the expression of lubricin, whereas the resistance to shear stress can be associated to the parallel orientation of collagen fibers in the superficial zone (Minns and Steven, 1977; Rhee et al., 2005; Schumacher et al., 1994). Lubricin is a mucinous glycoprotein which coats the cartilage surface to provide boundary lubrication that is superior to the lowest friction man-made material to date (Teflon) (Jay

and Waller, 2014). The expression of lubricin is a unique feature which distinguishes the superficial zone from the other zones in articular cartilage. Remarkably, the superficial zone only has a thickness of approximately 200  $\mu\text{m}$  and comparatively low mechanical properties ranging from  $0.020\pm 0.003$  MPa to  $1.16\pm 0.20$  MPa (Antons et al., 2018b; Chen et al., 2001a).

Mimicking the superficial zone of articular cartilage is believed to enhance lubrication at the cartilage surface and provide resistance to shear stress. Implementing superficial zone characteristics such as the mechanical properties in scaffolds for cartilage tissue engineering may increase the durability of the forming cartilage tissue by giving lubrication and shear resistance. To produce superficial zone characteristics, the chondrocytes should follow a zone-specific lineage commitment. Generally, in previous studies, zonal lineage commitment was controlled by modifying the composition as well as the mechanical properties of biomaterials or using external cues such as oxygen tension or growth factors (Grad et al., 2005; Khala et al., 2007; Mhanna et al., 2013; Nguyen et al., 2011b; Niikura and Reddi, 2007; Wise et al., 2009; Zhu et al., 2017). When targeting the superficial zone by biomaterial design, recent studies have focused on mimicking the characteristic parallel fiber orientation and/or the mechanical properties of the superficial zone. Thus, the parallel collagen fiber orientation in the superficial zone was obtained by electrospun PCL-fiber scaffolds which has been shown to enhance chondrogenesis (Wise et al., 2009). Further, the mechanical properties of the superficial zone were targeted in scaffolds with initial scaffold elastic moduli of  $199.71\pm 89.60$  kPa and likewise with a spatial gradient of mechanical properties of 5–60 kPa (Nguyen et al., 2011b; Zhu et al., 2017). Using the initial elastic modulus of  $199.71\pm 89.60$  led to superficial zone characteristics such as a higher collagen II (col II) content and lower glycosaminoglycan (GAG) content compared to scaffolds with higher elastic modulus (Nguyen et al., 2011b). In the elastic modulus range investigated (5–60 kPa), for the hydrogels seeded with either chondrocytes or MSCs, a zone-specific extracellular matrix deposition was observed (Zhu et al., 2017). Similar to the biomaterial design, external cues such as normoxic oxygen tension or growth factors could induce superficial zone cartilage indicating the characteristic lubricin expression (Lee et al., 2010; Mhanna et al., 2013)

One aspect, which has rarely been studied to discern zonal lineage commitment, is the use of decellularised tissue matrices. The advantage of using decellularised tissue matrices is their inherent bioactivity, which potentially allows to omit the use of external cues such as growth factors. Indeed, due to the reported chondrogenic effect of decellularised cartilage, this material would be an attractive approach to enhance zonal lineage commitment (Bautista et al., 2016; Beck et al., 2016; Cheng et al., 2009; Hwang et al., 2007). In one recent study,

zonal lineage commitment was observed in human mesenchymal stem cells (MSCs) when zone-specific growth factors were supplied in hydrogels fabricated from decellularised bovine articular cartilage (Moeinzadeh et al., 2018). We hypothesized that scaffolds fabricated from decellularised articular cartilage can induce the superficial zone phenotype without the use of additional growth factors. This hypothesis was based on the aforementioned observed effect of decellularised articular cartilage on zonal lineage commitment as well as on chondrogenesis. In contrast to other studies in cartilage tissue engineering, which mostly work with autologous, nasal-septum, polydactyly and auricular chondrocytes as well as MSCs and adipose-derived stem cells (Brittberg et al., 2018; Maehara et al., 2017; Martin et al., 2015; Mortazavi et al., 2017; Mumme et al., 2016; Nam et al., 2018; Wong et al., 2018; Zuk et al., 2002), we used human chondro-progenitors. The advantage of chondro-progenitors is their stable phenotype and that they don't require growth factors for chondrogenic lineage commitment (Darwiche et al., 2012; Studer et al., 2017).

The purpose of this study was, therefore, to fabricate decellularised articular cartilage based scaffolds with adjustable mechanical properties to induce chondro-progenitors in the superficial zone phenotype without the use of additional growth factors. The creation of the superficial zone in scaffolds would be a valuable feature to engineer hyaline cartilage with native structure and function in future cartilage treatments.

## 6.4 Materials and Methods

### 6.4.1 Scaffold Fabrication

Bovine articular cartilage was obtained from a local slaughterhouse and carefully harvested from the femoral condyle with a scalpel while working on ice. The processing of bovine cartilage into a porous and crosslinked scaffold is described in Figure 6.1. Briefly, cartilage was cut into small pieces (approximately 3 mm x 3 mm) using a scalpel. Thereafter, the cartilage was digested in 1 mg/ml hyaluronidase (H3506, Sigma-Aldrich, Buchs, Switzerland) in PBS at ambient temperature on an orbital shaker for 24 h. This was followed by a second digestion in 0.5 M acetic acid (695092, Sigma-Aldrich, Buchs, Switzerland) supplemented with 10 mg pepsin/100 mg (P7125, Sigma-Aldrich, Buchs, Switzerland) dry tissue at ambient temperature under mild agitation on an orbital shaker for 48 h. To modify the mechanical properties of the scaffolds, two different digest concentrations were chosen: 10 mg dry tissue/ml 0.5 M acetic acid (loose) and 50 mg dry tissue/ml 0.5 M acetic acid (dense). From now on, we refer to these digest conditions as loose and dense scaffolds, respectively.

Afterwards, the digest was carefully filtered through a 70  $\mu\text{m}$  cell strainer (Corning, New York, USA) by centrifuging at 3000 RPM for 5 min. The pH of the filtered cartilage digest was then adjusted to pH 7 using cold (4°C) 10 M NaOH to avoid premature gelation. Subsequently, 400  $\mu\text{l}$  of the digest was distributed in each well of a 48-well plate. To remove bubbles, the 48-well plate was centrifuged at 2000 RPM for 5 min. The samples were then frozen at -80°C for 3 h and subsequently lyophilized in a table top lyophilizer (FreeZone 2.5 Liter -50°C, Labconco, USA) at -0.200 mbar for 24 h. From now on these uncrosslinked samples are referred to as “Before treatment”. Later, samples were decellularised by treatment with  $\text{scCO}_2$  only (sample name:  $\text{scCO}_2$  only) and  $\text{scCO}_2/\text{EtOH}$  (sample name:  $\text{scCO}_2/\text{EtOH}$ ).

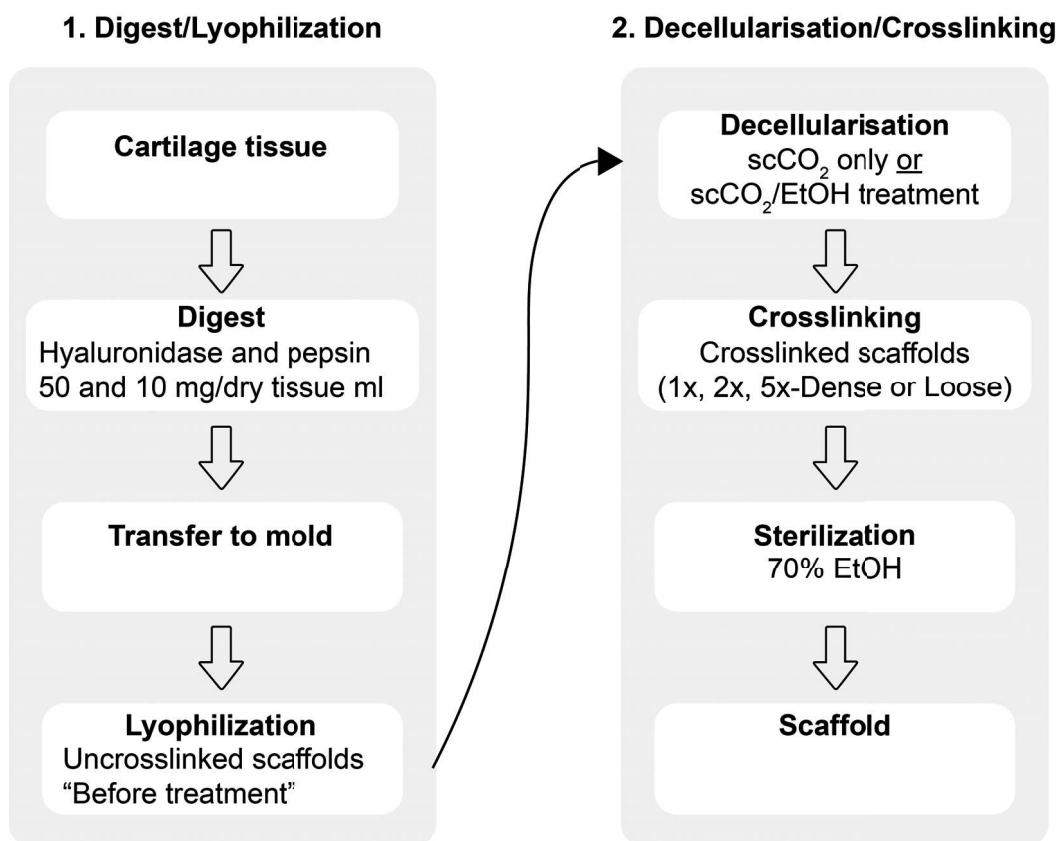


**Figure 6.1 Scaffold fabrication and decellularisation protocols.** 1. Bovine cartilage tissue is digested, transferred to a mold and lyophilized to yield uncrosslinked scaffolds ("before treatment"). 2. Next, the uncrosslinked scaffolds are decellularised either with  $\text{scCO}_2$  only or  $\text{scCO}_2/\text{EtOH}$  followed by crosslinking with EDC/NHS using different crosslinker concentrations (1x, 2x, 5x). Finally, scaffolds are sterilized by 70% EtOH.

### 6.4.2 Decellularisation with scCO<sub>2</sub>/EtOH

The scCO<sub>2</sub> treatment was similar to a previously reported procedure of our group (Antons et al., 2018a). The treatment was modified by using ethanol (EtOH) instead of a CO<sub>2</sub>-philic detergent to add polarity to scCO<sub>2</sub>. Briefly, an autoclave (SITEC AG, Switzerland) was filled with 5%(w/v) 70% EtOH. The lyophilized, but uncrosslinked cartilage samples were then sealed in sterilization bags (Medline Industries, USA) and placed in the autoclave. Carbon dioxide (99.9% pure, Carbagas AG, Lausanne Switzerland) was introduced into the pressure vessel (volume of vessel: 4 L) and the pressure was progressively increased to 250 bars using a high-pressure pump. The temperature was adjusted to 37°C. The samples were constantly treated for 1 h under these conditions. Later, the pressure vessel was rapidly depressurized using a manual valve at a depressurization rate of approximately 100 bars/min.

### 6.4.3 EDC/NHS Crosslinking

The obtained samples from the decellularisation treatments were then chemically crosslinked using EDC/NHS as previously described elsewhere (Rowland et al., 2013). Briefly, 11.5 mg EDC (22980, ThermoFisher, Waltham, USA) and 2.8 mg NHS (24510, ThermoFisher, Waltham, USA) were dissolved in 1 ml of 75% EtOH. We defined this condition (11.5 mg EDC and 2.8 mg NHS in 1 ml) as 1x crosslinker, whereas 2x (23 mg EDC and 5.6 mg NHS in 1 ml) and 5x (57.5 mg EDC and 14 mg NHS in 1 ml) corresponds to a multiplication of the concentration in the initial condition. The resulting scaffolds were named according to the digest and crosslinker concentration as described in Table 6.1.

**Table 6.1 Terminology of scaffolds depending on digest and crosslinker concentration.**

Scaffold name	Digest concentration	Crosslinker
1x-Dense	Dense	1x
2x-Dense	Dense	2x
5x-Dense	Dense	5x
1x-Loose	Loose	1x
2x-Loose	Loose	2x
5x-Loose	Loose	5x

Next, the crosslinking solution (EDC/NHS in 75% EtOH) was uniformly pipetted on the lyophilized and uncrosslinked cartilage digest to fully immerse the samples. The crosslinking reaction was performed for 2 h at ambient temperature under the laminar flow hood to ensure sterility. To remove remaining EtOH and crosslinker, the samples were thoroughly washed

under the laminar flow hood in sterile PBS for 5 cycles of 15 min. Finally, the samples were sterilized in 70% EtOH for 1 h.

#### **6.4.4 DNA Extraction**

To assess the effectiveness of the scCO<sub>2</sub>/EtOH decellularisation protocol, the total DNA content was quantified. Briefly, samples were completely dried using a bench top lyophilizer (FreeZone 2.5 Liter -50°C, Labconco, USA) at -0.200 mbar for 24 h and the dry weight was recorded. The samples were then thoroughly digested in papain buffer (100 mM Na<sub>2</sub>HPO<sub>4</sub>, 100 mM EDTA, 10 mM cysteine-HCL, pH 6.5) supplemented with 250 µg papain/ml at 65°C under agitation at 750 RPM overnight or until no visible scaffold material remained. Next, this digest was purified by Phenol:Chloroform:Isoamylalcohol (25:24:1, v/v). The aqueous phase was ethanol precipitated on ice for 30 min. Following centrifugation, the DNA pellet was carefully washed and reconstituted in nuclease free water. Finally, the DNA content was quantified by a NanoDrop spectrophotometer (Thermo Fisher Scientific, Waltham, MA, USA). Each sample condition (before treatment, scCO<sub>2</sub> only and scCO<sub>2</sub>/EtOH) was measured in quadruplicate.

#### **GAG Content**

To evaluate the effect of the decellularisation protocols on the GAG content, a 1,9-dimethylmethylene blue dye (DMMB) assay was performed to quantify GAGs. Briefly, a standard curve was prepared by chondroitin sulphate dilutions ranging from 0 to 100 µg. Scaffolds with a dry weight of approximately 10 mg were previously digested in 1 ml papain buffer (100 mM Na<sub>2</sub>HPO<sub>4</sub>, 100 mM EDTA, 10 mM cysteine-HCL, pH 6.5) supplemented with 250 µg papain/ml at 65°C under agitation at 750 RPM overnight. Subsequently, 100 µl of the scaffold digest was distributed into a 96-well plate in triplicate. Then DMMB solution was added and the absorbance was immediately read on a microplate reader (Wallac 1420 Victor2, Perkin Elmer, USA) at a wavelength of 595 nm. To determine the GAG content for the different scaffold conditions, the aforementioned chondroitin sulphate concentrations were plotted against their corresponding absorbance values. Each sample condition (before treatment, scCO<sub>2</sub> only and scCO<sub>2</sub>/EtOH) was measured in triplicate.

#### **Scanning Electron Microscopy**

To evaluate the ultrastructure of samples obtained with different digest and crosslinking concentrations, Scanning Electron Microscopy (SEM) was performed. Briefly, the samples were lyophilized using a bench top lyophilizer (FreeZone 2.5 Liter -50°C, Labconco, USA)

at -0.200 mbar for 24 h and subsequently coated with 10 nm carbon using a carbon coater. Images were acquired using a scanning electron microscope (Merlin resolution SEM, Zeiss, Germany) at three magnifications, namely: 200, 2,000 and 50,000 with an accelerating voltage of 1.2 kV.

### **Compression Test**

To assess the elastic modulus of the different sample conditions (before treatment, scCO<sub>2</sub> only and scCO<sub>2</sub>/EtOH), an unconfined compression test was performed on a uniaxial test system (Instron E3000, Instron, USA; load cell: 50 N). The same compression test was performed for the different digest (loose, dense) and crosslinker (1x, 2x, 5x) concentrations. Briefly, scaffolds (9.8 mm diameter and 3 mm height) were swollen in PBS at ambient temperature overnight. Then, each scaffold condition was compressed to 50% strain at a compression rate of 500  $\mu$ m/s. The elastic modulus was determined from the stress-strain curve between 20 and 40% of strain. Each sample condition was measured in quintuplicate.

### **Cell Seeding**

For the biological tests, human chondro-progenitors were used (Darwiche et al., 2012; Studer et al., 2017). Chondro-progenitors at passage 3 were expanded in cell culture flasks using DMEM medium (10% FBS, 1% L-glutamine, 1% pen-strep) until 80% confluence was reached. Subsequently, lyophilized and crosslinked scaffolds were distributed in a 48-well plate. One million chondro-progenitors at passage 4 in 20  $\mu$ l DMEM medium (10% FBS, 1% L-glutamine, 1% pen-strep) were evenly pipetted on the surface of the scaffolds. The plate was then transferred to a cell culture incubator with humidified atmosphere at 5% CO<sub>2</sub> and 37°C for 2 h to enable cell adhesion. Finally, 1 ml of fresh DMEM medium was added to the scaffolds, which were then re-transferred to the incubator. The medium was changed every other day.

### **Histology**

Samples were thoroughly fixed in 4% paraformaldehyde at ambient temperature overnight. Next, slices with a thickness of 5  $\mu$ m were processed with a microtome and stained by standard histology methods for cell nuclei by Hematoxylin Eosin (H&E) and DAPI, sulphated GAGs by Alcian Blue (AB) and collagen by Masson trichrome (MT) staining. Immunohistochemistry was performed to detect collagen type II (col II), fibronectin, lubricin and collagen type X (col X). The human articular cartilage tissue was obtained from the DAL/CHUV



biobank (Lausanne), under anonymous donation, in accordance with its regulation and approval by the Institutional Biobank. Briefly, samples were first incubated with lubricin (polyclonal, 1:200; MABT400, Sigma-Aldrich, Buchs, Switzerland), col II (polyclonal, 1:200; ab34712, Abcam, Cambridge, United Kingdom), col X (polyclonal 1:200; ab58632, Abcam, Cambridge, United Kingdom) and fibronectin (monoclonal, 1:200; 610077, BD Biosciences, USA) at 4°C overnight. A peroxidase reaction was used to detect lubricin, col II and col X (ImmPRESS™ HRP, Vectorlabs, USA), whereas fibronectin was detected by immunofluorescence (polyclonal, Alexa Fluor 568, 1:100; Invitrogen, USA at ambient temperature for 2 h). Tissue sections were examined under a widefield microscope (DM 5500, Leica, Germany). Each sample condition (before treatment, scCO<sub>2</sub> only and scCO<sub>2</sub>/EtOH) was evaluate in triplicate.

#### 6.4.5 Statistical Methods

An unpaired two-tailed Student's t-test was used to determine the statistical significance between the DNA and GAG content of each sample condition. The same statistical test was used to determine the difference between the mechanical measurements depending on the crosslinking degree (1x, 2x, 5x) and the digest concentration (loose and dense scaffold) depending on the cell culture time (14 and 28 days). Samples were statistically significant when \* $p < 0.05$  and named not statistically significant (n.s.) when  $p > 0.05$ .

## 6.5 Results

### DNA and GAG content

The decellularisation procedure with scCO<sub>2</sub>/EtOH significantly (\* $p < 0.05$ ) reduced the DNA content ( $111 \pm 77$  ng dsDNA/mg dry scaffold) compared to the scaffold before treatment ( $311 \pm 103$  ng dsDNA/mg dry scaffold) or scCO<sub>2</sub> only ( $286 \pm 79$  ng dsDNA/mg dry scaffold) (Figure 6.2). Another favorable decellularisation effect was seen in the H&E and DAPI staining's (Figure 6.7), where both staining's indicated no traces of visible cell nuclei. Simultaneously, GAG content was not affected by scCO<sub>2</sub> treatment only ( $2.90 \pm 0.54$   $\mu\text{g}/\text{mg}$  dry scaffold) or scCO<sub>2</sub>/EtOH ( $2.79 \pm 0.64$   $\mu\text{g}/\text{mg}$  dry scaffold) compared to the sample before treatment ( $2.52 \pm 0.23$   $\mu\text{g}/\text{mg}$  dry scaffold) (Figure 6.2).

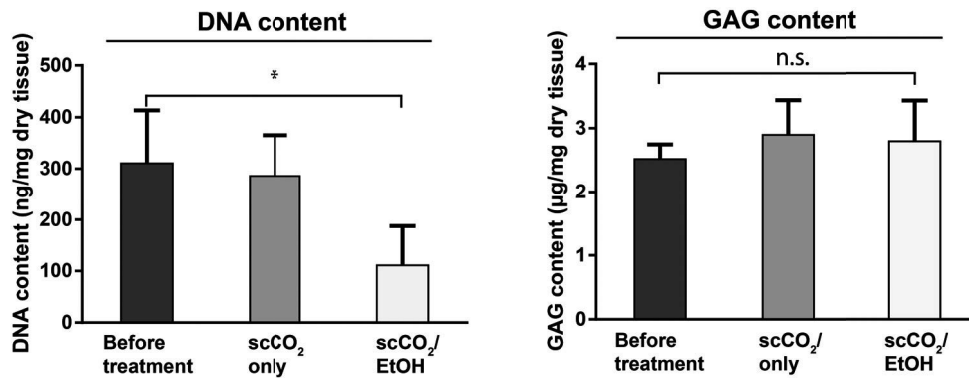


**Figure 6.2 DNA and GAG content of the decellularised articular cartilage scaffold.** n= 4 samples per condition (\*p<0.05), n.s.: not statistically significant.

## SEM

To assess the ultrastructure of the scaffolds before and after decellularisation as well as the effect of the different digest and crosslinker concentrations, SEM images were acquired (Figure 6.3). When compared, the non-treated, scCO<sub>2</sub> only and scCO<sub>2</sub>/EtOH treated scaffolds showed no change in the ultrastructure (Figure 6.3). In all conditions, aggregated spherical particles can be identified in the highest magnification. When analyzing the impact of the different digest and crosslinker concentrations on the ultrastructure of the scaffolds, alterations can be identified (Figure 6.4). Hence, the scaffolds with a higher crosslinker concentration (5x), showed aggregated spherical particles, whereas with lower crosslinker concentrations (1x, 2x) fiber-like structure were found in the highest magnification.

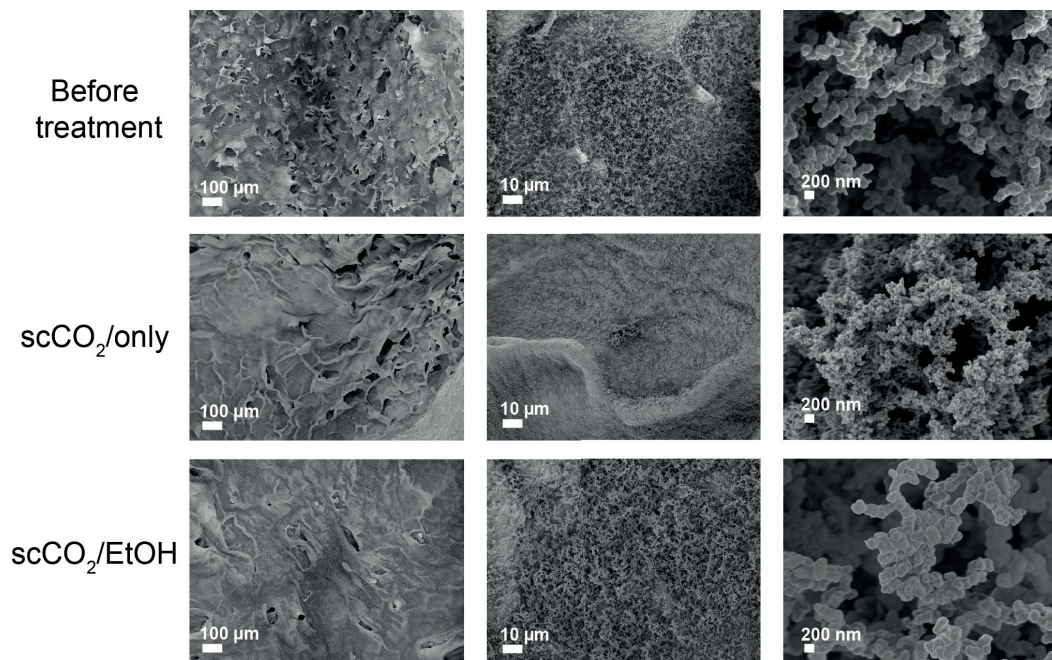


**Figure 6.3 Ultrastructure of scaffolds after decellularisation treatment.** Influence of scCO<sub>2</sub> and scCO<sub>2</sub>/EtOH treatment on the ultrastructure of the scaffolds. In particular in the middle, scale bar: 10 μm and highest magnification, scale bar: 200 nm, a change in ultrastructure was observed. All samples were crosslinked with the 5x crosslinker concentration.

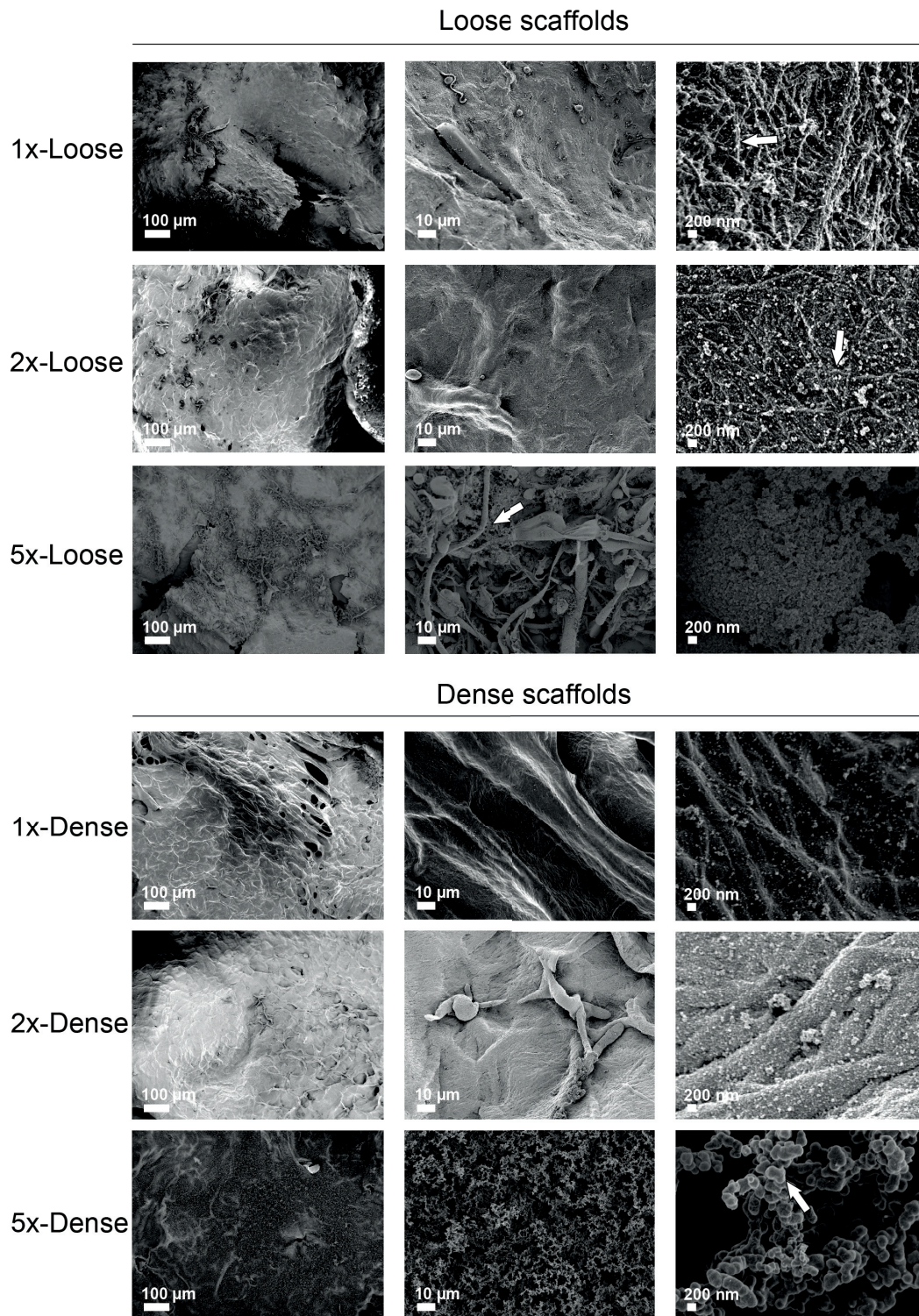


**Figure 6.4** Ultrastructure of the decellularised articular cartilage scaffolds depending on the digest and crosslinker concentration. The upper part shows the ultrastructure of loose scaffolds depending on different crosslinker proportions (1x, 2x, 5x). The lower part illustrates the ultrastructure of the dense scaffolds depending on the crosslinker concentration (1x, 2x, 5x). Arrows correspond to either fiber-like structures or granules.

### Mechanical Properties

To evaluate the effect of the scCO<sub>2</sub>/EtOH decellularisation treatment on the elastic modulus, the different treatment conditions were compared (before treatment, scCO<sub>2</sub> only and scCO<sub>2</sub>/EtOH) (Figure 6.5 A.). The elastic modulus of the treated scaffolds (scCO<sub>2</sub>/only: 25.33±7.53 kPa and scCO<sub>2</sub>/EtOH: 18.99±5.96 kPa) was slightly reduced compared to the samples before treatment: 29.75±6.15 kPa.

Next, the elastic modulus of the scaffolds depending on the digest and crosslinker concentration was measured (Figure 6.5 B.). In the case of the dense scaffolds, the different elastic moduli were: 28.27±7.81 kPa for 5x-Dense, 20.79±7.76 kPa for 2x-Dense and 28.85±12.37 kPa for 1x-Dense. For the loose scaffolds, the following values were measured: 2.80±1.77 kPa for 5x-Loose, 4.46±1.40 kPa for 2x-Loose and 6.10±4.58 kPa for 1x-Loose. The elastic modulus changed significantly (\*p<0.05) between dense and loose scaffolds, but no significant difference was observed between the crosslinker concentrations.

For the cell-seeded scaffolds, only the elastic modulus of the dense scaffold could be measured due to contraction of the loose scaffold (Figure 6.6). Comparing the different time points of each crosslinking condition, the elastic modulus has increased over time. For the 1x-Dense scaffolds, the elastic modulus has increased from 28.27±7.81 kPa (day 0) to 123.41±12.75 kPa (day 14) and 451.81±170.52 kPa (day 28), respectively. A similar trend was observed for the 2x-Dense and 5x-Dense scaffolds.

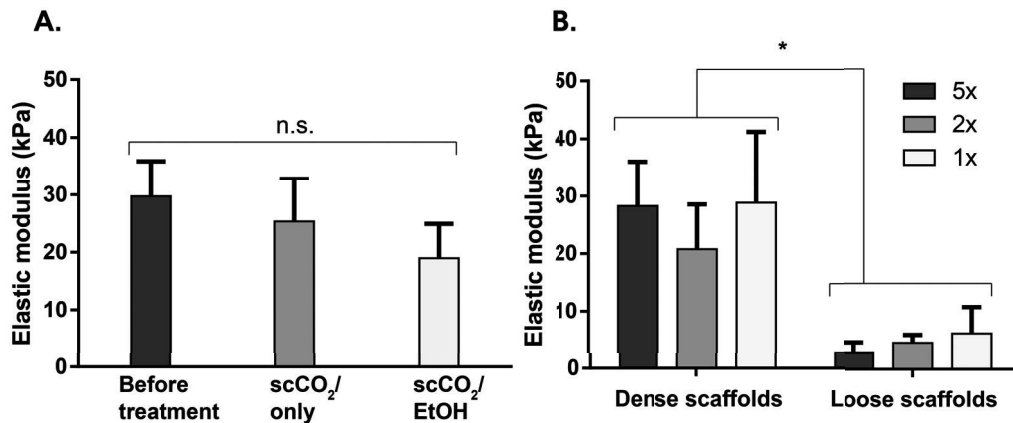


**Figure 6.5 Elastic modulus of the scaffolds depending on decellularisation, digest concentration and crosslinker concentration.** A. Effect of the decellularisation treatment. B. Effect of digest and crosslinker concentration. n.s.: not statistically significant.

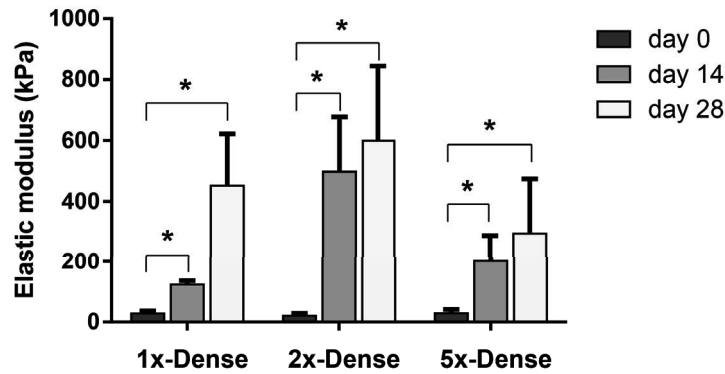


**Figure 6.6 Elastic modulus as a function of crosslinking in dense scaffolds increased over time when scaffolds were seeded with chondro-progenitors. (\* $p < 0.05$ ).** Note: Only the dense scaffolds were measured due to contraction of the loose scaffolds.

### Histology

First, immunohistochemistry was used to screen for specific extracellular matrix (ECM) molecules and to analyze the impact of the decellularisation protocol (before treatment, scCO<sub>2</sub> only and scCO<sub>2</sub>/EtOH). Hence, the presence of fibronectin, col II, col X and lubricin were evident (Figure 6.7). In native cartilage, fibronectin was detected in the superficial zone, whereas in all decellularisation conditions fibronectin was identified throughout the entire ECM. The same effect was observed for the lubricin staining. Lubricin was located at the surface of human articular cartilage and was only mildly detected in the scaffolds prior to cell seeding. Col II was ubiquitously present in the ECM. Col X was mainly identified around chondrocytes in native cartilage, but only weakly detected in the scaffolds.

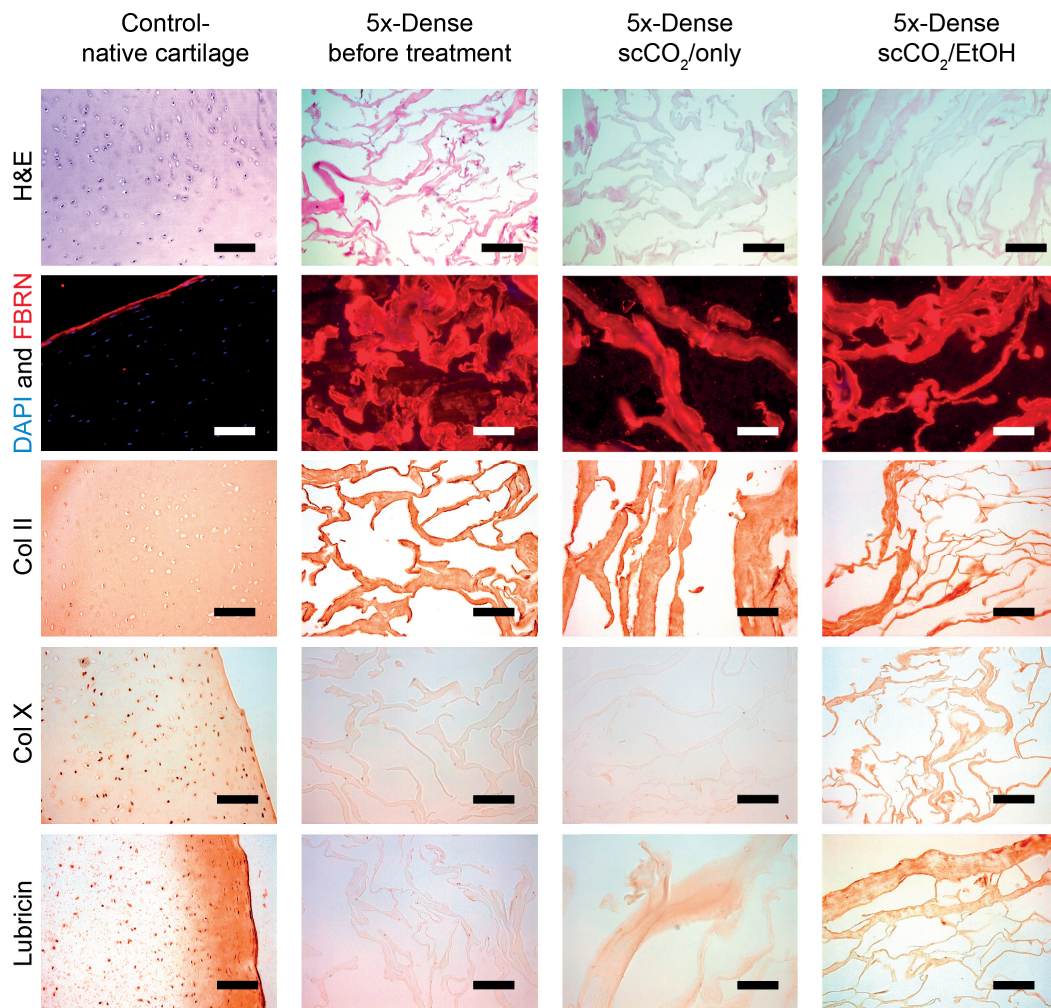


**Figure 6.7 Immunohistochemistry before and after decellularisation.** Presence of fibronectin (FBRN), collagen type II (col II), collagen type X (col X) and lubricin was corroborated, scale bar: 200  $\mu$ m.

Secondly, to evaluate the ECM secreted from the chondro-progenitors after 14 days and 28 days, GAGs (Alcian Blue (AB)) and collagen (Masson's Trichrome (MT)) were examined (Figure 6.8 and Figure 6.9, respectively) by histology. For the loose scaffolds, the chondro-progenitors formed aggregates (Figure 6.8, H&E- black arrows). Chondro-progenitors presented a moderate secretion of GAGs, indicated by AB staining surrounding the cells. In the case of the dense scaffolds, the cells were mainly located at the surface. Similar to the loose scaffolds, GAG expression was evident surrounding the cells. Finally, to further assess the zonal lineage commitment for the superficial zone, immunohistochemistry for lubricin and col II was performed (Figure 6.10). In the positive control (human articular cartilage), lubricin expression was identified mostly at the surface, whereas col II had a low intensity at the surface. For lubricin, a similar pattern was seen in the 1x-Dense scaffolds.

For the 1x-Loose scaffolds, intense lubricin staining was observed surrounding the cell aggregates. In case of col II, the staining intensity was quite homogeneous for the dense and loose scaffolds.

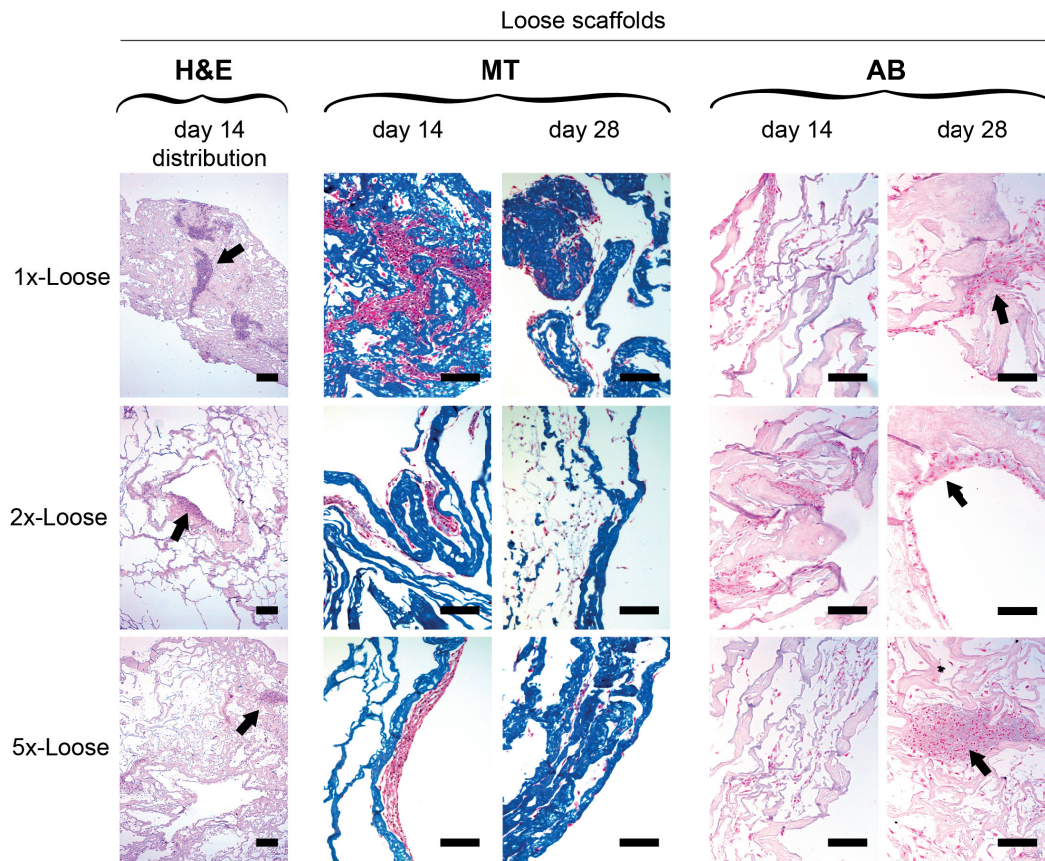


**Figure 6.8** ECM secretion in decellularised articular cartilage scaffolds after 14 days and 28 days (loose scaffold). H&E staining indicates cell distribution after 14 days cell culture. Black arrows point out cell aggregates (H&E) and secreted GAGs surrounding the cells (AB). Collagen can be detected throughout the scaffolds (MT). Scale bar: 200  $\mu\text{m}$ .



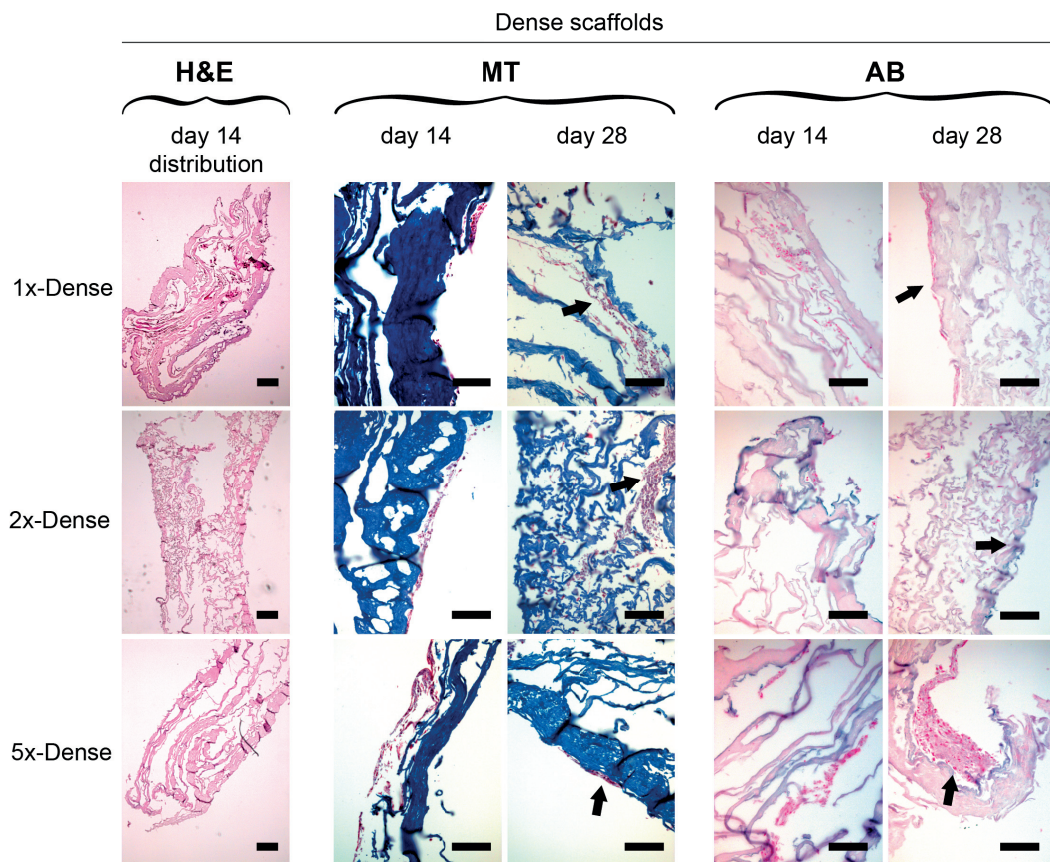


**Figure 6.9** ECM secretion in decellularised articular cartilage scaffolds after 14 days and 28 days (dense scaffold). H&E staining indicates cell distribution after 14 days cell culture. Black arrows point out cell aggregates (H&E) and secreted GAGs surrounding the cells (AB). Collagen can be detected throughout the scaffolds (MT). Scale bar: 200  $\mu\text{m}$ .

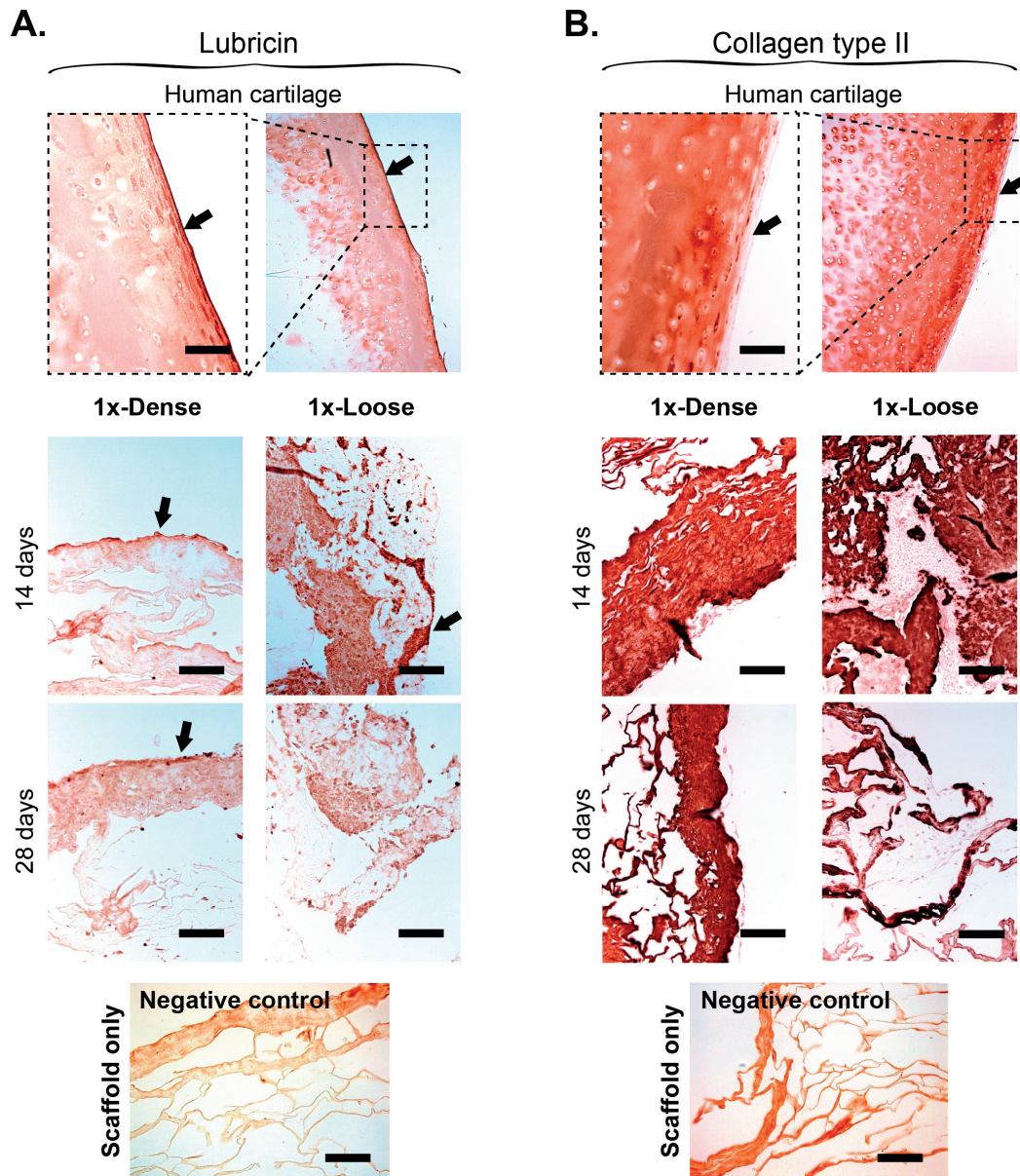


**Figure 6.10** Lubricin and collagen type II secretion in decellularised articular cartilage based scaffolds after 14 days and 28 days (loose and dense scaffold) compared to human articular cartilage (positive control). A. Black arrows indicate that lubricin expression is mainly located at the surface. Negative control indicates a light background staining of the unseeded scaffolds, but with chondro-progenitors, the staining intensity was considerably higher. B. Col II has a low intensity at the surface of articular cartilage. Negative control indicates the background staining of the scaffold without cells. Scale bar: 200  $\mu\text{m}$ .

## 6.6 Discussion

In the present work, we hypothesized that scaffolds fabricated from decellularised articular cartilage can induce zonal lineage commitment towards the superficial zone in human chondro-progenitors without additional growth factors. To validate this hypothesis, an approach to fabricate decellularised articular cartilage based scaffolds with adjustable mechanical properties was developed. To establish this approach, a multistep fabrication protocol was used. First, an optimized procedure adapted to decellularise the scaffolds with scCO<sub>2</sub>/EtOH, has demonstrated to efficiently remove cellular material while maintaining GAG content as well as ultrastructure and mechanical properties. Interestingly, human chondro-progenitors cultured within these scaffolds allow to increase over time the mechanical properties of the scaffolds so that it matched the values of the superficial zone known from literature (Antons et al., 2018b; Chen et al., 2001b). Finally, these same cells seeded within the scaffolds have demonstrated to secrete the superficial zone protein lubricin during 14 and 28 days of cell culture.

The base of the scaffolds in the present work was the decellularised ECM of articular cartilage. In previous attempts to decellularise bovine articular cartilage with scCO<sub>2</sub>, the use of a CO<sub>2</sub>-philic detergent was required (Antons et al., 2018a). Omitting this detergent would further simplify the procedure by reducing washing steps and by avoiding possible detergent residues in the final decellularised tissue. Hence, in the present work, we have decellularised articular cartilage by a more gentle approach based on scCO<sub>2</sub>/EtOH after processing it into a lyophilized porous scaffold. It was necessary to process the decellularised cartilage into scaffolds to facilitate cell infiltration due to the high ECM density in native cartilage (6 nm pore size) (Maroudas, 1976). Decellularisation by scCO<sub>2</sub>/EtOH has formerly demonstrated to produce biocompatible, acellular tissues (Casali et al., 2018; Guler et al., 2017; Halfwerk et al., 2018; Huang et al., 2017; Sawada et al., 2008; Wang et al., 2017a; Zambon et al., 2016). Using scCO<sub>2</sub>/EtOH, the DNA content of the scaffolds was significantly reduced (\*p<0.05) compared to the scaffolds before treatment. Similarly GAG content was not affected by the scCO<sub>2</sub> and scCO<sub>2</sub>/EtOH treatments compared to the scaffold before treatment (Figure 6.2), which emphasizes the mildness of the scCO<sub>2</sub>/EtOH treatment. Simultaneously, ECM molecules including fibronectin, col II, col X and lubricin were immunolocalized in the decellularised ECM (Figure 6.7). Furthermore, scCO<sub>2</sub>/EtOH only moderately affected the elastic modulus of the scaffolds compared to before treatment. Hence, with scCO<sub>2</sub>/EtOH decellularisation, 63.83±20.03% of the original elastic modulus of the scaffolds could be maintained in contrast to only 14.44±2.81% with the previous protocol using scCO<sub>2</sub>/LS-54 (Antons et al., 2018a). This further underlines the reduced impact of the scCO<sub>2</sub>/EtOH

decellularisation technique on the mechanical properties of the obtained scaffolds. Likewise, the ultrastructure of the scaffolds was somewhat affected by the scCO<sub>2</sub>/EtOH treatment and illustrated aggregated granules in all treatment conditions (Figure 6.3, 200 nm scale bar). This reconfirms the mildness of the decellularisation procedure since the ultrastructure was not further changed by the decellularisation treatment.

To induce the superficial zone phenotype, scaffolds with different properties were fabricated by modifying the digest and crosslinker concentrations. The different crosslinker concentrations (1x, 2x, 5x) did not have a significant influence on the mechanical properties within the evaluated concentration range. Nonetheless, the crosslinker concentration was able to modify the ultrastructure. Thus, lower crosslinker concentrations (2x, 1x) produced fiber-like structures (Figure 6.4, 200 nm scale bar, indicated by white arrow), whereas 5x crosslinker concentration generated aggregated granules. Indeed, lower crosslinker concentrations should be preferred since this favors fiber-like structures. This is in agreement with native articular cartilage, in which collagen fibers of different diameters and orientations can be detected (Minns and Steven, 1977; Weiss et al., 1968). Our results are also in line with another study, in which a lower crosslinker concentration resulted in fewer changes in ultrastructure and a higher bioactivity (Rowland et al., 2013). Since lowering the crosslinker concentrations seemed to be more favorable for the ultrastructure of the scaffolds (fiber-like structures), we mainly focused further analysis on the 1x crosslinked scaffolds.

As previously mentioned, the digest concentration showed a greater effect on the mechanical properties of the scaffold than the crosslinker concentration (Figure 6.5 B.). Additionally, a lower digest concentration (loose scaffold) was associated with collagen fibers of smaller diameter within the scaffolds than in the higher digest concentration (dense scaffold) (Figure 6.4, 200 nm scale bar, indicated by white arrow). This effect could also be used to implement a more native cartilage-like fiber appearance within the scaffolds. Hence, the fiber diameters could be adapted to match the collagen fiber diameters of the superficial zone, which have a smaller diameter than in the other cartilage zones (Muir et al., 1970). Comparing the mechanical properties of the loose and dense scaffolds reveals a 5-10 times lower elastic modulus in the loose scaffolds (\*p<0.05). For instance, within the dense scaffolds an initial elastic modulus of  $28.85 \pm 12.37$  kPa (1x crosslinker) compared to  $6.10 \pm 4.58$  kPa (1x crosslinker) for the loose scaffolds was measured. These initial scaffold properties are in the range of the superficial zone ( $0.020 \pm 0.003$  MPa) (Antons et al., 2018b).

Interestingly, in both digest conditions (loose and dense scaffolds), the presence of the superficial zone-specific protein lubricin was detected by immunohistochemistry (Figure 6.10 A.). Comparing the secretion of lubricin to human articular cartilage (positive control), confirmed a similar surface-located expression for the dense scaffolds. Similarly, previous experiments using the combination of different scaffold properties, revealed lubricin secretion at the surface of the scaffolds (Steele et al., 2014). On the contrary, lubricin secretion was located around cell aggregates in the loose scaffolds. This is comparable to another study in which lubricin expression was immunolocalized around cell aggregates in pellet culture of mesenchymal progenitor cells supplemented with growth factors (Lee et al., 2010). In general, cell aggregates establish important cell-cell contacts which mediate zonal lineage commitment depending on the initial cell density (Karimi et al., 2014; Ren et al., 2016). Even though the immunolocalization of lubricin indicated signs of superficial zone cartilage, this could not be confirmed for col II (Figure 6.10 B.). Usually, the superficial zone has the highest col II content compared to the other zones in articular cartilage (Muir et al., 1970). In contrast, we observed a lower staining intensity of col II at the outermost surface of human articular cartilage (positive control), whereas a bit deeper the col II staining intensity increases sharply (Figure 6.10 B.). This could be due to a possible osteoarthritis-inflicted degeneration in the human cartilage sample. It is known that osteoarthritis-inflicted degeneration usually starts at the cartilage surface (Hollander et al., 1995). Within the scaffolds col II was rather homogeneously expressed and did not indicate a different content at the surface. The commonly high col II content of superficial zone cartilage should be further corroborated in future studies to verify if this can also be induced in the developed scaffolds.

Looking more closely at the mechanical properties during cell culture reveals that the elastic modulus of the dense scaffold was significantly ( $*p<0.05$ ) increased (Figure 6.6). Thus, the elastic modulus of the 1x-Dense scaffolds increased from an initial  $28.27\pm 7.81$  kPa to  $123.41\pm 12.75$  kPa after 14 days and to  $451.81\pm 170.52$  kPa after 28 days. From the three investigated crosslinking concentrations, the 5x-Dense scaffolds showed the lowest increase of mechanical properties. This could be due to the ultrastructure which at high crosslinker concentrations (5x) showed granules instead of fiber-like structures and might thus be less favorable for cell proliferation and adhesion. Comparing these scaffold properties with other studies targeting the superficial zone, shows that the obtained values are in the same range ( $105.78\pm 26.89$  kPa to  $199.71\pm 89.60$  kPa) (Nguyen et al., 2011a,b). Indeed, in these aforementioned studies it was demonstrated that the mechanical properties of scaffolds turned out to be important for zonal lineage commitment. Thus, likewise hydrogels with gradients of mechanical properties could induce zonal lineage commitment (Nguyen et al.,

2011b; Zhu et al., 2017). Furthermore, the observed increase in elastic modulus remains in the range of the reported literature values of approximately  $0.020 \pm 0.003$  MPa and  $1.16 \pm 0.20$  MPa (Antons et al., 2018b; Chen et al., 2001a).

Despite these promising results, there are several limitations of the present study that should be considered. Only two digest concentrations (loose and dense scaffold) and three crosslinker concentrations were evaluated (1x, 2x, 5x). To further tailor the scaffold properties, the range of digest concentrations should be extended. Further, the initial elastic modulus of the loose scaffold was too low and thus the chondro-progenitors caused excessive scaffold contraction. This issue was resolved in previous studies by increasing the mechanical properties of the scaffolds in order to resist the contractile forces of the cells (Rowland et al., 2016). Secondly, external cues such as growth factors, oxygen tension, cell density gradients and mechanical stimulation might be implemented since these have been previously shown, to similarly influence zonal lineage commitment (Cheng et al., 2009; Grad et al., 2005; Karimi et al., 2014; Mhanna et al., 2013; Nguyen et al., 2011b; Wise et al., 2009). It should be emphasized that in the present work no specific growth factors were supplemented in the cell culture medium to induce zonal lineage commitment. We argued, that the seeded chondro-progenitors would not require additional growth factors for zonal lineage commitment due to their chondrogenic stability (Darwiche et al., 2012; Studer et al., 2017). Nonetheless, it would be interesting to investigate a potential synergistic effect of decellularised articular cartilage and external cues such as growth factors. Further, the porosity of the dense scaffolds should be increased to enable a more effective cell ingrowth. To implement a higher porosity of the scaffolds, salt leaching or unidirectional freezing could be utilized to enhance the control of scaffold porosity (Abdel-Sayed et al., 2014; Hou et al., 2003; Nasrollahzadeh et al., 2017; Rowland et al., 2016).

Taken together, the results of the present study suggest, that zonal lineage commitment towards the superficial zone can be achieved without additional growth factors in scaffolds, which are based on decellularised articular cartilage. Eventually these types of scaffolds could similarly be used for effective delivery of other cell sources for enhanced treatments of patients by inducing the cartilage superficial zone.

## 6.7 Acknowledgements

We would like to thank the Swiss National Science Foundation (#200021-150190 and IZLCZ3-156126) for their financial support. Additionally, we thank Sandra Jaccoud for

her assistance with immunohistochemistry, Anaelle Dubois for her help with the Electron Microscopy and the histology core facility of EPFL for their precious support with histology. Finally, we would like to express our gratitude to Dr. Ossama Khalaf and Dr. Ulrike Kettenberger for critical review and proof-reading of this manuscript.





# Chapter 7

## Discussion and Outlook

### 7.1 Clinical Situation

Articular cartilage defects cannot heal spontaneously as already stated by William Hunter in 1742: “From Hippocrates to the present age, it is universally allowed that ulcerated cartilage is a troublesome thing and that, once destroyed, is never recovered” (Hunter, 1742). Cartilage defects, if left untreated, further degrade over time and eventually cause degenerative joint diseases such as osteoarthritis (Ding et al., 2010). Therefore, the main objective of orthopedic surgeons is to treat cartilage defects as early as possible to prevent further damage (Vanlauwe et al., 2011). The major drawback of current clinical treatments is that they all can only create fibrocartilage or a mixture of fibro- and hyaline cartilage (Brun et al., 2008; Goldberg et al., 2017; Oussedik et al., 2015). Fibrocartilage, contrary to native hyaline cartilage, presents inferior mechanical properties and therefore degrades much faster than hyaline cartilage (Mankin, 1974). For successful and long-lasting cartilage regeneration, it would be crucial to have a treatment option that can create hyaline cartilage. One aspect that is believed to be important for the neoformation of hyaline cartilage is a scaffold with a zonal structure presenting mechanical properties similar to native cartilage (Klein et al., 2009; Levett et al., 2014; Tatman et al., 2015). In line with this hypothesis, providing zone-specific characteristics such as cell density, material composition or growth factors have formerly demonstrated to promote zonal lineage commitment (Cheng et al., 2009; Grad et al., 2005; Karimi et al., 2014; Mhanna et al., 2013; Nguyen et al., 2011b; Wise et al., 2009). It has also been shown that even, when only the zonal mechanical properties were implemented in scaffolds, the corresponding zone-specific cell behavior could be observed (Zhu et al., 2017). So far, the best results were achieved, when mechanical properties were combined with cell density and growth factors gradients (Karimi et al., 2014; Nguyen et al., 2011b). All scaffolds used in the aforementioned studies consisted of synthetic polymers requiring

further chemical modification to implement a certain bioactivity (Lutolf and Hubbell, 2005). This limitation can be overcome with the use of biological materials which provide a higher bioactivity due to presentation of extracellular matrix molecules with which cells can interact. It has been shown that decellularised articular cartilage without additional growth factors or chemical modifications has the ability of inducing chondrogenesis (Bautista et al., 2016; Beck et al., 2016; Cheng et al., 2009; Hwang et al., 2007). Those materials should give even better results when used with zone-specific mechanical properties. Therefore, the hypothesis of this thesis is that scaffolds based on decellularised articular cartilage with tailored mechanical properties can induce zonal lineage commitment without the use of additional zone-specific characteristics such as growth factors or cell density.

## 7.2 Summary of the Findings, Discussion and Outlook

For a verification of the hypothesis, a novel type of scaffolds made from decellularised articular cartilage needs to be developed. The development process was divided into three aims. The first aim was to determine the zonal mechanical properties of human articular cartilage with instrumented indentation (**chapter four**). This step was necessary, as no reliable data for human tissues was available in the literature. The measurements were performed on six freshly-frozen human cartilage samples retrieved during surgical intervention in patients of different ages (20-70 years old). The results from the indentations showed a consistent depth-dependent gradient of elastic modulus. Those measurements were correlated to histological sections to determine the quality of the cartilage and detect potential signs of degradation. The results of those measurements were later used to define the mechanical properties of the developed scaffold. Nonetheless, the study had inherent limitations. Instrumented indentation is quite sensitive to local differences and thus sample degradation, sample preparation, and the surrounding environment can influence the accuracy of the measurement. The interline-spacing of 800  $\mu\text{m}$  in the indentation protocol might have been too large and the elastic modulus in the adjacent lines already changed due to different structure or composition. It should be noted that the study exclusively focused on the elastic modulus. Yet, there are additional mechanical parameters such as the friction coefficient, creep, fatigue resistance and toughness which also should be considered for the scaffold design (Lu and Mow, 2008; Mow et al., 1984). Finally, the study only covered six human samples and therefore results need to be validated in consecutive studies covering patients of different age groups and disease stages. Extending the measurements in a larger study can eventually create a “map” of mechanical properties for the fabrication of scaffold designs

which are site-specific.

The second aim of the thesis was the development of an alternative decellularisation technique for bovine articular cartilage that could overcome the limitations of existing complex and time-consuming protocols. The novel protocol was based on supercritical carbon dioxide, a single-step technique which has already shown promising results in other tissues such as aorta, cornea, esophagus and adipose tissues (Guler et al., 2017; Huang et al., 2017; Sawada et al., 2008; Wang et al., 2017a) (**chapter five**). Supercritical carbon dioxide has liquid-like density and gas-like transport properties and can therefore enhance both diffusion and cell removal in articular cartilage (Schneider, 1978). Common decellularisation protocols consist of lengthy tissue-specific protocols combining chemical and physical methods (Crapo et al., 2011). The samples usually have to be immersed in rather aggressive detergents for a long time due to the slow diffusion in denser tissues. The long exposure of the tissues to chemicals negatively influences the bioactivity of the decellularised tissues (Gilbert et al., 2006) as well as the mechanical properties (Crapo et al., 2011). The first tests to decellularise the cartilage were performed with supercritical carbon dioxide and ethanol. Histology showed remaining cell nuclei indicating that the decellularisation was not efficient. Attempts to optimize the process parameters such as increasing the pressure, time and ethanol concentration were not successful. In a second step the ethanol was replaced by a CO<sub>2</sub>-philic detergent as it was hypothesized that the phospholipids of the cell membranes more easily dissolve in detergent than in ethanol. This could be confirmed as the remaining DNA content in the CO<sub>2</sub>-philic detergent-treated samples was lower than in the ones processed with ethanol. However, there were still visible cell nuclei and the DNA content was not below the required threshold of 50 ng dsDNA/mg dry tissue (Crapo et al., 2011). The only way to approach this limit was to add additional steps to the protocol such as freeze-thaw cycles, osmotic shock and enzymatic treatment. With this extended protocol a satisfying decellularisation of bovine articular cartilage was demonstrated. The initial theory of using the developed decellularisation protocol as a single-step technique for both decellularisation and sterilization of the cartilage was not achieved. However, it is not excluded that a more powerful set-up enabling a higher pressure with defined pressure cycles could still fully decellularise articular cartilage in a single step. Nevertheless, the developed technique could have the advantage of including decellularisation and sterilization in a single-step. This is due to the reported usability of supercritical carbon dioxide as gentle sterilization technique (Bernhardt et al., 2015). In future studies this effect has to be studied in more detail using standard sterility testing protocols. For the study presented in **chapter five**, no further sterilization was done and no problems with contamination were observed. Established immersion-based decellularisation

protocols require additional sterilization steps using acids, alcohols, ethylene oxide and gamma irradiation (Freytes et al., 2008; Hodde and Hiles, 2002). These sterilization methods have been shown to negatively influence the ECM and mechanical properties (Rosario et al., 2008; Sun and Leung, 2008). First attempts to recellularise the decellularised tissue samples failed due to the very dense matrix of cartilage which inhibits cell-ingrowth.

The third aim of the thesis was then the fabrication of porous scaffolds with tailorable mechanical properties from decellularised articular cartilage (**chapter six**). The developed protocol has four main steps. In a first step, bovine articular cartilage is enzymatically digested and filtered generating a viscous cartilage slurry. In a second step, this slurry was transferred into molds and lyophilized resulting in uncrosslinked scaffolds. Then, these scaffolds were decellularised with supercritical carbon dioxide. As the digestion and lyophilization of articular cartilage increased the porosity of the samples, it was found that the decellularisation procedure described in **chapter five** was already efficient with ethanol. It could be shown that the scaffold were successfully decellularised while conserving mechanical properties, ultrastructure and cell adhesion molecules. Contrary to the detergent, the use of the less aggressive and volatile ethanol has the advantage of not requiring long washing steps after decellularisation. Digestion prior to lyophilization also allows tailoring the mechanical properties of the scaffolds by changing the cartilage digest concentration. As a result, the mechanical properties of the superficial zone could be mimicked. However, with the chosen digest concentration the higher mechanical properties of middle, deep and calcified zone of human articular cartilage were not achieved (Antons et al., 2018b). When seeding those scaffolds with human chondro-progenitors it could be confirmed that for scaffolds based on decellularised cartilage the matching mechanical properties alone are sufficient to induce zone-specific cell behavior without additional stimuli. Immunohistochemistry revealed that after 14 and 28 days of cell culture without additional growth factors the chondro-progenitors expressed the superficial zone-specific protein lubricin. Those results are not only aligned with earlier findings that decellularised matrices have a chondrogenic effect even without the use of additional growth factors (Cheng et al., 2009, 2011; Ghosh et al., 2018), but also confirm the hypothesis of this thesis. Nonetheless, the study had several limitations. Firstly, only few digest and crosslinker concentrations were investigated. The selection of the digest concentration was based on a former study using digested decellularised cartilage for bioinks (Pati et al., 2014; Visser et al., 2015). Similarly, the crosslinking concentration was inspired by a previous study with decellularised cartilage (Rowland et al., 2013). It would be interesting to study more digest concentrations and test the effect of different crosslinker modalities and concentrations. Secondly, the presence of lubricin was examined

only qualitatively by immunohistochemistry, quantitative tests should be conducted in future studies for the evaluation of different scaffold conditions. An enzyme-linked immunosorbent assay (ELISA) or gene expression analysis of zone-specific genes could be used for this purpose (Khala et al., 2007; Mhanna et al., 2013; Niikura and Reddi, 2007). Thirdly, there is also high interest in mimicking the other zones of articular cartilage. As it will be very challenging to reproduce those rather rigid zones with comparably soft decellularised cartilage scaffolds, structural support by other materials could be a possible solution. It has been shown that these properties can be achieved for example with 3D printed matrices which target the deep and calcified zone of articular cartilage (Marascio et al., 2017). Those dense structures could then be immersed with the here presented scaffold material. Finally, the cell penetration into the developed scaffolds should be improved by further enhancement of their porosity. One possible porogene technique is salt-leaching with defined salt-crystal sizes (Abdel-Sayed et al., 2014; Hou et al., 2003; Nasrollahzadeh et al., 2017).

Taken together, the here presented scaffolds are a first step towards improved scaffolds for articular cartilage repair. By providing enhanced bioactivity with matching mechanical properties the scaffolds could support the formation of pure hyaline cartilage. As a direct application, this could significantly improve the outcome of Autologous Chondrocytes Implantation and Microfracture.



# References

- Abdel-Sayed, P., Darwiche, S. E., Kettenberger, U., and Pioletti, D. P. (2014). The role of energy dissipation of polymeric scaffolds in the mechanobiological modulation of chondrogenic expression. *Biomaterials*, 35(6):1890–1897.
- Aldrian, S., Zak, L., Wondrasch, B., Albrecht, C., Stelzeneder, B., Binder, H., Kovar, F., Trattnig, S., and Marlovits, S. (2014). Clinical and radiological long-term outcomes after matrix-induced autologous chondrocyte transplantation: a prospective follow-up at a minimum of 10 years. *The American journal of sports medicine*, 42:2680–8.
- Alford, J. W. and Cole, B. J. (2005). Cartilage restoration, part 1: basic science, historical perspective, patient evaluation, and treatment options. *The American journal of sports medicine*, 33(2):295–306.
- Anders, S., Goetz, J., Schubert, T., Grifka, J., and Schaumburger, J. (2012). Treatment of deep articular talus lesions by matrix associated autologous chondrocyte implantation - Results at five years. *International Orthopaedics*, 36(11):2279–2285.
- Angele, P., Fritz, J., Albrecht, D., Koh, J., and Zellner, J. (2015). Defect type, localization and marker gene expression determines early adverse events of matrix-associated autologous chondrocyte implantation. *Injury*, 46:S2–S9.
- Antons, J., Marascio, M., Aeberhard, P., Weissenberger, G., Hirt-Burri, N., Applegate, L., Bourban, P., and Pioletti, D. (2018a). Decellularised tissues obtained by a CO<sub>2</sub>-philic detergent and supercritical CO<sub>2</sub>. *European Cells and Materials*, 36:81–95.
- Antons, J., Marascio, M. G., Nohava, J., Martin, R., Applegate, L. A., Bourban, P. E., and Pioletti, D. P. (2018b). Zone-dependent mechanical properties of human articular cartilage obtained by indentation measurements. *Journal of Materials Science: Materials in Medicine*, 29(5).
- Applegate, L. A., Scaletta, C., Hirt-Burri, N., Raffoul, W., and Pioletti, D. (2009). Whole-cell bioprocessing of human fetal cells for tissue engineering of skin.
- Applegate, L. A., Weber, D., Simon, J.-P., Scaletta, C., Hirt-Burri, N., de Buys Roessingh, A., and Raffoul, W. (2013). Organ donation and whole-cell bioprocessing in the Swiss Fetal progenitor cell Transplantation Platform. *Organ Donation and Organ Donors: Issues, Challenges and Perspectives*, pages 125–147.
- Armitage, O. E. and Oyen, M. L. (2017). Indentation across interfaces between stiff and compliant tissues. *Acta Biomaterialia*, 56:36–43.

- Armstrong, C. G. and Mow, V. C. (1982). Variations in the intrinsic mechanical properties of human articular cartilage with age, degeneration, and water content. *The Journal of bone and joint surgery. American volume*, 64(1):88–94.
- Aspberg, A. (2016). Cartilage proteoglycans. *Cartilage: Volume 1: Physiology and Development*, 12:1–22.
- Athanasiou, K. A., Darling, E. M., and Hu, J. C. (2009). Articular Cartilage Tissue Engineering. *Synthesis Lectures on Tissue Engineering*, 1(1):1–182.
- Athanasiou, K. A., Rosenwasser, M. P., Buckwalter, J. A., Malinin, T. I., and Mow, V. C. (1991). Interspecies comparisons of in situ intrinsic mechanical properties of distal femoral cartilage. *Journal of Orthopaedic Research*, 9(3):330–340.
- Aubin, H., Kranz, A., Hülsmann, J., Lichtenberg, A., and Akhyari, P. (2013). Decellularized whole heart for bioartificial heart. *Methods in Molecular Biology*, 1036:163–178.
- Badylak, S. F. and Gilbert, T. W. (2008). Immune response to biologic scaffold materials.
- Badylak, S. F., Hoppo, T., Nieponice, A., Gilbert, T. W., Davison, J. M., and Jobe, B. A. (2011). Esophageal preservation in five male patients after endoscopic inner-layer circumferential resection in the setting of superficial cancer: a regenerative medicine approach with a biologic scaffold. *Tissue engineering. Part A*, 17(11-12):1643–50.
- Barthel, T., Fensky, F., Noth, U., Rudert, M., Reichert, J., Siebenlist, S., Rackwitz, L., Andereya, S., Schneider, U., and Loer, I. (2011). A Prospective Multicenter Study on the Outcome of Type I Collagen Hydrogel-Based Autologous Chondrocyte Implantation (CaReS) for the Repair of Articular Cartilage Defects in the Knee.
- Basad, E., Ishaque, B., Bachmann, G., Stürz, H., and Steinmeyer, J. (2010). Matrix-induced autologous chondrocyte implantation versus microfracture in the treatment of cartilage defects of the knee: A 2-year randomised study. *Knee Surgery, Sports Traumatology, Arthroscopy*, 18(4):519–527.
- Bauer, S., Khan, R. J. K., Ebert, J. R., Robertson, W. B., Breidahl, W., Ackland, T. R., and Wood, D. J. (2012). Knee joint preservation with combined neutralising High Tibial Osteotomy (HTO) and Matrix-induced Autologous Chondrocyte Implantation (MACI) in younger patients with medial knee osteoarthritis: A case. *Knee*, 19(4):431–439.
- Bautista, C. A., Park, H. J., Mazur, C. M., Aaron, R. K., and Bilgen, B. (2016). Effects of chondroitinase ABC-Mediated proteoglycan digestion on decellularization and recellularization of articular cartilage. *PLoS ONE*, 11(7):1–15.
- Beck, E. C., Barragan, M., Tadros, M. H., Gehrke, S. H., and Detamore, M. S. (2016). Approaching the compressive modulus of articular cartilage with a decellularized cartilage-based hydrogel. *Acta Biomaterialia*, 38:94–105.
- Bedi, A., Feeley, B. T., and Williams, R. J. (2010). Management of articular cartilage defects of the knee. *The Journal of bone and joint surgery. American volume*, 92(4):994–1009.
- Benya, P. D. and Shaffer, J. D. (1982). Dedifferentiated chondrocytes reexpress the differentiated collagen phenotype when cultured in agarose gels. *Cell*, 30(1):215–224.



- Bernhardt, A., Wehrl, M., Paul, B., Hochmuth, T., Schumacher, M., Schütz, K., and Gelinsky, M. (2015). Improved Sterilization of Sensitive Biomaterials with Supercritical Carbon Dioxide at Low Temperature. *PloS one*, 10(6):e0129205.
- Blacker, T. S., Duchon, M. R., Sibbons, P., and Roberts, S. J. (2018). Decellularized Cartilage Directs Chondrogenic Differentiation. *00(00):1–17*.
- Bottagisio, M., Pellegata, A. F., Boschetti, F., Ferroni, M., Moretti, M., and Lovati, A. B. (2016). A new strategy for the decellularisation of large equine tendons as biocompatible tendon substitutes. *European Cells and Materials*, 32:58–73.
- Brittberg, M., Lindahl, A., Nilsson, A., Ohlsson, C., Isaksson, O., and Peterson, L. (1994). Treatment of deep cartilage defects in the knee with autologous chondrocyte transplantation. *The New England journal of medicine*, 331(14):889–895.
- Brittberg, M., Recker, D., Ilgenfritz, J., and Saris, D. B. (2018). Matrix-Applied Characterized Autologous Cultured Chondrocytes Versus Microfracture: Five-Year Follow-up of a Prospective Randomized Trial. *American Journal of Sports Medicine*, 46(6):1343–1351.
- Brown, T. D., Dalton, P. D., and Hutmacher, D. W. (2011). Direct writing by way of melt electrospinning. *Advanced Materials*, 23(47):5651–5657.
- Brown, T. D., Dalton, P. D., and Hutmacher, D. W. (2015). Melt electrospinning today: An opportune time for an emerging polymer process.
- Brun, P., Dickinson, S. C., Zavan, B., Cortivo, R., Hollander, A. P., and Abatangelo, G. (2008). Characteristics of repair tissue in second-look and third-look biopsies from patients treated with engineered cartilage: Relationship to symptomatology and time after implantation. *Arthritis Research and Therapy*, 10(6).
- Burk, J., Erbe, I., Berner, D., Kacza, J., Kasper, C., Pfeiffer, B., Winter, K., and Brehm, W. (2014). Freeze-Thaw Cycles Enhance Decellularization of Large Tendons. *Tissue Engineering Part C: Methods*, 20(4):276–284.
- Caione, P., Boldrinic, R., Salerno, A., and Nappo, S. G. (2012). Bladder augmentation using acellular collagen biomatrix: A pilot experience in exstrophic patients. *Pediatric Surgery International*, 28(4):421–428.
- Campbell, S. E., Ferguson, V. L., and Hurley, D. C. (2012). Nanomechanical mapping of the osteochondral interface with contact resonance force microscopy and nanoindentation. *Acta Biomaterialia*, 8(12):4389–4396.
- Candrian, C., Vonwil, D., Barbero, A., Bonacina, E., Miot, S., Farhadi, J., Wirz, D., Dickinson, S., Hollander, A., Jakob, M., Li, Z., Alini, M., Heberer, M., and Martin, I. (2008). Engineered cartilage generated by nasal chondrocytes is responsive to physical forces resembling joint loading. *Arthritis and Rheumatism*, 58(1):197–208.
- Casali, D. M., Handleton, R. M., Shazly, T., and Matthews, M. A. (2018). A novel supercritical CO<sub>2</sub>-based decellularization method for maintaining scaffold hydration and mechanical properties. *The Journal of Supercritical Fluids*, 131(July 2017):72–81.

- Castell, M. V., Van Der Pas, S., Otero, A., Siviero, P., Dennison, E., Denking, M., Pedersen, N., Sanchez-Martinez, M., Queipo, R., Van Schoor, N., Zambon, S., Edwards, M., Peter, R., Schaap, L., and Deeg, D. (2015). Osteoarthritis and frailty in elderly individuals across six European countries: Results from the European Project on OsteoArthritis (EPOSA). *BMC Musculoskeletal Disorders*, 16(1).
- Charalambous, C. P. (2014). Articular cartilage. Part II: Degeneration and osteoarthrosis, repair, regeneration, and transplantation. In *Classic Papers in Orthopaedics*, pages 389–391.
- Chen, A. C., Bae, W. C., Schinagl, R. M., and Sah, R. L. (2001a). Depth-and strain-dependent mechanical and electromechanical properties of full-thickness bovine articular cartilage in confined compression. *Journal of Biomechanics*, 34:1–12.
- Chen, S. S., Falcovitz, Y. H., Schneiderman, R., Maroudas, A., and Sah, R. L. (2001b). Depth-dependent compressive properties of normal aged human femoral head articular cartilage : relationship to fixed charge density. pages 561–569.
- Cheng, N.-C., Estes, B. T., Awad, H. a., and Guilak, F. (2009). Chondrogenic differentiation of adipose-derived adult stem cells by a porous scaffold derived from native articular cartilage extracellular matrix. *Tissue engineering. Part A*, 15(2):231–241.
- Cheng, N. C., Estes, B. T., Young, T. H., and Guilak, F. (2011). Engineered cartilage using primary chondrocytes cultured in a porous cartilage-derived matrix. *Regenerative Medicine*, 6(1):81–93.
- Chia, H. N. and Wu, B. M. (2015). Recent advances in 3D printing of biomaterials. *Journal of Biological Engineering*, 9:4.
- Clar, H., Pascher, A., Kastner, N., Gruber, G., Robl, T., and Windhager, R. (2010). Matrix-assisted autologous chondrocyte implantation into a 14cm<sup>2</sup> cartilage defect, caused by steroid-induced osteonecrosis. *Knee*, 17(3):255–257.
- Clements, K. M., Bee, Z. C., Crossingham, G. V., Adams, M. A., and Sharif, M. (2001). How severe must repetitive loading be to kill chondrocytes in articular cartilage? *Osteoarthritis and Cartilage*, 9(5):499–507.
- Cole, B. J., Pascual-Garrido, C., and Grumet, R. C. (2009). Surgical management of articular cartilage defects in the knee. *The Journal of bone and joint surgery. American volume*, 91(7):1778–90.
- Collins, D. (1949). The Pathology of Articular and Spinal Diseases. *Edward Arnold, London*, 9(2):181.(9):76–115.
- Crapo, P. M., Gilbert, T. W., and Badylak, S. F. (2011). An overview of tissue and whole organ decellularization processes. *Biomaterials*, 32(12):3233–3243.
- Crawford, D. C., DeBerardino, T. M., and Williams, R. J. (2012). NeoCart, an autologous cartilage tissue implant, compared with microfracture for treatment of distal femoral cartilage lesions: An FDA phase-II prospective, randomized clinical trial after two years. *Journal of Bone and Joint Surgery - Series A*, 94(11):979–989.

- Crawford, D. C., Heveran, C. M., Cannon, W. D., Foo, L. F., and Potter, H. G. (2009). An autologous cartilage tissue implant neocart for treatment of grade III chondral injury to the distal femur: Prospective clinical safety trial at 2 years. *American Journal of Sports Medicine*, 37(7):1334–1343.
- Dalton, P. D., Joergensen, N. T., Groll, J., and Moeller, M. (2008). Patterned melt electrospun substrates for tissue engineering. *Biomedical materials (Bristol, England)*, 3(3):034109.
- Darwiche, S., Scaletta, C., Raffoul, W., Pioletti, D. P., and Applegate, L. A. (2012). Epiphyseal Chondroprogenitors Provide a Stable Cell Source for Cartilage Cell Therapy. *Cell Medicine*, 4(1):23–32.
- de Vries-van Melle, M. L., Tihaya, M. S., Kops, N., Koevoet, W. J. L. M., Murphy, J. M., Verhaar, J. a. N., Alini, M., Eglin, D., van Osch, G. J. V. M., Melle, M. L. D. V.-v., Tihaya, M. S., Kops, N., Koevoet, W. J. L. M., Murphy, J. M., Verhaar, J. a. N., Alini, M., Eglin, D., and Osch, G. J. V. M. V. (2014). Chondrogenic differentiation of human bone marrow-derived mesenchymal stem cells in a simulated osteochondral environment is hydrogel dependent. *European cells & materials*, 27:112–23.
- Deeken, C. R., White, A. K., Bachman, S. L., Ramshaw, B. J., Cleveland, D. S., Loy, T. S., and Grant, S. A. (2011). Method of preparing a decellularized porcine tendon using tributyl phosphate. *Journal of Biomedical Materials Research - Part B Applied Biomaterials*, 96 B(2):199–206.
- Degen, R. M., Tetreault, D., Mahony, G. T., and Williams, R. J. (2016). Acute Delamination of Commercially Available Decellularized Osteochondral Allograft Plugs: A Report of Two Cases. *Cartilage*, 7(4):316–321.
- Ding, C., Jones, G., Wluka, A. E., and Cicuttini, F. (2010). What can we learn about osteoarthritis by studying a healthy person against a person with early onset of disease? *Current Opinion in Rheumatology*, 22(5):520–527.
- Dong, S., Huangfu, X., Xie, G., Zhang, Y., Shen, P., Li, X., Qi, J., and Zhao, J. (2015). Decellularized Versus Fresh-Frozen Allografts in Anterior Cruciate Ligament Reconstruction: An in Vitro Study in a Rabbit Model. *American Journal of Sports Medicine*, 43(8):1924–1934.
- Dorotka, R., Windberger, U., Macfelda, K., Bindreiter, U., Toma, C., and Nehrer, S. (2005). Repair of articular cartilage defects treated by microfracture and a three-dimensional collagen matrix. *Biomaterials*, 26(17):3617–3629.
- Dunford, N. T. and Temelli, F. (1995). Extraction of phospholipids from canola with supercritical carbon dioxide and ethanol. *Journal of the American Oil Chemists' Society*, 72(9):1009–1015.
- Ebenstein, D. M., Kuo, A., Rodrigo, J. J., Reddi, A. H., Ries, M., and Pruitt, L. (2011). A nanoindentation technique for functional evaluation of cartilage repair tissue. *Journal of Materials Research*, 19(1):273–281.

- Ebert, J. R., Robertson, W. B., Woodhouse, J., Fallon, M., Zheng, M. H., Ackland, T., and Wood, D. J. (2011). Clinical and Magnetic Resonance Imaging–Based Outcomes to 5 Years After Matrix-Induced Autologous Chondrocyte Implantation to Address Articular Cartilage Defects in the Knee. *The American Journal of Sports Medicine*, 39(4):753–763.
- Eberwein, P., Nohava, J., Schlunck, G., and Swain, M. (2014). Nanoindentation Derived Mechanical Properties of the Corneoscleral Rim of the Human Eye. *Key Engineering Materials*, 606:117–120.
- Erggelet, C., Kreuz, P. C., Mrosek, E. H., Schagemann, J. C., Lahm, A., Ducommun, P. P., and Ossendorf, C. (2010). Autologous chondrocyte implantation versus ACI using 3D-bioresorbable graft for the treatment of large full-thickness cartilage lesions of the knee. *Archives of Orthopaedic and Trauma Surgery*, 130(8):957–964.
- Ethgen, O., Bruyère, O., Richy, F., Dardennes, C., and Reginster, J.-Y. (2004). Health-related quality of life in total hip and total knee arthroplasty. A qualitative and systematic review of the literature. *The Journal of bone and joint surgery. American volume*, 86-A(5):963–74.
- Eyre, D. R., Weis, M. A., and Wu, J. J. (2006). Articular cartilage collagen: An irreplaceable framework?
- Farhadi, J., Fulco, I., Miot, S., Wirz, D., Haug, M., Dickinson, S. C., Hollander, A. P., Daniels, A. U., Pierer, G., Heberer, M., and Martin, I. (2006). Precultivation of engineered human nasal cartilage enhances the mechanical properties relevant for use in facial reconstructive surgery. *Annals of Surgery*, 244(6):978–985.
- Farnebo, S., Woon, C. Y., Schmitt, T., Joubert, L.-M., Kim, M., Pham, H., and Chang, J. (2014). Design and Characterization of an Injectable Tendon Hydrogel: A Novel Scaffold for Guided Tissue Regeneration in the Musculoskeletal System. *Tissue Engineering Part A*, 20(9-10):1550–1561.
- Fermor, H. L., Russell, S. L., Williams, S., Fisher, J., and Ingham, E. (2015). Development and characterisation of a decellularised bovine osteochondral biomaterial for cartilage repair. *Journal of Materials Science: Materials in Medicine*, 26(5):1–11.
- Fickert, S., Schattenberg, T., Niks, M., Weiss, C., and Thier, S. (2014). Feasibility of arthroscopic 3-dimensional, purely autologous chondrocyte transplantation for chondral defects of the hip: A case series. *Archives of Orthopaedic and Trauma Surgery*, 134(7):971–978.
- Fontana, A., Bistolfi, A., Crova, M., Rosso, F., and Massazza, G. (2012). Arthroscopic treatment of hip chondral defects: Autologous chondrocyte transplantation versus simple debridement-A pilot study. *Arthroscopy - Journal of Arthroscopic and Related Surgery*, 28(3):322–329.
- Forster, H. and Fisher, J. (1996). The Influence of Loading Time and Lubricant on the Friction of Articular Cartilage. *Proceedings of the Institution of Mechanical Engineers, Part H: Journal of Engineering in Medicine*, 210(2):109–119.
- Franke, O., Durst, K., Maier, V., Göken, M., Birkholz, T., Schneider, H., Hennig, F., and Gelse, K. (2007). Mechanical properties of hyaline and repair cartilage studied by nanoindentation. *Acta Biomaterialia*, 3(6):873–881.

- Franke, O., Göken, M., Meyers, M. a., Durst, K., and Hodge, a. M. (2011). Dynamic nanoindentation of articular porcine cartilage. *Materials Science and Engineering C*, 31(4):789–795.
- Freytes, D. O., Stoner, R. M., and Badylak, S. F. (2008). Uniaxial and biaxial properties of terminally sterilized porcine urinary bladder matrix scaffolds. *Journal of Biomedical Materials Research - Part B Applied Biomaterials*, 84(2):408–414.
- Gawlitta, D., Benders, K. E., Visser, J., van der Sar, A. S., Kempen, D. H., Theyse, L. F., Malda, J., and Dhert, W. J. (2015). Decellularized Cartilage-Derived Matrix as Substrate for Endochondral Bone Regeneration. *Tissue Engineering Part A*, 21(3-4):694–703.
- Ghosh, P., Gruber, S. M., Lin, C. Y., and Whitlock, P. W. (2018). Microspheres containing decellularized cartilage induce chondrogenesis in vitro and remain functional after incorporation within a poly(caprolactone) filament useful for fabricating a 3D scaffold. *Biofabrication*, 10(2).
- Gilbert, T. W., Sellaro, T. L., and Badylak, S. F. (2006). Decellularization of tissues and organs. *Biomaterials*, 27(19):3675–3683.
- Goldberg, A., Mitchell, K., Soans, J., Kim, L., and Zaidi, R. (2017). The use of mesenchymal stem cells for cartilage repair and regeneration: A systematic review. *Journal of Orthopaedic Surgery and Research*, 12(1):1–30.
- Gomoll, A. H. (2013). Osteochondral allograft transplantation using the chondrofix implant. *Operative Techniques in Sports Medicine*, 21(2):90–94.
- Gotte, L., Stern, P., Elsdén, D. F., and Partridge, S. M. (1963). The chemistry of connective tissues. 8. The composition of elastin from three bovine tissues. *Biochem. J.*, 87:344–351.
- Grad, S., Lee, C. R., Gorna, K., Gogolewski, S., Wimmer, M. A., and Alini, M. (2005). Surface Motion Upregulates Superficial Zone Protein and Hyaluronan Production in Chondrocyte-Seeded Three-Dimensional Scaffolds. *Tissue Engineering*, 11(1-2):249–256.
- Guilak, F., Butler, D. L., and Goldstein, S. A. (2001). Functional tissue engineering: the role of biomechanics in articular cartilage repair. *Clinical Orthopaedics and Related Research*, (391 Suppl):295–305.
- Guler, S., Aslan, B., Hosseinian, P., and Aydin, H. M. (2017). Supercritical Carbon Dioxide-Assisted Decellularization of Aorta and Cornea. *Tissue engineering. Part C, Methods*, 23(9):540–547.
- Gupta, H. S., Schratte, S., Tesch, W., Roschger, P., Berzlanovich, A., Schoeberl, T., Klaushofer, K., and Fratzl, P. (2005). Two different correlations between nanoindentation modulus and mineral content in the bone-cartilage interface. *Journal of Structural Biology*, 149(2):138–148.
- Haddo, O., Mahroof, S., Higgs, D., David, L., Pringle, J., Bayliss, M., Cannon, S. R., and Briggs, T. W. (2004). The use of chondroglide membrane in autologous chondrocyte implantation. *Knee*, 11(1):51–55.

- Halfwerk, F. R., Rouwkema, J., Gossen, J. A., and Grandjean, J. G. (2018). Supercritical carbon dioxide decellularised pericardium: Mechanical and structural characterisation for applications in cardio-thoracic surgery. *Journal of the Mechanical Behavior of Biomedical Materials*, 77(September 2017):400–407.
- Hardingham, T. E. (1979). The Role of Link-Protein in the Structure of Cartilage Proteoglycan Aggregates. *Biochem. J*, 177:237–247.
- Hardingham, T. E. and Muir, H. (1972). The specific interaction of hyaluronic acid with cartilage proteoglycans. *BBA - General Subjects*, 279(2):401–405.
- Harkness, R. D. (1961). Biological Functions of Collagen. *Biological reviews*, 36(4):399–463.
- Hayes, W. C. and Mockros, L. F. (1971). Viscoelastic properties of human articular cartilage. *Journal of Applied Physiology*, 31(4):562–568.
- Heisel, J. and Kipshoven, C. (2013). Safety and efficacy findings from a non-interventional study of a new hyaluronic acid/sorbitol formulation (GO-ON® matrix) for intra-articular injection to relieve pain and disability in osteoarthritis patients.
- Hodde, J. and Hiles, M. (2002). Virus safety of a porcine-derived medical device: Evaluation of a viral inactivation method. *Biotechnology and Bioengineering*, 79(2):211–216.
- Hollander, A. P., Pidoux, I., Reiner, A., Rorabeck, C., Bourne, R., and Poole, A. R. (1995). Damage to type II collagen in aging and osteoarthritis starts at the articular surface, originates around chondrocytes, and extends into the cartilage with progressive degeneration. *Journal of Clinical Investigation*, 96(6):2859–2869.
- Hollister, S. J. (2005). Porous scaffold design for tissue engineering. *Nature materials*, 4(July):518–24.
- Hou, Q., Grijpma, D. W., and Feijen, J. (2003). Porous polymeric structures for tissue engineering prepared by a coagulation, compression moulding and salt leaching technique. *Biomaterials*, 24(11):1937–1947.
- Huang, Y.-h., Tseng, F.-w., Chang, W.-h., Peng, I., Hsieh, D.-j., and Wu, S.-w. (2017). Preparation of acellular scaffold for corneal tissue engineering by supercritical carbon dioxide extraction technology. *Acta Biomaterialia*, 58:238–243.
- Hunter, W. (1742). Of the Structure and Diseases of Articulating Cartilages. *Philosophical Transactions (1683-1775)*, 42:514–521.
- Hutmacher, D. W. (2000). Scaffolds in tissue engineering bone and cartilage. *Biomaterials*, 21(24):2529–2543.
- Hwang, N. S., Varghese, S., Lee, H. J., Theprungsirikul, P., Canver, A., Sharma, B., and Elisseeff, J. (2007). Response of zonal chondrocytes to extracellular matrix-hydrogels. *FEBS Letters*, 581:4172–4178.
- Illien-Jünger, S., Sedaghatpour, D. D., Laudier, D. M., Hecht, A. C., Qureshi, S. A., and Iatridis, J. C. (2016). Development of a bovine decellularized extracellular matrix-biomaterial for nucleus pulposus regeneration. *Journal of Orthopaedic Research*, 34(5):876–888.

- Jakes, J., Frihart, C., Beecher, J., Moon, R., Resto, P., Melgarejo, Z., Suárez, O., Baumgart, H., Elmustafa, A., and Stone, D. (2009). Nanoindentation near the edge. *J. Mater. Res.*, 24:1016–1031.
- Jakes, J. E. and Stone, D. S. (2011). The edge effect in nanoindentation. *Philosophical Magazine*, 91(91):7–9.
- Jay, G. D. and Waller, K. A. (2014). The biology of Lubricin: Near frictionless joint motion. *Matrix Biology*, 39:17–24.
- Jeffrey, J. E., Gregory, D. W., and Aspden, R. M. (1995). Matrix damage and chondrocyte viability following a single impact load on articular cartilage.
- Jeon, J. E., Malda, J., Schrobback, K., Irawan, D., Masuda, K., Sah, R. L., Hutmacher, D. W., Klein, T. J., Yarmush, M. L., and Langer, R. (2010). Engineering Cartilage Tissue with Zonal Properties. *3-D Tissue Engineering*, (January 2016):225–236.
- J.R., E., A., S., M., F., D.J., W., and T.R., A. (2014). Correlation Between Clinical and Radiological Outcomes After Matrix-Induced Autologous Chondrocyte Implantation in the Femoral Condyles. *The American journal of sports medicine*, 42(8):1857–1864.
- Juanssilfero, A. B., Akmal, F., Mutalib, A., Zulaikha, W., Zulkifli, W., and Jahim, J. (2011). Characterization of Copolymer Dehypon ® LS 54 and Its Application for Aqueous Two-Phase Systems Paired with the Waxy Maize Starch for Protein Extraction. *Water*, (January).
- Kafienah, W., Jakob, M., Démarteau, O., Frazer, A., Barker, M. D., Martin, I., and Hollander, A. P. (2002). Three-Dimensional Tissue Engineering of Hyaline Cartilage: Comparison of Adult Nasal and Articular Chondrocytes. *Tissue Engineering*, 8(5):817–826.
- Kang, H., Peng, J., Lu, S., Liu, S., Zhang, L., Huang, J., Sui, X., Zhao, B., Wang, A., Xu, W., Luo, Z., and Guo, Q. (2014). In vivo cartilage repair using adipose-derived stem cell-loaded decellularized cartilage ECM scaffolds. *Journal of Tissue Engineering and Regenerative Medicine*, 8(6):442–453.
- Karimi, T., Barati, D., Karaman, O., and Moeinzadeh, S. (2014). Integrative Biology and biochemical signaling approach on zonal lineage commitment of mesenchymal stem cells in articular cartilage regeneration. *Integrative Biology*, 7:112–127.
- Keane, T. J., Londono, R., Turner, N. J., and Badylak, S. F. (2012). Consequences of ineffective decellularization of biologic scaffolds on the host response. *Biomaterials*, 33(6):1771–1781.
- Kempson, G. E., Freeman, M. A. R., and Swanson, S. A. V. (1968). Tensile Properties of Articular Cartilage. *Nature*, 220(5172):1127–1128.
- Kevin R. Stone, Gustavo Ayala, J. G. R. H. A. W., Galili, and Uri (1998). Porcine cartilage transplants in the cynomolgus monkey: III Transplantation of  $\alpha$ -galactosidase treated porcine cartilage. 65(12):1577–1583.
- Khala, A., Schmid, T. M., Neu, C., and Reddi, A. H. (2007). Increased Accumulation of Super cial Zone Protein (SZP) in Articular Cartilage in Response to Bone Morphogenetic Protein-7 and Growth Factors. *Journal of Orthopaedic Research*, 4(March):11–13.

- Klein, T. J., Malda, J., Sah, R. L., and Hutmacher, D. W. (2009). Tissue engineering of articular cartilage with biomimetic zones. *Tissue engineering. Part B, Reviews*, 15(2):143–157.
- Knutsen, G., Drogset, J. O., Engebretsen, L., Grøntvedt, T., Isaksen, V., Ludvigsen, T. C., Roberts, S., Solheim, E., Strand, T., and Johansen, O. (2007). A randomized trial comparing autologous chondrocyte implantation with microfracture: Findings at five years. *Journal of Bone and Joint Surgery - Series A*, 89(10):2105–2112.
- Koga, H., Engebretsen, L., Brinchmann, J. E., Muneta, T., and Sekiya, I. (2009). Mesenchymal stem cell-based therapy for cartilage repair: a review. *Knee surgery, sports traumatology, arthroscopy : official journal of the ESSKA*, 17(11):1289–97.
- Koga, H., Shimaya, M., Muneta, T., Nimura, A., Morito, T., Hayashi, M., Suzuki, S., Ju, Y.-J., Mochizuki, T., and Sekiya, I. (2008). Local adherent technique for transplanting mesenchymal stem cells as a potential treatment of cartilage defect. *Arthritis research & therapy*, 10(4):R84.
- Kon, E., Filardo, G., Gobbi, A., Berruto, M., Andriolo, L., Ferrua, P., Crespiatico, I., and Marcacci, M. (2016). Long-term Results after Hyaluronan-based MACT for the Treatment of Cartilage Lesions of the Patellofemoral Joint. *American Journal of Sports Medicine*, 44(3):602–608.
- Könst, Y. E., Benink, R. J., Veldstra, R., van der Krieke, T. J., Helder, M. N., and van Royen, B. J. (2012). Treatment of severe osteochondral defects of the knee by combined autologous bone grafting and autologous chondrocyte implantation using fibrin gel. *Knee surgery, sports traumatology, arthroscopy : official journal of the ESSKA*, 20(11):2263–9.
- Kreuz, P. C., Müller, S., von Keudell, A., Tischer, T., Kaps, C., Niemeyer, P., and Erggelet, C. (2013). Influence of Sex on the Outcome of Autologous Chondrocyte Implantation in Chondral Defects of the Knee. *The American Journal of Sports Medicine*, 41(7):1541–1548.
- Laasanen, M. S., Töyräs, J., Korhonen, R. K., Rieppo, J., Saarakkala, S., Nieminen, M. T., Hirvonen, J., and Jurvelin, J. S. (2003). Biomechanical properties of knee articular cartilage. *Biorheology*, 40(1-3):133–40.
- Lai, W. M., Hou, J. S., and Mow, V. C. (1991). A Triphasic Theory for the Swelling and Deformation Behaviors of Articular Cartilage. *Journal of Biomechanical Engineering*, 113(3):245.
- Last, J., Liliensiek, S., Nealey, P., and Murphy, C. (2009). Determining the mechanical properties of human corneal basement membranes with atomic force microscopy. *Journal of structural biology*, 167(1):19–24.
- Lee, S. Y., Nakagawa, T., and Reddi, A. H. (2010). Mesenchymal Progenitor Cells Derived from Synovium and Infrapatellar Fat Pad as a Source for Superficial Zone Cartilage Tissue Engineering: Analysis of Superficial Zone Protein/Lubricin Expression. *Tissue Engineering Part A*, 16(1):317–325.



- Levett, P. a., Melchels, F. P. W., Schrobback, K., Hutmacher, D. W., Malda, J., and Klein, T. J. (2014). A biomimetic extracellular matrix for cartilage tissue engineering centered on photocurable gelatin, hyaluronic acid and chondroitin sulfate. *Acta Biomaterialia*, 10(1):214–223.
- Lin, X., Chen, J., Qiu, P., Zhang, Q., Wang, S., Su, M., Chen, Y., Jin, K., Qin, A., Fan, S., Chen, P., and Zhao, X. (2018). Biphasic hierarchical extracellular matrix scaffold for osteochondral defect regeneration. *Osteoarthritis and Cartilage*, 26(3):433–444.
- Linn, F. C. and Sokoloff, L. (1965). Movement and composition of interstitial fluid of cartilage. *Arthritis & Rheumatism*, 8(4):481–494.
- Liu, H., Yang, L., Zhang, E., Zhang, R., Cai, D., Zhu, S., Ran, J., Bunpetch, V., Cai, Y., Heng, B. C., Hu, Y., Dai, X., Chen, X., and Ouyang, H. (2017). Biomimetic tendon extracellular matrix composite gradient scaffold enhances ligament-to-bone junction reconstruction. *Acta Biomaterialia*, 56:129–140.
- Liu, J., Han, B., Zhang, J., Li, G., and Zhang, X. (2002). Formation of Water-in-CO<sub>2</sub> Microemulsions with Non-fluorous Surfactant. (6):1356–1360.
- Loeser, R. F., Goldring, S. R., Scanzello, C. R., and Goldring, M. B. (2012). Osteoarthritis: A disease of the joint as an organ. *Arthritis and Rheumatism*, 64(6):1697–1707.
- Long, W. J., Greene, J. W., and Cushner, F. D. (2016). Early Clinical Outcomes Associated with a Novel Osteochondral Allograft Transplantation System in the Knee. *Advances in Orthopedic Surgery*, 2016:1–6.
- Lorenzo, P., Bayliss, M. T., and Heinegård, D. (1998). A novel cartilage protein (CILP) present in the mid-zone of human articular cartilage increases with age. *Journal of Biological Chemistry*, 273(36):23463–23468.
- Lovekamp, J. J., Simionescu, D. T., Mercuri, J. J., Zubiante, B., Sacks, M. S., and Vyavahare, N. R. (2006). Stability and function of glycosaminoglycans in porcine bioprosthetic heart valves. *Biomaterials*, 27(8):1507–1518.
- Lu, X. L. and Mow, V. C. (2008). Biomechanics of articular cartilage and determination of material properties. *Medicine and Science in Sports and Exercise*, 40(2):193–199.
- Luo, L., Eswaramoorthy, R., Mulhall, K. J., and Kelly, D. J. (2015). Decellularization of porcine articular cartilage explants and their subsequent repopulation with human chondroprogenitor cells. *Journal of the Mechanical Behavior of Biomedical Materials*, 55:21–31.
- Lutolf, M. P. and Hubbell, J. a. (2005). Synthetic biomaterials as instructive extracellular microenvironments for morphogenesis in tissue engineering. *Nature biotechnology*, 23(1):47–55.
- Macchiarini, P., Jungebluth, P., Go, T., Asnaghi, M. A., Rees, L. E., Cogan, T. A., Dodson, A., Martorell, J., Bellini, S., Parnigotto, P. P., Dickinson, S. C., Hollander, A. P., Mantero, S., Conconi, M. T., and Birchall, M. A. (2008). Clinical transplantation of a tissue-engineered airway. *The Lancet*, 372(9655):2023–2030.

- Maehara, M., Sato, M., Toyoda, E., Takahashi, T., Okada, E., Kotoku, T., and Watanabe, M. (2017). Characterization of polydactyly-derived chondrocyte sheets versus adult chondrocyte sheets for articular cartilage repair. *Inflammation and regeneration*, 37:22.
- Mancini, D. and Fontana, A. (2014). Five-year results of arthroscopic techniques for the treatment of acetabular chondral lesions in femoroacetabular impingement. *International Orthopaedics*, 38(10):2057–2064.
- Mankin, H. (1974). The Reaction of Articular Cartilage to injury and osteoarthritis. *The New England Journal of Medicine*, 291(24):1285–1292.
- Marascio, M. G. M., Antons, J., Pioletti, D. P., and Bourban, P. E. (2017). 3D Printing of Polymers with Hierarchical Continuous Porosity. *Advanced Materials Technologies*, 2(11):1–7.
- Marlovits, S., Aldrian, S., Wondrasch, B., Zak, L., Albrecht, C., Welsch, G., and Trattnig, S. (2012). Clinical and radiological outcomes 5 years after matrix-induced autologous chondrocyte implantation in patients with symptomatic, traumatic chondral defects. *Am J Sports Med*, 40(10):2273–2280.
- Maroudas, A. (1973). Physico-chemical properties of articular cartilage. *Adult Articular Cartilage*, pages 131–170.
- Maroudas, A. and Bullough, P. (1968). Permeability of Articular Cartilage. *Nature*, 219(5160):1260–1261.
- Maroudas, A., Muir, H., and Wingham, J. (1969). The correlation of fixed negative charge with glycosaminoglycan content of human articular cartilage. *Biochimica et Biophysica Acta (BBA) - General Subjects*, 177(3):492–500.
- Maroudas, A. I. (1976). Balance between swelling pressure and collagen tension in normal and degenerate cartilage. *Nature*, 260(5554):808–809.
- Martin, I., Ireland, H., Baldomero, H., and Passweg, J. (2015). The Survey on Cellular and Engineered Tissue Therapies in Europe in 2012\*. *Tissue Engineering Part A*, 21(1-2):1–13.
- Masuda, K., Sah, R. L., Hejna, M. J., and Thonar, E. J. M. a. (2003). A novel two-step method for the formation of tissue-engineered cartilage by mature bovine chondrocytes: The alginate-recovered-chondrocyte (ARC) method. *Journal of Orthopaedic Research*, 21(1):139–148.
- Mathews, M. B., Lozaityte, I., Hay, H., and Foundation, W. (1958). Sodium Chondroitin Sulfate-Protein Complexes of Cartilage . 1 . Molecular Weight and Shape ' evident from a later study by Partridge ( 3 ) that crude preparations of and the. pages 158–174.
- McLeod, M. a., Wilusz, R. E., and Guilak, F. (2013). Depth-dependent anisotropy of the micromechanical properties of the extracellular and pericellular matrices of articular cartilage evaluated via atomic force microscopy. *Journal of Biomechanics*, 46(3):586–592.
- Merrilees, M. J. and Flint, M. H. (1980). Ultrastructural study of tension and pressure zones in a rabbit flexor tendon. *American Journal of Anatomy*, 157(1):87–106.

- Mhanna, R., Öztürk, E., Schlink, P., and Zenobi-Wong, M. (2013). Probing the microenvironmental conditions for induction of superficial zone protein expression. *Osteoarthritis and Cartilage*, 21(12):1924–1932.
- Miller, E. J. and Lunde, L. G. (1973). Isolation and characterization of the cyanogen bromide peptides from the  $\alpha 1(\text{II})$  chain of bovine and human cartilage collagen. *Biochemistry*, 12(17):3153–3159.
- Minns, R. J. and Steven, F. S. (1977). The collagen fibril organization in human articular cartilage. *Journal of anatomy*, 123:437–457.
- Mithoefer, K., Mcadams, T., Williams, R. J., Kreuz, P. C., and Mandelbaum, B. R. (2009). Clinical efficacy of the microfracture technique for articular cartilage repair in the knee: An evidence-based systematic analysis. *American Journal of Sports Medicine*, 37(10):2053–2063.
- Mithoefer, K., Peterson, L., Zenobi-Wong, M., and Mandelbaum, B. R. (2015). Cartilage issues in football—today’s problems and tomorrow’s solutions. *British Journal of Sports Medicine*, 49(9):590–596.
- Moeinzadeh, S., Monavarian, M., Kader, S., and ESMAIEL, J. (2018). Sequential Zonal Chondrogenic Differentiation of Mesenchymal Stem Cells in Cartilage Matrices. *Tissue Engineering Part A*, 8022(803):ten.TEA.2018.0083.
- Montanari, L., Fantozzi, P., Snyder, J. M., and King, J. W. (1999). Selective extraction of phospholipids from soybeans with supercritical carbon dioxide and ethanol. *The Journal of Supercritical Fluids*, 14(2):87–93.
- Mortazavi, F., Shafaei, H., Soleimani Rad, J., Rushangar, L., Montaceri, A., and Jamshidi, M. (2017). High Quality of Infant Chondrocytes in Comparison with Adult Chondrocytes for Cartilage Tissue Engineering. *World Journal of Plastic Surgery*, 6(2):183–189.
- Mouser, V. H. M., Levato, R., Bonassar, L. J., DLima, D. D., Grande, D. A., Klein, T. J., Saris, D. B. F., Zenobi-Wong, M., Gawlitta, D., and Malda, J. (2016). Three-Dimensional Bioprinting and Its Potential in the Field of Articular Cartilage Regeneration. *Cartilage*, page 1947603516665445.
- Moutos, F. T., Freed, L. E., and Guilak, F. (2007). A biomimetic three-dimensional woven composite scaffold for functional tissue engineering of cartilage. *Nature materials*, 6(February):162–167.
- Mow, V. C., Gibbs, M. C., Lai, W. M., Zhu, W. B., and Athanasiou, K. A. (1989). Biphasic indentation of articular cartilage-II. A numerical algorithm and an experimental study. *Journal of Biomechanics*, 22(8-9):853–861.
- Mow, V. C., Holmes, M. H., and Michael Lai, W. (1984). Fluid transport and mechanical properties of articular cartilage: A review.
- Mow, V. C., Ratcliffe, A., and Robin Poole, A. (1992). Cartilage and diarthrodial joints as paradigms for hierarchical materials and structures.

- Mow, V. C., Zhu, W., and Ratcliffe, A. (1991). Structure and function of articular cartilage and meniscus. *Basic Orthopaedic Biomechanics*. Raven Press. New York., pages 143–1998.
- Muir, H., Bullough, P., and Maroudas, A. (1970). The distribution of collagen in human articular cartilage with some of its physiological implications. *The Journal of bone and joint surgery. British volume*, 52(3):554–563.
- Mumme, M., Barbero, A., Miot, S., Wixmerten, A., Feliciano, S., Wolf, F., Asnaghi, A. M., Baumhoer, D., Bieri, O., Kretzschmar, M., Pagenstert, G., Haug, M., Schaefer, D. J., Martin, I., and Jakob, M. (2016). Nasal chondrocyte-based engineered autologous cartilage tissue for repair of articular cartilage defects: an observational first-in-human trial. *The Lancet*, 388(10055):1985–1994.
- Nam, Y., Rim, Y. A., Lee, J., and Ju, J. H. (2018). Current Therapeutic Strategies for Stem Cell-Based Cartilage Regeneration. *Stem Cells International*, 2018:1–20.
- Nasrollahzadeh, N., Applegate, L. A., and Pioletti, D. P. (2017). Development of an Effective Cell Seeding Technique: Simulation, Implementation, and Analysis of Contributing Factors. *Tissue Engineering Part C: Methods*, 23(8):485–496.
- Nejadnik, H., Hui, J. H., Feng Choong, E. P., Tai, B.-C., and Lee, E. H. (2010). Autologous Bone Marrow–Derived Mesenchymal Stem Cells Versus Autologous Chondrocyte Implantation. *The American Journal of Sports Medicine*, 38(6):1110–1116.
- Nguyen, L. H., Kudva, A. K., Guckert, N. L., Linse, K. D., and Roy, K. (2011a). Unique biomaterial compositions direct bone marrow stem cells into specific chondrocytic phenotypes corresponding to the various zones of articular cartilage. *Biomaterials*, 32(5):1327–1338.
- Nguyen, L. H., Kudva, A. K., Saxena, N. S., and Roy, K. (2011b). Engineering articular cartilage with spatially-varying matrix composition and mechanical properties from a single stem cell population using a multi-layered hydrogel. *Biomaterials*, 32(29):6946–6952.
- Nichols, A., Burns, D. C., and Christopher, R. (2009). Studies On The Sterilization Of Human Bone And Tendon Musculoskeletal Allograft Tissue Using Supercritical Carbon Dioxide. *Journal of Orthopaedics*, 6(2):e9.
- Niethammer, T. R., Pietschmann, M. F., Horng, A., Roßbach, B. P., Ficklscherer, A., Jansson, V., and Müller, P. E. (2014). Graft hypertrophy of matrix-based autologous chondrocyte implantation: A two-year follow-up study of NOVOCART 3D implantation in the knee. *Knee Surgery, Sports Traumatology, Arthroscopy*, 22(6):1329–1336.
- Niikura, T. and Reddi, A. H. (2007). Differential regulation of lubricin/superficial zone protein by transforming growth factor  $\beta$ /bone morphogenetic protein superfamily members in articular chondrocytes and synoviocytes. *Arthritis and Rheumatism*, 56(7):2312–2321.
- Nourissat, G., Berenbaum, F., and Duprez, D. (2015). Tendon injury: from biology to tendon repair. *Nature reviews. Rheumatology*, 11(4):223–233.
- Nuernberger, S., Cyran, N., Albrecht, C., Redl, H., Vécsei, V., and Marlovits, S. (2011). The influence of scaffold architecture on chondrocyte distribution and behavior in matrix-associated chondrocyte transplantation grafts. *Biomaterials*, 32(4):1032–1040.

- Oliver-Welsh, L., Griffin, J. W., Meyer, M. A., Gitelis, M. E., and Cole, B. J. (2016). Deciding How Best to Treat Cartilage Defects. *Orthopedics*, 39(6):343–350.
- Onuora, S. (2016). Regenerative medicine: A nose for cartilage repair. *Nature Reviews Rheumatology*, 12(12):691.
- Orth, P., Rey-Rico, A., Venkatesan, J. K., Madry, H., and Cucchiaroni, M. (2014). Current perspectives in stem cell research for knee cartilage repair. *Stem Cells and Cloning: Advances and Applications*, 7(1):1–17.
- Ott, H. C., Clippinger, B., Conrad, C., Schuetz, C., Pomerantseva, I., Ikonomou, L., Kotton, D., and Vacanti, J. P. (2010). Regeneration and orthotopic transplantation of a bioartificial lung. *Nature Medicine*, 16(8):927–933.
- Ott, H. C., Matthiesen, T. S., Goh, S.-K., Black, L. D., Kren, S. M., Netoff, T. I., and Taylor, D. a. (2008). Perfusion-decellularized matrix: using nature's platform to engineer a bioartificial heart. *Nature medicine*, 14(2):213–221.
- Oussedik, S., Tsitskaris, K., and Parker, D. (2015). Treatment of articular cartilage lesions of the knee by microfracture or autologous chondrocyte implantation: A systematic review. *Arthroscopy - Journal of Arthroscopic and Related Surgery*, 31(4):732–744.
- Park, J., Gelse, K., Frank, S., von der Mark, K., Aigner, T., and Schneider, H. (2006). Transgene-activated mesenchymal cells for articular cartilage repair: A comparison of primary bone marrow-, perichondrium/periosteum- and fat-derived cells. *Journal of Gene Medicine*, 8(1):112–125.
- Park, S. M., Yang, S., Rye, S. M., and Choi, S. W. (2018). Effect of pulsatile flow perfusion on decellularization. *BioMedical Engineering Online*, 17(1).
- Park, S. S., Jin, H. R., Chi, D. H., and Taylor, R. S. (2004). Characteristics of tissue-engineered cartilage from human auricular chondrocytes. *Biomaterials*, 25(12):2363–2369.
- Pati, F., Jang, J., Ha, D.-H., Won Kim, S., Rhie, J.-W., Shim, J.-H., Kim, D.-H., and Cho, D.-W. (2014). Printing three-dimensional tissue analogues with decellularized extracellular matrix bioink. *Nature Communications*, 5:1–11.
- Patton, J. H., Berry, S., and Kralovich, K. A. (2007). Use of human acellular dermal matrix in complex and contaminated abdominal wall reconstructions. *American Journal of Surgery*, 193(3):360–363.
- Pelttari, K., Winter, A., Steck, E., Goetzke, K., Hennig, T., Ochs, B. G., Aigner, T., and Richter, W. (2006). Premature induction of hypertrophy during in vitro chondrogenesis of human mesenchymal stem cells correlates with calcification and vascular invasion after ectopic transplantation in SCID mice. *Arthritis and Rheumatism*, 54(10):3254–3266.
- Petersen, T. H. T., Calle, E. A. E., Zhao, L., Lee, E. J., Gui, L., Raredon, M. B., Gavrillov, K., Yi, T., Zhuang, Z. W., Breuer, C., Herzog, E., and Niklason, L. E. (2010). Tissue-engineered lungs for in vivo implantation. *Science*, 329(5991):538–541.

- Peterson, L., Minas, T., Brittberg, M., Nilsson, A., Sjögren-Jansson, E., and Lindahl, A. (2000). Two- to 9-year outcome after autologous chondrocyte transplantation of the knee. *Clinical orthopaedics and related research*, (374):212–34.
- Petrella, R. J., DiSilvestro, M. D., and Hildebrand, C. (2002). Effects of Hyaluronate Sodium on Pain and Physical Functioning in Osteoarthritis of the Knee. *Archives of Internal Medicine*, 162(3):292.
- Pittenger, M. F. (1999). Multilineage Potential of Adult Human Mesenchymal Stem Cells. *Science*, 284(5411):143–147.
- Portocarrero, G. and Livinston, A. T. (2013). Challenges In Cartilage Tissue Engineering. *Journal of Tissue Science & Engineering*, 04(1):1–2.
- Quarto, R., Mastrogiacomo, M., Cancedda, R., Kutepov, S. M., Mukhachev, V., Lavroukov, A., Kon, E., and Marcacci, M. (2001). Repair of Large Bone Defects with the Use of Autologous Bone Marrow Stromal Cells. *New England Journal of Medicine*, 344(5):385–386.
- Quintin, A., Hirt-Burri, N., Scaletta, C., Schizas, C., Pioletti, D. P., and Applegate, L. A. (2007). Consistency and safety of cell banks for research and clinical use: preliminary analysis of fetal skin banks. *Cell transplantation*, 16(7):675–84.
- R Lakes, S. S. (1979). Cement Line Motion in Bone Abstract. *Science*, 204(4392):501–503.
- Raghavan, S. S., Woon, C. Y. L., Kraus, A., Megerle, K., Choi, M. S. S., Pridgen, B. C., Pham, H., and Chang, J. (2012). Human flexor tendon tissue engineering: decellularization of human flexor tendons reduces immunogenicity in vivo. *Tissue engineering. Part A*, 18(7-8):796–805.
- Redler, I., Mow, V. C., Zimny, M. L., and Mansell, J. (1975). The ultrastructure and biomechanical significance of the tidemark of articular cartilage. *Clinical orthopaedics and related research*, (112):357–62.
- Ren, X., Wang, F., Chen, C., Gong, X., Yin, L., and Yang, L. (2016). Engineering zonal cartilage through bioprinting collagen type II hydrogel constructs with biomimetic chondrocyte density gradient. *BMC Musculoskeletal Disorders*, 17(1):1–10.
- Revell, C. M. and Athanasiou, K. A. (2009). Success Rates and Immunologic Responses of Autogenic, Allogenic, and Xenogenic Treatments to Repair Articular Cartilage Defects. *Tissue Engineering Part B: Reviews*, 15(1):1–15.
- Reynolds, K. L. and Bishai, S. K. (2014). In situ evaluation of chondrofix® osteochondral allograft 25 months following implantation: A case report. *Osteoarthritis Cartilage*, 22:S155–S156.
- Rhee, D. K., Marcelino, J., Baker, M., Gong, Y., Smits, P., Lefebvre, V., Jay, G. D., Stewart, M., Wang, H., Warman, M. L., and Carpten, J. D. (2005). The secreted glycoprotein lubricin protects cartilage surfaces and inhibits synovial cell overgrowth. 115(3).

- Ronga, M., Grassi, F. A., and Bulgheroni, P. (2004). Arthroscopic Autologous Chondrocyte Implantation for the Treatment of a Chondral Defect in the Tibial Plateau of the Knee. *Arthroscopy - Journal of Arthroscopic and Related Surgery*, 20(1):79–84.
- Rosario, D. J., Reilly, G. C., Ali Salah, E., Glover, M., Bullock, A. J., and Macneil, S. (2008). Decellularization and sterilization of porcine urinary bladder matrix for tissue engineering in the lower urinary tract. *Regenerative medicine*, 3(2):145–156.
- Rosenthal, D. I., Rosenberg, A. E., Schiller, A. L., and Smith, R. J. (1983). Destructive arthritis due to silicone: a foreign-body reaction. *Radiology*, 149(1):69–72.
- Roth, S. P., Glauche, S. M., Plenge, A., Erbe, I., Heller, S., and Burk, J. (2017). Automated freeze-thaw cycles for decellularization of tendon tissue - a pilot study. *BMC Biotechnology*, 17(1):1–10.
- Rotter, N., Bonassar, L. J., Tobias, G., Lebl, M., Roy, A. K., and Vacanti, C. A. (2002). Age dependence of biochemical and biomechanical properties of tissue-engineered human septal cartilage. *Biomaterials*, 23(15):3087–3094.
- Rowland, C. R., Colucci, L. A., and Guilak, F. (2016). Fabrication of anatomically-shaped cartilage constructs using decellularized cartilage-derived matrix scaffolds. *Biomaterials*, 91:57–72.
- Rowland, C. R., Lennon, D. P., Caplan, A. I., and Guilak, F. (2013). The effects of crosslinking of scaffolds engineered from cartilage ECM on the chondrogenic differentiation of MSCs. *Biomaterials*, 34(23):5802–5812.
- Rutjes, A. W. S., Ju, P., Costa, B. R., Trelle, S., and Nu, E. (2013). Annals of Internal Medicine Viscosupplementation for Osteoarthritis of the Knee. *Annals of Internal Medicine*, (157):180–191.
- Saris, D., Price, A., Widuchowski, W., Bertrand-Marchand, M., Caron, J., Drogset, J. O., Emans, P., Podskubka, A., Tsuchida, A., Kili, S., Levine, D., and Brittberg, M. (2014). Matrix-Applied Characterized Autologous Cultured Chondrocytes Versus Microfracture: Two-Year Follow-up of a Prospective Randomized Trial. *The American journal of sports medicine*, 42(6):1384–1394.
- Sawada, K., Terada, D., Yamaoka, T., Kitamura, S., and Fujisato, T. (2008). Cell removal with supercritical carbon dioxide for acellular artificial tissue. *Journal of Chemical Technology and Biotechnology*, 83(6):943–949.
- Schmidt, T. A., Gastelum, N. S., Nguyen, Q. T., Schumacher, B. L., and Sah, R. L. (2007). Boundary lubrication of articular cartilage: Role of synovial fluid constituents. *Arthritis and Rheumatism*, 56(3):882–891.
- Schneider, C., Lehmann, J., van Osch, G. J., Hildner, F., Teuschl, A., Monforte, X., Miosga, D., Heimel, P., Priglinger, E., Redl, H., Wolbank, S., and Nürnberger, S. (2016). Systematic Comparison of Protocols for the Preparation of Human Articular Cartilage for Use as Scaffold Material in Cartilage Tissue Engineering. *Tissue Engineering Part C: Methods*, 22(12):1095–1107.

- Schneider, G. M. (1978). Physicochemical Principles of Extraction with Supercritical Gases. *Angewandte Chemie International Edition in English*, 17(10):716–727.
- Schumacher, B. L., Block, J. A., Schmid, T. M., Aydelotte, M. B., and Kuettner, K. E. (1994). A novel proteoglycan synthesized and secreted by chondrocytes of the superficial zone of articular cartilage. *Archives of Biochemistry and Biophysics*, 311(1):144–152.
- Sharkey, P. F., Lichstein, P. M., Shen, C., Tokarski, A. T., and Parvizi, J. (2013). Why are total knee arthroplasties failing today-has anything changed after 10 years? *Journal of Arthroplasty*, 29(9):1774–1778.
- Shin, H., Jo, S., and Mikos, A. G. (2003). Biomimetic materials for tissue engineering.
- Siebold, R., Lichtenberg, S., and Habermeyer, P. (2003). Combination of microfracture and periosteal-flap for the treatment of focal full thickness articular cartilage lesions of the shoulder: a prospective study. *Knee surgery, sports traumatology, arthroscopy : official journal of the ESSKA*, 11(3):183–189.
- Simon, T. M. and Jackson, D. W. (2018). Articular Cartilage: Injury Pathways and Treatment Options. *Sports Medicine and Arthroscopy Review*, 26(1):146–154.
- Simonsen, J. L., Rosada, C., Serakinci, N., Justesen, J., Stenderup, K., Rattan, S. I. S., Jensen, T. G., and Kassem, M. (2002). Telomerase expression extends the proliferative life-span and maintains the osteogenic potential of human bone marrow stromal cells. *Nature Biotechnology*, 20(6):592–596.
- Song, J. J., Guyette, J. P., Gilpin, S. E., Gonzalez, G., Vacanti, J. P., and Ott, H. C. (2013). Regeneration and experimental orthotopic transplantation of a bioengineered kidney. *Nature Medicine*, 19(5):646–651.
- Steadman, J. R., Rodkey, W. G., and Rodrigo, J. J. (2001). Microfracture: surgical technique and rehabilitation to treat chondral defects. *Clin Orthop Relat Res*, (391 Suppl):362–9.
- Steele, J. A., McCullen, S. D., Callanan, A., Autefage, H., Accardi, M. A., Dini, D., and Stevens, M. M. (2014). Combinatorial scaffold morphologies for zonal articular cartilage engineering. *Acta Biomaterialia*, 10(5):2065–2075.
- Steinhagen, J., Bruns, J., Deuretzbacher, G., Ruether, W., Fuerst, M., and Niggemeyer, O. (2010). Treatment of osteochondritis dissecans of the femoral condyle with autologous bone grafts and matrix-supported autologous chondrocytes. *International Orthopaedics*, 34(6):819–825.
- Stockwell, R. A. (1967). The cell density of human articular and costal cartilage. *Journal of Anatomy*, 101(4):753–763.
- Strangeways, T. S. P. (1920). The nutrition of articular cartilage. *Br Med J*, 15:661–663.
- Studer, D., Cavalli, E., Formica, F. A., Kuhn, G. A., Salzmann, G., Mumme, M., Steinwachs, M. R., Laurent-Applegate, L. A., Maniura-Weber, K., and Zenobi-Wong, M. (2017). Human chondroprogenitors in alginate–collagen hybrid scaffolds produce stable cartilage in vivo. *Journal of Tissue Engineering and Regenerative Medicine*, 11(11):3014–3026.



- Sun, W. Q. and Leung, P. (2008). Calorimetric study of extracellular tissue matrix degradation and instability after gamma irradiation. *Acta Biomaterialia*, 4(4):817–826.
- Sutherland, A. J., Beck, E. C., Dennis, S. C., Converse, G. L., Hopkins, R. a., Berkland, C. J., and Detamore, M. S. (2015). Decellularized Cartilage May Be a Chondroinductive Material for Osteochondral Tissue Engineering. *Plos One*, 10(5):e0121966.
- Swain, M. V., Nohava, J., and Eberwein, P. (2017). A simple basis for determination of the modulus and hydraulic conductivity of human ocular surface using nano-indentation. *Acta Biomaterialia*, 50:312–321.
- Szarko, M., Muldrew, K., and Bertram, J. E. (2010). Freeze-thaw treatment effects on the dynamic mechanical properties of articular cartilage. *BMC musculoskeletal disorders*, 11(1):231.
- Tanaka, Y., Sakaki, I., and Ohkubo, T. (2004). Extraction of Phospholipids from Salmon Roe with Supercritical Carbon Dioxide and an Entrainer. *Journal of Oleo Science*, 53(9):417–424.
- Tatman, P. D., Gerull, W., Sweeney-Easter, S., Davis, J. I., Gee, A. O., and Kim, D.-H. (2015). Multiscale Biofabrication of Articular Cartilage: Bioinspired and Biomimetic Approaches. *Tissue Engineering Part B: Reviews*, 21(6):543–559.
- Temenoff, J. S. and Mikos, A. G. (2000). Review: Tissue engineering for regeneration of articular cartilage. *Biomaterials*, 21(5):431–440.
- Tiziana Martinello<sup>1</sup>, Ilaria Bronzini<sup>1</sup>, A. V. V. V. L. M. G. C. F. B. M. P. (2014). Successful recellularization of human tendonscaffolds using adipose-derived mesenchymal stemcells and collagen gel. *Journal of tissue engineering and regenerative medicine*, 8(8):612–619.
- Tomkoria, S., Patel, R. V., and Mao, J. J. (2004). Heterogeneous nanomechanical properties of superficial and zonal regions of articular cartilage of the rabbit proximal radius condyle by atomic force microscopy. *Medical Engineering and Physics*, 26(10):815–822.
- Trueta, J. and Little, K. (1960). The vascular contribution to osteogenesis. II. Studies with the electron microscope. *The Journal of bone and joint surgery. British volume*, 42-B:367–76.
- Uygun, B. E., Soto-Gutierrez, A., Yagi, H., Izamis, M.-L., Guzzardi, M. A., Shulman, C., Milwid, J., Kobayashi, N., Tilles, A., Berthiaume, F., Hertl, M., Nahmias, Y., Yarmush, M. L., and Uygun, K. (2010). Organ reengineering through development of a transplantable recellularized liver graft using decellularized liver matrix. *Nature medicine*, 16(7):814–20.
- Vanlauwe, J., Saris, D. B. F., Victor, J., Almqvist, K. F., Bellemans, J., and Luyten, F. P. (2011). Five-year outcome of characterized chondrocyte implantation versus microfracture for symptomatic cartilage defects of the knee: early treatment matters. *American Journal of Sports Medicine*, 39(12):2566–2574.
- Vinatier, C., Gauthier, O., Masson, M., Malard, O., Moreau, A., Fellah, B. H., Bilban, M., Spaethe, R., Daculsi, G., and Guicheux, J. (2009). Nasal chondrocytes and fibrin sealant for cartilage tissue engineering. *Journal of Biomedical Materials Research - Part A*, 89(1):176–185.

- Visser, J., Levett, P. A., te Moller, N. C. R., Besems, J., Boere, K. W. M., van Rijen, M. H. P., de Grauw, J. C., Dhert, W. J. A., van Weeren, P. R., and Malda, J. (2015). Crosslinkable hydrogels derived from cartilage, meniscus, and tendon tissue. *Tissue engineering. Part A*, 21(7-8):1195–206.
- Visser, J., Peters, B., Burger, T. J., Boomstra, J., Dhert, W. J. A., Melchels, F. P. W., and Malda, J. (2013). Biofabrication of multi-material anatomically shaped tissue constructs. *Biofabrication*, 5(3):035007.
- Von Der Mark, K., Gauss, V., Von Der Mark, H., and Müller, P. (1977). Relationship between cell shape and type of collagen synthesised as chondrocytes lose their cartilage phenotype in culture [26]. *Nature*, 267(5611):531–532.
- Wainwright, J. M., Czajka, C. a., Patel, U. B., Freytes, D. O., Tobita, K., Gilbert, T. W., and Badylak, S. F. (2010). Preparation of cardiac extracellular matrix from an intact porcine heart. *Tissue engineering. Part C, Methods*, 16(3):525–32.
- Wakitani, S., Imoto, K., Yamamoto, T., Saito, M., Murata, N., and Yoneda, M. (2002). Human autologous culture expanded bone marrow-mesenchymal cell transplantation for repair of cartilage defects in osteoarthritic knees. *Osteoarthritis and Cartilage*, 10(3):199–206.
- Wang, J. K., Luo, B., Guneta, V., Li, L., Foo, S. E. M., Dai, Y., Tan, T. T. Y., Tan, N. S., Choong, C., and Wong, M. T. C. (2017a). Supercritical carbon dioxide extracted extracellular matrix material from adipose tissue. *Materials Science and Engineering C*, 75:349–358.
- Wang, X., Jiang, M., Zhou, Z., Gou, J., and Hui, D. (2017b). 3D printing of polymer matrix composites: A review and prospective.
- Weiss, C., Rosenberg, L., and Helfet, A. J. (1968). An ultrastructural study of normal young adult human articular cartilage. *The Journal of bone and joint surgery. American volume*, 50(4):663–674.
- Wise, J. K., Yarin, A. L., Megaridis, C. M., and Cho, M. (2009). Chondrogenic Differentiation of Human Mesenchymal Stem Cells on Oriented Nanofibrous Scaffolds: Engineering the Superficial Zone of Articular Cartilage. *Tissue Engineering Part A*, 15(4):913–921.
- Wondrasch, B., Zak, L., Welsch, G. H., and Marlovits, S. (2009). Effect of accelerated weightbearing after matrix-associated autologous chondrocyte implantation on the femoral condyle on radiographic and clinical outcome after 2 years: a prospective, randomized controlled pilot study. *The American journal of sports medicine*, 37 Suppl 1:88S–96S.
- Wong, C. C., Chen, C. H., Chiu, L. H., Tsuang, Y. H., Bai, M. Y., Chung, R. J., Lin, Y. H., Hsieh, F. J., Chen, Y. T., and Yang, T. L. (2018). Facilitating In Vivo Articular Cartilage Repair by Tissue-Engineered Cartilage Grafts Produced From Auricular Chondrocytes. *American Journal of Sports Medicine*, 46(3):713–727.
- Xu, K., Kuntz, L. A., Foehr, P., Kuempel, K., Wagner, A., Tuebel, J., Deimling, C. V., and Burgkart, R. H. (2017). Efficient decellularization for tissue engineering of the tendon-bone interface with preservation of biomechanics. *PLoS ONE*, 12(2).

- Yanaga, H., Yanaga, K., Imai, K., Koga, M., Soejima, C., and Ohmori, K. (2006). Clinical application of cultured autologous human auricular chondrocytes with autologous serum for craniofacial or nasal augmentation and repair. *Plastic and Reconstructive Surgery*, 117(6):2019–2030.
- Yang, G., Rothrauff, B. B., Lin, H., Gottardi, R., Alexander, P. G., and Tuan, R. S. (2013). Enhancement of tenogenic differentiation of human adipose stem cells by tendon-derived extracellular matrix. *Biomaterials*, 34(37):9295–9306.
- Yang, Q., Peng, J., Guo, Q., Huang, J., Zhang, L., Yao, J., Yang, F., Wang, S., Xu, W., Wang, A., and Lu, S. (2008). A cartilage ECM-derived 3-D porous acellular matrix scaffold for in vivo cartilage tissue engineering with PKH26-labeled chondrogenic bone marrow-derived mesenchymal stem cells. *Biomaterials*, 29(15):2378–2387.
- Yang, Z., Shi, Y., Wei, X., He, J., Yang, S., Dickson, G., Tang, J., Xiang, J., Song, C., and Li, G. (2010). Fabrication and repair of cartilage defects with a novel acellular cartilage matrix scaffold. *Tissue engineering. Part C, Methods*, 16(5):865–876.
- Youngstrom, D. W., Barrett, J. G., Jose, R. R., and Kaplan, D. L. (2013). Functional Characterization of Detergent-Decellularized Equine Tendon Extracellular Matrix for Tissue Engineering Applications. *PLoS ONE*, 8(5).
- Yu, H., Grynepas, M., and Kandel, R. A. (1997). Composition of cartilagenous tissue with mineralized and non-mineralized zones formed in vitro. *Biomaterials*, 18(21):1425–1431.
- Zadpoor, A. A. and Malda, J. (2016). Additive Manufacturing of Biomaterials, Tissues, and Organs. *Annals of Biomedical Engineering*.
- Zak, L., Albrecht, C., Wondrasch, B., Widhalm, H., Vekszler, G., Trattinig, S., Marlovits, S., and Aldrian, S. (2014). Results 2 years after matrix-associated autologous chondrocyte transplantation using the Novocart 3D scaffold: An analysis of clinical and radiological data. *American Journal of Sports Medicine*, 42(7):1618–1627.
- Zambon, A., Vetralla, M., Urbani, L., Pantano, M. F., Ferrentino, G., Pozzobon, M., Pugno, N. M., Coppi, P. D., Elvassore, N., and Spilimbergo, S. (2016). Dry acellular oesophageal matrix prepared by supercritical carbon dioxide. *The Journal of Supercritical Fluids*, 115:33–41.
- Zein, I., Hutmacher, D. W., Tan, K. C., and Teoh, S. H. (2002). Fused deposition modeling of novel scaffold architectures for tissue engineering applications. *Biomaterials*, 23(4):1169–1185.
- Zhang, Q., Johnson, J. A., Dunne, L. W., Chen, Y., Iyyanki, T., Wu, Y., Chang, E. I., Branch-Brooks, C. D., Robb, G. L., and Butler, C. E. (2016). Decellularized skin/adipose tissue flap matrix for engineering vascularized composite soft tissue flaps. *Acta Biomaterialia*, 35:166–184.
- Zhang, Z., Zhong, X., Ji, H., Tang, Z., Bai, J., Yao, M., Hou, J., Zheng, M., Wood, D. J., Sun, J., Zhou, S.-F., and Liu, A. (2014). Matrix-induced autologous chondrocyte implantation for the treatment of chondral defects of the knees in Chinese patients. *Drug Des Devel Ther.*, 8:2439–2448.

- Zheng, M.-H., Willers, C., Kirilak, L., Yates, P., Xu, J., Wood, D., and Shimmin, A. (2007). Matrix-induced autologous chondrocyte implantation (MACI®): biological and histological assessment. *Tissue Engineering*, 13(4):737–746.
- Zhu, D., Tong, X., Trinh, P., and Yang, F. (2017). Mimicking Cartilage Tissue Zonal Organization by Engineering Tissue-scale Gradient Hydrogels as 3D Cell Niche. *Tissue Engineering Part A*, 24:ten.TEA.2016.0453.
- Zuk, P. A., Zhu, M., Ashjian, P., De Ugarte, D. A., Huang, J. I., Mizuno, H., Alfonso, Z. C., Fraser, J. K., Benhaim, P., and Hedrick, M. H. (2002). Human adipose tissue is a source of multipotent stem cells. *Mol Biol Cell*, 13(12):4279–4295.



# Jens Antons

Ph.D. in Bioengineering  
(Expected in 01/2019)

Rue de l'industrie 9  
CH-1020 Renens  
+41764945452  
Jens.Antons@gmail.com  
Date of birth: 14th June 1988  
Nationality: German  
Resident status: Permit B  
Marital Status: Single

**Summary:** A bioengineer with essential skills and experience to manage projects in a multidisciplinary environment. A passionate and focused problem-solver as well as process- and results-driven. Analytically strong, self-motivated and keen to reach desired outcome by setting up and following a plan.

<b>Technical</b>	Experience in supercritical carbon dioxide, nanoindentation, biocompatibility tests and biomaterial characterization
<b>IT-Skills</b>	Advanced computer skills, Adobe Illustrator, Microsoft Office, LaTeX
<b>Communication</b>	Fluency in English, German, French and intermediate in Spanish. Ongoing participation in public speaking training, mentoring and competitions

## Professional Experience

01/2015-Present	<b>Ph.D. Researcher</b> -Writing of scientific publications -Coordination between labs and companies -Teaching of courses -Mentoring of students	Lab of Biomechanical Orthopedics, EPFL Lausanne, Switzerland
10/2014–12/2014	<b>Research Assistant</b> Improvement of optical coating	Fraunhofer Institute for Ceramic Technologies, Dresden, Germany
02/2013-10/2014	<b>Student Assistant</b> Maintenance of light microscopes	Max Planck Institute, MPI-CBG, Dresden, Germany
02/2012-08/2012	<b>Application Lab Intern</b> Bachelor thesis on robotic system for DNA extraction	Promega, Lyon, France
08/2008-08/2009	<b>Gap Year: Work and Travel</b> Improvement of English skills, guiding sea kayaking tourist groups	Melbourne, Australia

## Education

01/2015-Present	<b>Ph.D. in Bioengineering</b> Supervisors: Prof. Dominique P. Pioletti Prof. Lee Ann Laurent-Applegate  <u>Ph.D. thesis:</u> Development of a new decellularisation method for articular cartilage	Lab of Biomechanical Orthopedics, EPFL Lausanne, Switzerland
10/2012-10/2014	<b>M.Sc. Molecular Bioengineering</b> International Master (100% English) <u>Master thesis:</u> on local surface plasmon resonance biosensor	TU Dresden, Dresden, Germany
10/2009-10/2012	<b>B.Sc. Biology</b> <u>Bachelor thesis:</u> on robotic DNA extraction system	University of Würzburg, Würzburg, Germany



## Additional Courses

2017	Scientific Writing for Biomedical Articles (1 ECTS)	Lausanne, Switzerland
2016	3D Printing and Biofabrication (2 ECTS)	Utrecht, Netherlands
2016	Additive Manufacturing (2 ECTS)	Lausanne, Switzerland
2016	CTI Business Concept (4 ECTS)	Lausanne, Switzerland
2013-2014	Course in Intellectual Property Rights (12 ECTS)	Dresden, Germany



## Teaching

2018-Present	<b>Teaching Assistant</b> ME-380-(Bachelor course) "Experimental Methods in Biomechanics"	Supervisor: Prof. Dominique Pioletti
2016-Present	<b>Teaching Assistant</b> ME-482-(Master course) "Biomechanics of the Musculoskeletal System"	Supervisor: Prof. Dominique Pioletti
2015-Present	<b>Student Supervisor</b> Supervision of master, semester projects and interns	



## Peer-reviewed Publications

**Antons, J.**, et al. 2018. Zonal Mechanical Properties of Human Articular Cartilage obtained by Nanoindentation. *Journal of Materials Science: Materials in Medicine*

**Antons, J.**, et al. 2018. Decellularised tissues obtained by a CO<sub>2</sub>-philic detergent and supercritical CO<sub>2</sub>. *European cells & materials*, 36, pp.81-95

Marascio, M.G.M., **Antons, J.**, Pioletti, D.P. and Bourban, P.E., 2017. 3D Printing of Polymers with Hierarchical Continuous Porosity. *Advanced Materials Technologies*, 2(11)



## Oral Presentations

06/2018	"Decellularised tissue matrices in orthopedics"	Orthopedic Research day EPFL, Lausanne
05/2018	"Decellularised tissues obtained by a CO <sub>2</sub> -philic detergent and supercritical carbon dioxide"	SBMS Summer School Interlaken, Switzerland
07/2017	"Depth-dependent mechanical properties of human articular cartilage"	ESB 2017, Sevilla, Spain
06/2017	"Decellularisation potential of biological matrix for musculoskeletal tissue repair"	Orthopedic Research day EPFL, Lausanne



## Poster Presentations

09/2018	"Decellularised tissues obtained by a CO <sub>2</sub> -philic detergent and supercritical CO <sub>2</sub> "	Termis 2018 Kyoto, Japan
07/2017	"Depth-dependent mechanical properties of human articular cartilage obtained by indentation measurements"	EU Termis 2017, Davos, Switzerland
03/2017	"An extracellular matrix based hydrogel as in vitro model to study zone-specific chondrocyte differentiation"	ORS 2017 San Diego, California USA
08/2016	"Cartilage decellularised extracellular matrix as photocrosslinkable hydrogel for mechanical gradients in near native environments"	Biointerfaces 2016 ETH Zürich, Zürich



## Extracurricular Activities

2015-Present	Public Speaking Club president (2017-2018)	Toastmasters EPFL, Lausanne, Switzerland
Sport	Rock climbing, hiking, diving	



## References

Prof. Dominique P. Pioletti	Thesis director	<a href="mailto:Dominique.Pioletti@epfl.ch">Dominique.Pioletti@epfl.ch</a>
Prof. Lee Ann Laurent-Applegate	Thesis co-director	<a href="mailto:Lee.Laurent-Applegate@chuv.ch">Lee.Laurent-Applegate@chuv.ch</a>

